Role of the Actin Depolymerizing Factors ADF and Cofilin in Murine Macrophages (*Mus musculus*; Linnaeus 1758)

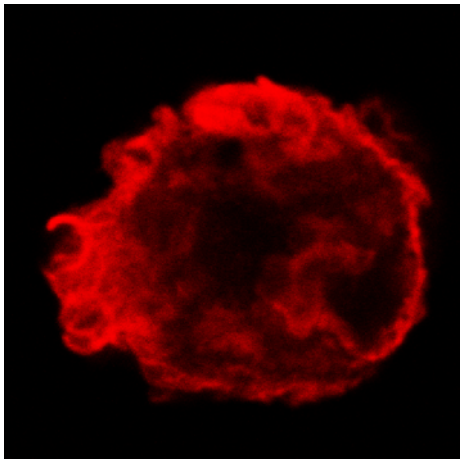

INAUGURAL-DISSERTATION

Submitted in partial fulfilment of the requirements for the doctoral degree

- Dr. rer. nat. -

Department of Biology,

Faculty of Mathematics, Informatics and Natural Sciences,

University of Hamburg, Germany

by

Friederike Jönsson

Hamburg, Germany

2007

,

Genehmigt vom Department Biologie
der Fakultät für Mathematik, Informatik und Naturwissenschaften
an der Universität Hamburg
auf Antrag von Professor Dr. B. FLEISCHER
Weiterer Gutachter der Dissertation:
Herr Priv.-Doz Dr. H. QUADER
Tag der Disputation: 16. Februar 2007

Hamburg, den 25. Januar 2007

Professor Dr. Reinhard Lieberei
Leiter des Departments Biologie

Role of the Actin Depolymerizing Factors ADF and Cofilin in Murine Macrophages (*Mus musculus*; Linnaeus 1758)

Summary

The actin cytoskeleton is a structure found in all eukaryotes, known to be essential for a wide range of cellular processes. The remodelling of the actin cytoskeleton is regulated by a large number of proteins, commonly known as actin binding proteins.

Recently the actin cytoskeleton as a central component of cellular architecture has gained attention as a regulator of immune functions. One goal of this thesis was to shed some light on the regulation of the actin cytoskeleton in murine macrophages, by investigating the function of the two actin depolymerizing factors ADF and cofilin. ADF and cofilin are highly conserved molecules that enhance actin filament turnover by severing and depolymerization of filaments.

Using a genetic approach, I studied the loss-of-function of ADF and cofilin in murine macrophages. My work demonstrated that cofilin is essential for macrophage polarization, migration, and cytokinesis. Lack of cofilin resulted in a decreased ability to re-organize the actin cytoskeleton as indicated by the accumulation of cortical F-actin and the alterations in cell morphology. Interestingly, other actin dependent processes like phagocytosis or cell attachment were not disturbed in cofilin null macrophages. In terms of immunological functions, I could demonstrate that cofilin is required for antigen presentation by macrophages, suggesting an important role of cofilin in the formation of the immunological synapse.

One unexpected, finding described in my thesis is that the cofilin homolog ADF has a distinct role *in vivo*. Macrophages lacking ADF showed no functional defects and were similar to wild type cells in all the experiments performed.

In order to better characterize the common and distinct activities of cofilin and ADF, I developed two different strategies. First, I generated a conditional allele in the mouse which will allow tissue specific exchange of the cofilin expression by ADF.

Second, using a proteomics approach, I was able to identify novel binding partners for cofilin and ADF. These protein ligands characterized from ADF/cofilin complexes suggested a not yet recognized role of the two proteins also in the nucleus. There ADF and cofilin might regulate actin in controlling chromatin structure, transcription, and mRNA processing.

In conclusion, ADF and cofilin play distinct roles in macrophages in the regulation of immune cell functions, suggesting that both proteins are working in independent pathways to control actin turnover. The potential differences in regulation and the selective interaction of cofilin/ADF with partners other than actin will be an interesting and important aspect of future work. A better understanding of ADF and cofilin function and regulation might eventually allow to modify or interfere with immune cell responses under pathological conditions.

Supervisor: Dr. Walter Witke
First referee: Professor Dr. Bernhard Fleischer
Second referee: PD Dr. Hartmut Quader

Acknowledgements

I want to thank Professor Dr. Bernhard Fleischer who allowed me to follow this particular PhD project and made it possible to finish this project in Hamburg.

My special thanks go to Dr. Walter Witke for welcoming me in his lab, being an excellent teacher and for his support throughout the entire time of my PhD.

I want to thank Dr. Christine Gurniak for her help with the cloning and many fruitful discussions and of course the generous permission to use the cofilin conditional and ADF knockout mice for my experiments.

All the members of the Witke group who made my time in Italy a unique experience: Gian-Carlo Bellenchi, Marzia Massimi, Emerald Perlas, Pietro Pilo Boyl, Marco Rust, Agnieszka Sadowska, Ekaterina Salimova and Denise Sofia.

The department of Immunology of the Bernhard Nocht Institute who made me feel welcome after this long stay in Italy.

In addition I want to thank:
Christel Schmetz who prepared the samples for the scanning electron microscopy.
The Proteomics Facility of the EMBL Heidelberg for the mass spectrometry analysis of the AC complexes.
Jeannette Rientjes who provided the BAC derived subclones for the targeting construct.
Dr. Manolis Pasparakis who kindly provided the CD11bCre mice.
PD Dr. Uwe Ritter and his group for sharing their limited mouse space with me.
Dr. Minka Breloer and all members of the lab 222 for providing me a bench to finish my experiments.
The Gottlieb Daimler- and Karl Benz-Foundation and the Olympus Europa Foundation for the financial support.

My sister and my parents always supported me and it felt good to know that there is a home to come back to.

Most importantly, Olivier and my friends for listening to me and for sharing some good time with me, reminding me that there is so much more than “just” science.

Table of content

Figure list

List of abbreviations

Ab	antibody
AC	ADF/cofilin
ADP	adenosine 5´-diphosphate
APC	antigen presenting cell
APS	ammonium persulfate
ATP	adenosine 5´-trisphosphate
bm	bone marrow
BMM	bone marrow-derived macrophages
bp	base pair
BrdU	5-bromo-2′-deoxyuridine
BSA	bovine serum albumine
CD	clusters of differentiation
cDNA	complementary deoxyribonucleic acid
cof	cofilin
Cre	recombinase Cre
DC	dendritic cells
DMSO	dimethyl sulfoxide
dNTP	deoxyribonucleic triphosphate
EDTA	ethylenediamine-tetraacetic acid
ELISA	enzyme linked immunosorbent assay
ES cell	embryonic stem cell
F-actin	filamentous actin
FCS	fetal calf serum
FITC	fluorescein isothiocyanate
flx	floxed (flanked by loxP sites)
G-actin	globular actin
GST	glutathione-S-transferase
HEPES	4-(2-hydroxyethyl)-1-piperazineethanesulfonic acid
hnRNP	heterogeneous nuclear ribonucleoprotein
hr	hour
HSC	hematopoietic stem cells
i.p.	intraperitoneal
IFN	interferon
IL	interleukin
IPTG	isopropylthio-β-galactoside
kDa	kilodalton
LPS	lipopolysaccharide
LysM	lysozyme M
M	molar
MHC	major histocompatibility complex
min	minute
mM	millimolar
mRNA	messenger ribonucleic acid

neo	neomycin
ng	nanogram
o.n.	over night
OD	optical density
PBS	phosphate buffered saline
PCR	polymerase chain reaction
PE	phycoerythrin
PEC	peritoneal exsudate cells
PFA	paraformaldehyde
PI	phosphoinositides
polyI:C	polyinosinic-polycytidylic acid
rpm	rounds per minute
RT	room temperature
Ser	serine
TEMED	N,N,N′,N′-tetramethylethylenediamine
Thr	threonine
Tris	2-amino-2-hydroxymethyl-propan-1,3-diol
TUNEL	terminal transferase dUTP nick end labeling
Tyr	tyrosine
µg	microgram
µl	microliter
wt	wild type

1 INTRODUCTION

1.1 The immune system

The immune system of mammals is composed of a complex network of cells, characterized by dynamic communications and fast responses. Its main function is to protect the host against invasion by pathogenic organisms. Moreover, it has to eliminate malignant cells without damaging the surrounding healthy tissue.

The immune system is generally divided into two branches: The innate immune system, which provides a first line of defence and the more versatile adaptive immune system, which in addition endows increased protection against subsequent re-infection with the same pathogen (overview in Janeway, 2004). Lately, the actin cytoskeleton has been identified to be a key regulator in immune cell function and the underlying mechanisms have moved into the focus of immune regulation.

1.1.1 Innate immune system

The innate immune system is the evolutionary ancient branch of the immune system. Many of its components can be found in mammals as well as in insects, worms and plants. It is often referred to as the “non-specific” immune response since the same effector mechanisms are generated against an entire group of pathogens. This feature results in a fast and effective but rather unspecific response to pathogens.

The first line of defence is the endothelium of skin and mucosa. This physiological barrier protects the host by mechanical (tight junctions, air and liquid fluids) and chemical (pH, enzymes, peptides etc) as well as microbial mechanisms (e.g. flora of the gut).

If a pathogen breaches this barrier, it first faces the complement system. The complement system is comprised of serum proteins that can be activated by a biochemical cascade. In general, this cascade starts with the spontaneous cleavage of factor C3 (alternative mechanism of complement activation) and ends with the formation of a pore complex that integrates into the membrane of the target cell, leading to cytolysis. At the same time, small complement components attach to the membrane of the pathogen, marking it as foreign. This process is known as opsonization and involves either complement factors or antibodies (reviewed by Kohl, 2006).

Phagocytes, in particular polymorph-nucleated neutrophils, monocytes or macrophages take up pathogens easier when they are opsonized. These cells engulf large particles and digest them in vacuoles containing potent enzymes for protein and lipid degradation, called lysosomes.

Taken together, the innate immune system is acting at the earliest stages of infection and often effectively prevents the spreading of pathogens in the host. Many pathogens, however, have developed strategies that allow them to hide or escape from innate immune control. In this case, the innate response to infection sets the scene for the specialized functions of the adaptive immune system.

1.1.2 Adaptive immune system

The adaptive immune system is characterized by its ability to recognize foreign structures (antigens), unique to a given pathogen, and to develop an immune response directed against these targets. The adaptive immune system is cell-mediated which in turn requires a clonal expansion of the cells suitable for a specific pathogen, leading to a 4 - 7 days delay before the adaptive immune response can effectively act against a pathogen.

In contrast to the innate immune system, the adaptive immune system is capable of building up a memory. This is achieved by maintaining a few highly specific memory cells after an infection in the circulation. If the same pathogen infects the host a second time, these cells can rapidly multiply and protect the organism.

B and T lymphocytes are the main effector cells of the adaptive immunity. They derive from a common pluripotent precursor cell in the bone marrow (Lemischka et al., 1986). While B cells also mature in the bone marrow, T cell precursors migrate to the thymus, where they undergo differentiation through complex selection processes, before they are released as naïve T lymphocytes.

B cells are responsible for the humoral immunity that is based on the production of antibodies to specific antigens (Poljak, 1991). They recognize extracellular pathogens directly via their cell-surface bound immunoglobins. In contrast, T lymphocytes exclusively recognize peptide antigens that are presented in major histocompatibility (MHC) molecules (MHC restriction) (reviewed by Zinkernagel and Doherty, 1997). The receptor for this MHC-peptide complex is the T cell receptor (TCR) complex consisting of α,β-chain that and associated co-receptors, like CD3, CD4 or CD8. According to their co-receptor different T cell subclasses are discriminated that have distinct functions *in vivo*: Cytotoxic T cells (CTL) kill infected target cells directly. They express co-receptor CD8 that

recognizes endogenous or viral antigen peptides presented in MHC class I molecules (Gao et al., 1997). T helper cells on the other hand express co-receptor CD4; they deliver additional signals to other immune cells and thus modify immune responses. CD4 T cells recognize peptides from endocytosed extracellular pathogens presented in MHC class II molecules (Cammarota et al., 1992). Upon activation, T cells produce IL-2 and start to proliferate. Depending on their subset, they produce a variety of cytokines like IFN-γ, IL-4, IL-5, IL10 or TNF-α.

However, antigen contact alone is not sufficient to activate naïve T cells and a second, co-stimulatory signal is required (Croft and Dubey, 1997). The best-studied co-stimulatory molecules are the members of the B7 family, like CD80 or CD86 (Carreno and Collins, 2002). They interact with CD28 on the surface of T lymphocytes. These signals are exclusively provided by professional antigen presenting cells (APC) like dendritic cells, macrophages or B cells. Therefore, APCs are important regulators of the adaptive immunity.

1.1.3 Macrophages

Macrophages (greek: *macros* = large, *phagein* = eat) were first described by Elie Metchnikoff over a hundred years ago (Metchnikoff, 1891). These long-living cells originate from progenitors of the myeloid lineage in the bone marrow. Immature mononuclear cells, called monocytes, emigrate from the bone marrow into the blood, where they circulate for a short period. Monocytes are recruited to all tissues, especially to those strategically relevant to microbial invasions. It is only there that they mature to fully differentiated macrophages. According to their location different types of macrophages are discriminated: alveolar macrophages in the lung, Kupffer cells in the liver, osteoclasts in the bone, microglia cells in the neuronal tissue and histiocytes in the connective tissue.

Although macrophages display a heterogeneous cell population, the mechanisms by which they accomplish their functions is identical to all types. Thus, they are known overall as the mononuclear phagocytic system (MPS). Macrophages take part in innate as well as in the adaptive immune control and therefore are key regulators for the host defence.

Resting macrophages express few MHC class II molecules and almost no co-stimulatory molecules on their surface. Their main function is to migrate through the tissues and to engulf cell debris and opsonized pathogens in a process known as phagocytosis. The degradation of these particles occurs in acidic compartments inside the magrophages (phagosomes). Pattern recognition receptors (PRR) browse the ingested material for the presence of foreign structures. The PRR bind

to molecules common to a group of pathogens, e.g. LPS for gram-negative bacteria or double stranded RNA for viruses. Recognition of those pathogen-associated molecular patterns (PAMP) leads to the macrophage activation.

Upon activation, macrophages change their expression profile completely. Inflammatory cytokines are produced that can influence almost all cells of the immune system. Among those are IL-1, IL-6, IL-8, IL-12 and TNF-α. These cytokines lead to a systemic activation of the immune system. Additionally, tissue hormones like prostaglandins or leucotrienes get expressed that cause dilation of the small surrounding blood vessels. Consequently, endothelial cells express more adhesion molecules leading to an increase of leukocyte extravasation at the site of infection.

Reactive oxygen and nitrogen species that are produced by macrophages can damage the pathogens directly, displaying the potential of the innate immune response to act against invaders.

Moreover, expression of MHC class II molecules is induced and peptides generated in the lysosomes are presented on the surface of the macrophage. The expression of co-stimulatory receptors is up-regulated while the phagocytic activity is almost abolished, turning the macrophage into a professional antigen presenting cell that is equipped to present these antigens to naïve T cells and to induce an adaptive immune response.

Taken together, macrophages are key switches between innate and adaptive immune response and their proper regulation is a pre-requisite for an appropriate immune rection. Therefore, macrophages are interesting candidates to study the influence of proteins on immune functions.

1.2 The cytoskeleton

Many of the immune functions depend on active remodelling of cell shape, polarization or distribution of receptors and adaptor molecules on the cell surface. These structural reorganization processes are known to be controlled by the cytoskeleton, a dynamic structure found in all eukaryotes. It is composed of three distinct elements: actin microfilaments, microtubules and intermediate filaments. Microtubules are thought to form a polarized network allowing organelle and protein movement throughout the cell (Etienne-Manneville, 2004). Intermediate filaments are generally considered the most rigid component, responsible for the maintenance of the overall cell shape.

The actin cytoskeleton has been shown to be involved in a plethora of basic cellular activities, including cytokinesis (Sanger et al., 1977), endo- and exocytosis (Perrin et al., 1992), cell motility (Stossel, 1993), cell polarity and intracellular trafficking (Witke, 2004). Moreover, the unique importance of the actin cytoskeleton in immune cell function has recently come into focus since actin has been shown to be involved in immune cell migration and chemotaxis (reviewed by Lambrechts et al., 2004; Van Haastert and Devreotes, 2004), phagocytosis (Castellano et al., 2001), antigen presentation (Gordy et al., 2004; Stradal et al., 2006) and in the production of reactive oxygen and nitrogen species by macrophages and neutrophils (Webb et al., 2001; Su et al., 2005). During these immune cell functions, the actin cytoskeleton serves as a platform that integrates diverse signals from the cellular environment.

1.2.1 Actin

Actin is one of the most abundant proteins in eukaryotic cells with up to 5% of total protein. It is a 45 kDa protein, which in the cell exists in two forms, monomeric (G-actin) and polymeric (F-actin). Structural analysis revealed that the molecule consists of two lobes clasping an ATPase pocket (Kabsch et al., 1990). Each actin molecule can bind one molecule of ATP, which is hydrolyzed irreversibly to ADP + Pi after incorporation of the actin monomer into the filament. Thus, the ATPase activity serves as a timer, marking the age of an existing filament (Pollard, 1986). Actin monomers polymerize spontaneously at a suitable concentration of G-actin and salt in a head-to-tail fashion to form long helical filaments, whose ends are structurally and dynamically distinct. Although energy is not required for incorporation of actin monomers into the filaments, it can increase the rate of polymerization since ATP-bound actin is added faster to growing filaments than ADP-bound actin (Pollard, 1986). This difference in binding affinity leads to a polarization of the growing filament - the fast-growing end (barbed end) capped with ATP-actin, and the slow-growing end (pointed end) capped with ADP-actin.

Since ADP-actin has lower affinity than ATP-actin for the filament, ATP-actin monomers add on to the fast growing end of the filament while ADP-actin monomers are lost from the slow-growing end, in a process known as treadmilling (Fig. 1).

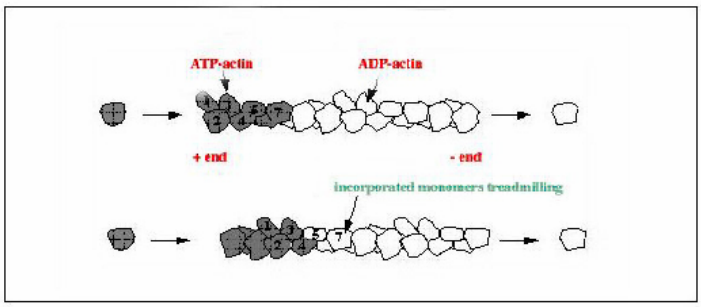

Figure 1: Actin filament treadmilling
ATP-actin monomers add to the fast growing (+)-end of actin filaments, while ADP-actin is released from the (-)-end. Over time ATP is hydrolysed and marks the filament as "old".

Actin forms filaments; however, it is not capable of regulating the length and three-dimensional structure of filaments independently. Moreover, there exist major discrepancies between the *in vitro* behaviour of purified actin and its behaviour inside living cells: First, the concentration of monomeric actin inside cells is about 100-fold higher than the critical concentration at which actin starts to polymerize. And second, the turnover of dynamic structures is up to 100fold faster (Theriot and Mitchison, 1991) inside cells than observed *in vitro*. This is possible because a broad range of cytosolic molecules - actin binding proteins - bind to actin and modify its polymerization, kinetic and structure.

1.2.2 Actin-binding proteins

Proteins that bind actin can modulate the actin cytoskeleton in many ways. They can control filament length, bundle and branch actin filaments or connect the scaffold to membranes (Ayscough, 1998). Thus, most actin-binding proteins are classified by their *in vivo* functions: proteins that nucleate filaments (Arp2/3 complex (Pollard et al., 2000)), cross-link filaments (like α-actinin or fimbrin), cap the free filament ends (like capG and capZ), sequester monomeric actin (like thymosin β4, profilin) and proteins that sever or disassemble actin filaments (like gelsolin, cofilin, actin depolymerizing factor (ADF)). These proteins ultimately convey signals to the actin cytoskeleton.

1.2.3 Actin depolymerizing factors

Actin depolymerizing factors are small (15-20 kDa) proteins that can bind to both monomeric and filamentous actin. ADF/cofilin proteins (AC) are evolutionary highly conserved molecules that are found throughout the animal kingdom as well as in plants. While yeast (Moon et al., 1993) and nematodes (Ono et al., 1999) have only one cofilin/ADF-like gene, some plants have evolved six to twelve ADF related genes (Maciver and Hussey, 2002; Feng et al., 2006). Mammals express three highly conserved genes termed n-cofilin for non-muscle cofilin or cofilin1

(Nishida et al., 1984), m-cofilin for muscle cofilin or cofilin2 (Abe et al., 1989) and ADF (Moriyama et al., 1990). In addition, related genes named coactosin (de Hostos et al., 1993) and twinfilin (Goode et al., 1998) have been also identified in mammals sharing sequence homology with the ADF domain. The present thesis will focus on the function of ADF and n-cofilin (hereafter referred to as cofilin) in murine macrophages.

1.2.3.1 AC Localization

AC appear to have multiple functions, as they show a complex association with monomeric and filamentous actin. The proteins localize to cellular regions with a high turnover of actin filaments (Bamburg and Bray, 1987), e.g. the leading edge of moving cells (Dawe et al., 2003) or the growth cones of neurons (Kuhn et al., 2000). On the other hand, AC contain a nuclear localization signal (NLS) close to the amino terminus and it has been shown that they translocate into the nucleus upon heat shock or DMSO treatment of cells (Abe et al., 1993). It has been speculated that this is a pathway to actively transport actin into the nucleus, where it has been shown to play a role in chromatin remodelling, mRNA processing and transcription (Vieu and Hernandez, 2006).

1.2.3.2 AC Activity

AC activity was discussed controversially until now. Cofilin/ADF binds to actin in a 1:1 fashion (Nishida et al., 1984), having a 100 fold higher affinity to ADP-actin than to ATP-actin (Carlier et al., 1997). The binding to old actin filaments is cooperative (Ressad et al., 1998), where one ADF/cofilin intercalates between two actin molecules (Renoult et al., 1999). Due to this binding, the helical rotation of the filament changes from -167° to -162° per actin molecule (McGough et al., 1997; Bamburg et al., 1999), which leads to a weakening of the actin-actin interactions. Thus, actin monomer depolymerization from the pointed end is enhanced 30fold. In addition, the twist increases the probability for the filament to break. This severing activity of ADF/cofilin generates new uncapped barbed ends that can serve as new sites of actin polymerization. Interestingly, these newly polymerized filaments are preferential sites for the formation of branches by the Arp2/3 complex (Ichetovkin et al., 2002). It has been shown that the activity of AC in combination with proteins that sequester actin monomers (profilins) enhances the actin treadmilling 125fold (Fig. 1 and (Didry et al., 1998)).

1.2.3.3 Regulation of AC activity

ADF/cofilin proteins are regulated in a precise temporal and spatial manner. Several mechanisms have been shown to regulate their activity: phosphorylation, pH, phosphoinositides and interactions with other proteins. This allows locally restricted activation of cofilin/ADF, while the bulk of proteins can remain inactive in the cytoplasma.

Phosphorylation:

The main switch to regulate ADF/cofilin activity is the phosphorylation on Ser3 (Fig. 2, (Moriyama et al., 1996)). Phosphorylated AC do not bind to actin (Morgan et al., 1993). At least four AC kinases have been described: LIM kinases 1 (Arber et al., 1998; Yang et al., 1998) and 2 (Sumi et al., 1999) (LIMK1 and LIMK2), testicular protein kinase 1 (Toshima et al., 2001a) and 2 (Toshima et al., 2001c) (TESK1/2). LIM kinases are ubiquitous and function downstream of the Rho-family GTPases. LIM kinases are activated through phosphorylation by the Rac- and Cdc42-activated kinase PAK, or by the Rho-associoted kinase (ROCK). Tes kinases were first described as testis specific, but are now known to be expressed in several tissues (Toshima et al., 2001b). TES kinase 1 is activated downstream of Rho, but independent of ROCK. Activation of Rho GTPases is linked to their translocation to the membrane, where they interact with cytoplasmatic domains of receptors and signalling complexes.

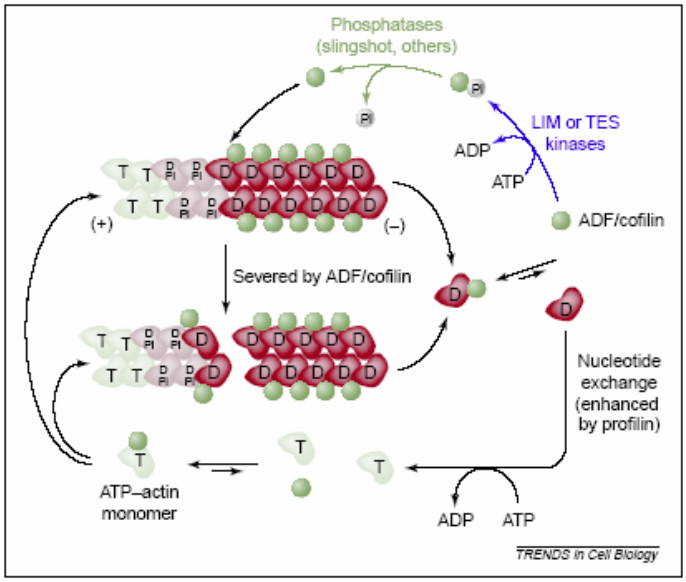

Figure 2: Biochemical activity and phosphoregulation of AC proteins
Actin treadmilling is enhanced by ADF/cofilin severing and depolymerizing activity. ADF/cofilin are inactivated through phosphorylation by LIM or TES kinases and their activity can be reconstituted through dephosphorylation by phosphateses like slingshot (taken from Bamburg and Wiggan, 2002).

The way dephosphorylation (activation) of AC proteins is regulated is less well understood. One mechanism appears to be the restriction of availability of the phosphorylated serine residue to phosphatases. It has been shown that the protein 14-3-3ζ, an isoform of a family of phosphoserine- and threonine-binding proteins, can sequester phosphorylated cofilin, thus protecting the phosphorylated serine from phosphatases.

Recently, a phosphatase named slingshot (SSH) has been identified that dephosphorylates cofilin *in vitro* and *in vivo* (Niwa et al., 2002). However, little is known about upstream regulators of SSH. In *drosophila* SSH has been found to act downstream of receptor-tyrosin kinase Sevenless (Rogers et al., 2005) and *in vitro* insulin signalling via phosphoinositide 3-kinase (PI3K) leads to SSH activation (Nishita et al., 2004). Besides SSH, several other phosphatases have been described to dephosporylate ADF/cofilin *in vitro* and *in vivo*, among those the conventional serine/threonin phosphatases type I, 2a and 2b (PP1, PP2A and PP2B) (Takuma et al., 1996; Meberg et al., 1998; Ambach et al., 2000), as well as a novel phosphatase called chronophin (Gohla et al., 2005).

Phosphoinositides:

Phosphoinositides (PI) are important secondary messengers for the regulation of the actin cytoskeleton (Yin and Janmey, 2003). The membrane-bound phosphatidylinositol (PI), phosphatidylinositol-4-monophosphate (PIP) and phosphatidylinositol-4,5-bisphosphate (PIP_2) can bind to AC in the region that forms the actin-binding domain. As a consequence binding of phosphoinositides inhibits actin-binding (Yonezawa et al., 1991) and inactives AC.

pH-Regulation:

The ability of actin depolymerizing factors to influence actin filament turnover is pH dependent *in vitro* (Yonezawa et al., 1985; Bernstein et al., 2000). F-actin is stabilized by ADF/cofilin in a slightly acidic environment (pH<6.8), whereas depolymerization is accelerated in a slightly basic milieu (pH>7.3). It has been suggested that this mechanism might play a role in proximity to membrane-integrated Na^+/H^+-antiporters, where large changes in pH can transiently occur (Bamburg, 1999). Nevertheless, conclusive evidence is missing that proves the significance of this pH dependence *in vivo*.

Accessory proteins:

Another way to modulate AC activity is the interaction with other proteins. Several proteins have been proposed to interact with ADF/cofilin.

Tropomyosin and ADF/cofilin compete for binding places on actin filaments (Bernstein and Bamburg, 1982). Presumably this mutually exclusive binding involves the change in actin filament twist by ADF/cofilin (McGough et al., 1997). Tropomyosin appears to be a physiological counterpart for AC (Ono and Ono, 2002) because this competition results in a division of the actin filament pool: one stable pool of actin-tropomyosin and a dynamic one with actin-AC interactions

(Cooper, 2002). This distinction is important for cell differentiation and polarity (DesMarais et al., 2002).

The actin interacting protein1 (Aip1) supports AC to further accelerate actin filament turnover (Okada et al., 1999). Aip1 has been described to interact with cofilin during actin depolymerization from the pointed end (Rodal et al., 1999), acting as a co-foactor of AC (Fujibuchi et al., 2005).

Cyclase associated protein (CAP or Srv2) was first described in yeast. It consists of three domains, of which the C-terminal one mediates the binding to G-actin (Freeman et al., 1995). Two reports suggest that CAP increases actin filament turnover by recycling cofilin from cofilin-ADP-Actin complexes and exchanging it with profilin (Moriyama and Yahara, 2002; Balcer et al., 2003).

1.2.3.4 ADF versus cofilin

At first glance, murine ADF and cofilin are very similar proteins. They show the same conserved genomic organization comprising four exons with the first exon encoding only the start methionine. The length of the following exons 2, 3 and 4 is identical and encode proteins of 146 amino acids. The coding regions of cofilin and ADF are 70% identical on the protein level, and biochemical characterization confirmed the F-actin binding and depolymerizing properties of both proteins (Vartiainen et al., 2002). Compared to cofilin, ADF is more potent to promote actin turnover and shows stronger pH dependence (Vartiainen et al., 2002; Yeoh et al., 2002). Given the molecular and biochemical similarities, it is conceivable that cofilin and ADF could be functionally equivalent *in vivo*, thus explaining why many publications do not discriminate between the different AC members.

However, there is evidence that AC have distinct roles *in vivo*. In mouse, ADF and cofilin are generally expressed with a reciprocal pattern. ADF is highly expressed in tissues that are rich in lining epithelia such as uterus, stomach and gut, while it is absent in T and B lymphocytes. Cofilin on the other hand is more abundant and shows its highest expression in lymphatic organs such as spleen, thymus and lymph nodes (Fig. 3, (Gurniak et al., 2005)).

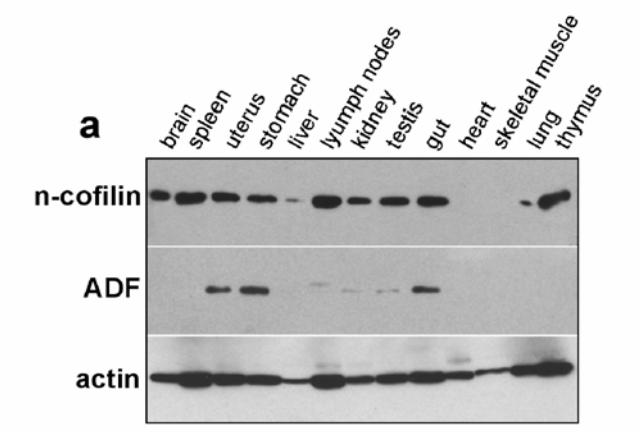

Figure 3: Tissue western blot for cofilin and ADF expression in mouse
Cofilin is expressed in a wide range of tissues, while ADF is restricted to the gastrointestinal tract, uterus, testis and kidney (taken from Gurniak et al., 2005).

The different phenotypes found in mutant mice further underline the differences between ADF and cofilin. Mice with a spontaneous autosomal recessive mutation, corneal disease-1 (*corn1*) that codes for ADF (Ikeda et al., 2003), develop a roughened opaque corneal surface accompanied by corneal stromal neovascularization and lymph angiogenesis (Smith et al., 1996; Cursiefen et al., 2005). Apart from this, they do not show any obvious phenotype.

In contrast, cofilin knockout mice die during embryonic development around day 10.5 (Gurniak et al., 2005). The main defects are observed in neural crest cell delamination and migration, affecting the development of neural crest derived tissues. In addition, it has been shown that cofilin is required for neuronal precursor cell proliferation and scattering. These defects result in a lack of neural tube closure in cofilin mutant embryos. Although ADF is over-expressed in mutant embryos, it can not compensate for the lack of cofilin (Gurniak et al., 2005).

1.2.3.5 ADF/cofilin in the immune system

The knowledge about the specific function of AC proteins in immune cells is very limited. Nevertheless, the importance of actin for immune cell function is widely accepted, thus it is likely that ADF/cofilin also contribute to their proper function. Lately, the use of antisense oligonucleotides and peptide homologues led to some insights about immune cell functions that are controlled by ADF/cofilin.

The group of Yvonne Samstag has studied the role of cofilin in T cells. In resting human T lymphocytes, the majority of cofilin is inactivated by phosphorylation at Ser3. Upon stimulation, cofilin is dephosphorylated, transiently interacts with the actin cytoskeleton and translocates from the cytosol into the nucleus (Samstag et al., 1994; Nebl et al., 1996). A PKC-Ras-MEK/PI3K-cascade transmits the activation signal from costimulation of TCR and costimulatory receptors, like CD2 or CD28, to the dephosphorylation of cofilin (Wabnitz et al., 2006); thus linking T cell stimulation to cytoskeletal rearrangement (Lee et al.,

2000). The functional importance of cofilin for T lymphocyte activation has been shown employing cell permeable peptides that block binding of cofilin to actin. In human T lymphocytes, these peptides impair the formation of the immunological synapse and inhibit the induction of T lymphocyte proliferation and cytokine production (Eibert et al., 2004).

In the human Jurkat T cell line, that has a different cofilin phosphorylation status than resting T cells, the activation of LIMK, and thus the deactivation of cofilin, is involved in chemotaxis induced by stromal cell derived factor 1 alpha (SDF-1α) (Nishita et al., 2002). Moreover, it was shown that the correct spatial and temporal activation of Slingshot and LIMK is crucial for directed cell migration (Nishita et al., 2005).

Interestingly, measles virus act on the PI3K pathway, leading to reduced phosphorylation levels of cofilin and proteins of the ERM family in human T lymphocytes. After contact with measles virus glycoprotein, T cells are impaired in cell spreading, polarization and CD3 clustering (Muller et al., 2006).

The role of cofilin in B cells has not been studied in detail yet. In superantigen-induced T cell-B cell conjugates, cofilin localizes in T cells, but not in the B cells, to the periphery of the immunological synapse (IS, (Eibert et al., 2004)). The mechanism of cofilin targeting to the IS has not been tested but likely occurs as a direct result of actin binding.

In macrophages, cofilin is up-regulated upon stimulation with LPS (Dax et al., 1998), thus indicating a role in inflammatory immune responses. The implication of cofilin in phagocytosis has been described with contradicting results: Using neutrophil-like HL-60 cells it has been shown that cofilin is dephosphorylated upon activation (Suzuki et al., 1995; Nagaishi et al., 1999a). However, this could not be confirmed employing macrophage-like U937 cells (Nagaishi et al., 1999b). Moreover, cofilin antisense oligonucleotides have been found to enhance phagocytosis and the production of nitric oxide (NO) in the J774.1 macrophage cell line (Adachi et al., 2002).

The involvement of cofilin in chemotaxis has been suggested in various settings. Upon recruitment of murine peritoneal exsudate cells towards alpha2M-proteinase complexes, LIMK is activated and subsequently phosphorylates cofilin (Misra et al., 2005). Using neutrophil-like HL-60 cells, Adachi et al. showed that cofilin has to be translocated to the plasma membrane before the cells can migrate towards an NO source (Adachi et al., 2000) and Riol-Blanco et al. suggested that cofilin determines the migratory speed in CCR7 dependent chemotaxis of dendritic cells (Riol-Blanco et al., 2005).

Taken together, the role of ADF and cofilin in the immune system has mainly been studied in lymphocytes while little is known about AC function in antigen presenting cells like macrophages and dendritic cells.

1.3 Aim of thesis

The aim of this thesis was to provide a detailed analysis of the actin depolymerizing factors ADF and cofilin in mouse macrophages and to study their function in these cells, using a genetic approach and gene inactivation in the mouse. Furthermore, I wanted to address the question if ADF and cofilin play distinct or redundant roles *in vivo*. This should be achieved by the use of specific AC antibodies and by the generation of a new transgenic mouse, in which cofilin can be replaced by ADF in a conditional manner.

Furthermore, additional interaction partners of ADF and cofilin should be identified using a proteomics approach that could further reveal the regulation and potentially novel cellular functions of these important proteins.

2 RESULTS

My results showed that cofilin is essential in macrophages to reorganize their actin cytoskeleton during cytoskinesis and migration as well as antigen presentation. Interestingly, phagocytosis was not impaired in cofilin null macrophages. On the contrary, ADF was not essential for all tested actin dependent processes such as proliferation, migration and phagocytosis. However, the morphology of $ADF^{-/-}$ macrophages was slightly altered, since cells appeared elongated and more polarized. This suggests that cofilin and ADF are not redundant proteins in macrophages. Evidence that support this hypothesis was found in purified ADF/cofilin complexes from different tissues. Some interaction partners, like CAP1, exclusively showed an affinity for cofilin, whereas other could be found in both complexes. Additionally, the purification of several nuclear proteins argues for a yet unknown function of AC proteins in the nucleus.

The following chapters of the thesis are divided as follows. Chapter 2.1 focuses on ADF and cofilin expression in wild type cells, while chapter 2.2 describes the different approaches to generate ADF and cofilin null macrophages. The characterization of these mutant bone marrow cultures is the topic of chapter 2.3, whereas chapter 2.4 concerns the functionality of mutant macrophages.

The last two chapters (2.5 and 2.6) present experiments I carried out to further investigate similarities and differences between ADF and cofilin using a conditional replacement of cofilin by ADF in the mouse, as well as biochemical studies addressing the binding partners of ADF and cofilin.

2.1 Role of ADF/cofilin in murine macrophages

2.1.1 Cofilin and ADF are expressed in cells of the myeloid lineage

Cofilin is expressed in a variety of tissues, while ADF is mainly expressed in tissues with a lining endothelia (see Fig. 3, (Gurniak et al., 2005)). For the present project it was crucial to determine the precise expression of ADF and cofilin in cells of myeloid origin, in particular, in macrophages. For this, different cell types of the myeloid lineage were isolated and tested by Western blotting for the levels of ADF and cofilin (Fig. 4).

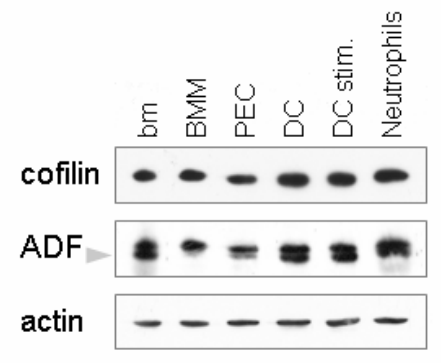

Figure 4: Expression of ADF and cofilin in cells of the myeloid lineage
Total lysates of different cell types (bm: bone marrow, BMM: bone marrow derived macrophages, PEC: peritoneal exsudate cells, DC: dendritic cells, stim: teated with LPS for 24hrs and neutrophils) were analysed by Western blotting for the levels of cofilin and ADF proteins. The lower band in the ADF blot is the actual ADF signal, whereas the upper band remained from the previous cofilin probing. Actin was used as loading control.

Cofilin is expressed in all cells of myeloid origin, with no major differences in the expression levels. Contrarily, ADF is expressed at appreciable levels in total bone marrow, dendritic cells and neutrophils, while in macrophages ADF seemed to be down-regulated during their differentiation, as suggested by rather low levels of expression in bone marrow derived macrophages and peritoneal exsudate cells (PEC).

To determine the absolute amount and the ratio of ADF/cofilin in macrophages, I performed quantitative Western blots using recombinant GST-fusion proteins as a standard (Fig. 5).

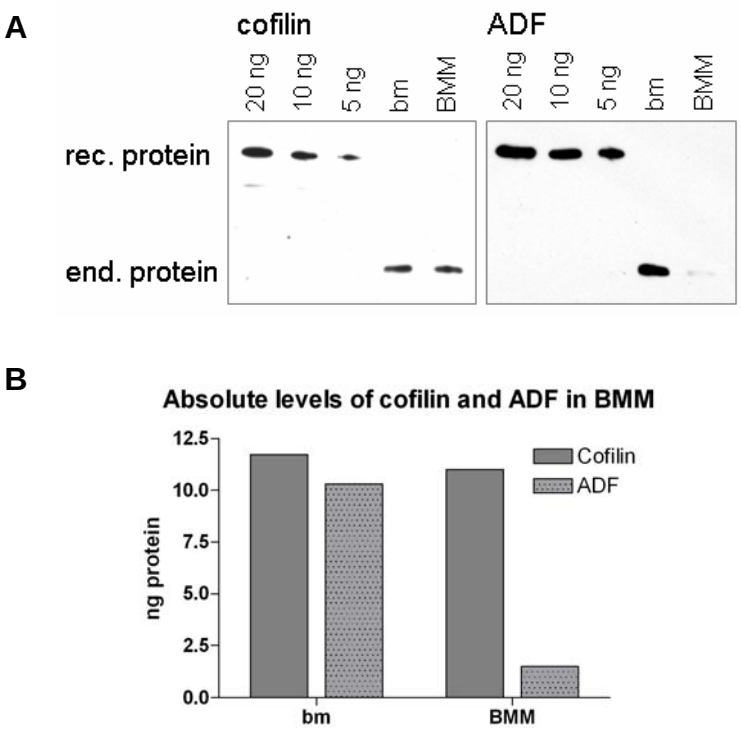

Figure 5: Comparison of ADF and cofilin expression levels in bm and BMM
A) 20 μg of bm (bone marrow) and BMM (bone marrow derived macrophages) lysates were loaded on a western blot for ADF/cofilin with different amounts of the respective GST-fusion protein. A program developed in the lab by H.Stöffler, called Radames, was used to evaluate the peak intensities and thus to determine the expression levels of ADF and cofilin.
B) Densiometric evaluation of ADF and cofilin protein levels.

In total murine bone marrow ADF and cofilin was found at comparable levels. In bone marrow derived macrophages cofilin expression exceeded ADF expression almost eight-fold. This difference seems to be due to a down-regulation of ADF upon adherence of differentiating macrophages. As shown total bone marrow cells and neutrophils that are directly purified from the bm, or dendritic cells, which grow in suspension, express much higher levels of ADF than adherent macrophages.

Consistently with these data, mRNA expression profiles of murine macrophages, mast cells, osteoblasts and osteoclasts generated in the FANTOM project (D. Hume in collaboration with the Genomics Institute of the Novartis Research Foundation) showed that ADF (destrin) RNA is expressed comparatively low in bone marrow derived macrophages compared to cofilin (Fig. 6).

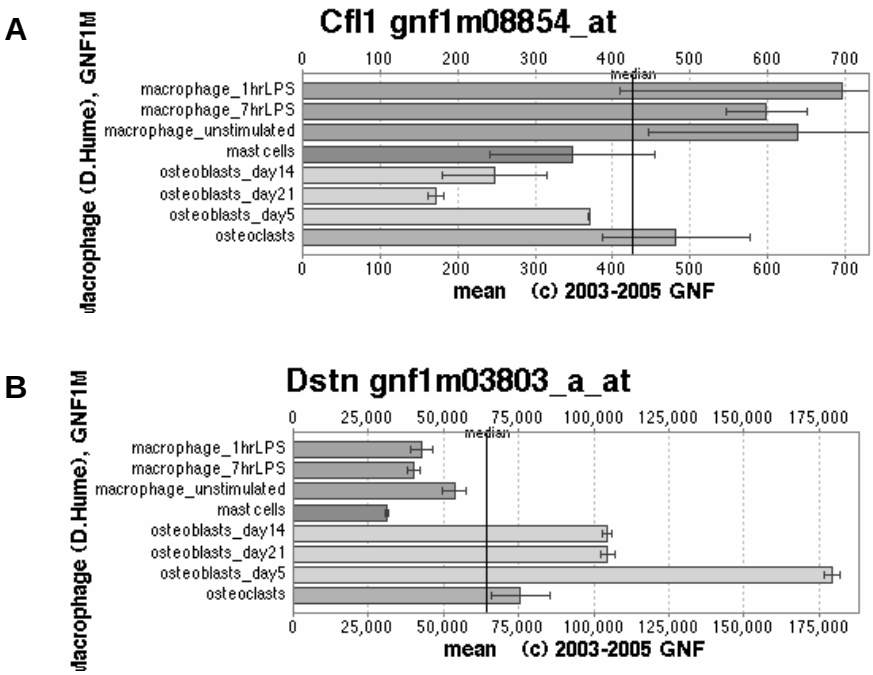

Figure 6: Gene expression data from the FANTOM project
RNA levels of cofilin (A) and ADF/destrin (B) were determined using Affymetrix microarrays (data taken from Genomics Institute of the Novartis Research Foundation in collaboration with D. Hume (http://symatlas.gnf.org/SymAtlas/ or http://www.macrophages.com)).

2.1.2 Subcellular localization of ADF and cofilin in murine macrophages

In general, AC proteins have been shown to localize in cells to regions with a high turnover of actin filaments (Bamburg and Bray, 1987), namely lamellipodia or growth cones in neurons (Kuhn et al., 2000). We therefore wanted to investigate whether the location of ADF and cofilin protein in macrophages also correlated with dynamic structures.

For the available antibody for cofilin I had to establish a protocol in order to make it work in immunofluorescence. Briefly, the cells were fixed with 15% picric acid/4% PFA followed by several stringent extractions. The best anti-cofilin antibody was the affinity purified rabbit antibody KG40. This protocol interfered with phalloidin staining for F-actin, a problem, which I resolved by using instead the actin antibody (C-4). Under these conditions, we expected that the C-4 staining mostly represents F-actin, since most monomeric actin (G-actin) is washed out of the cells (Fig. 7).

The ADF antibody (GV13) could be used with a standard PFA fixation protocol and in this case actin was visualized with phalloidin.

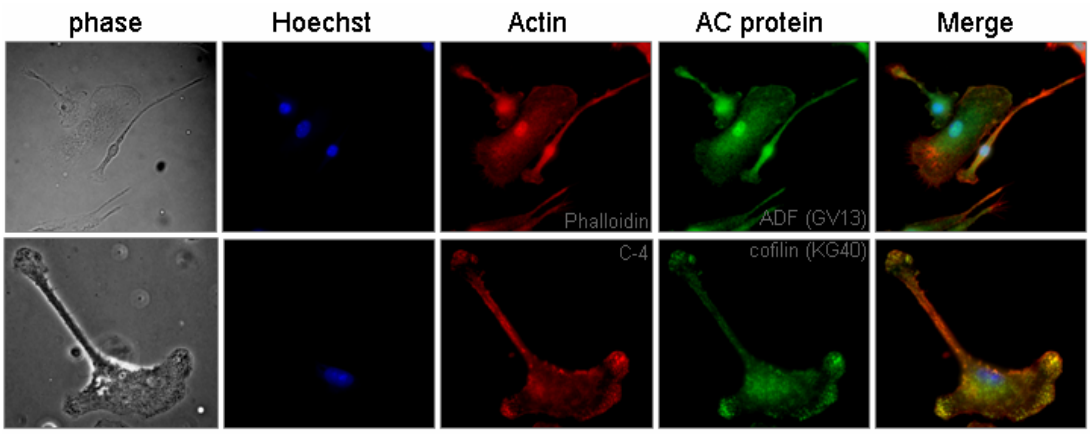

Figure 7: ADF and cofilin can be detected in macrophages using specific antibodies
In BMM, nuclei were visualized with Hoechst; actin and AC proteins were detected with specific antibodies (KG40 and GV13) and phalloidin. The overlay shows a high degree of co-localization of AC proteins with the actin staining. The KG40 antibody recognizes not only cofilin1 but also the muscle isoform cofilin2; however, the amount of cofilin2 is negligible in macrophages (data not shown).

Both, cofilin as well as ADF strongly co-localized with F-actin rich structures. To better examine the specific localization of AC proteins, we performed microscopical analysis at high resolution (Fig. 8).

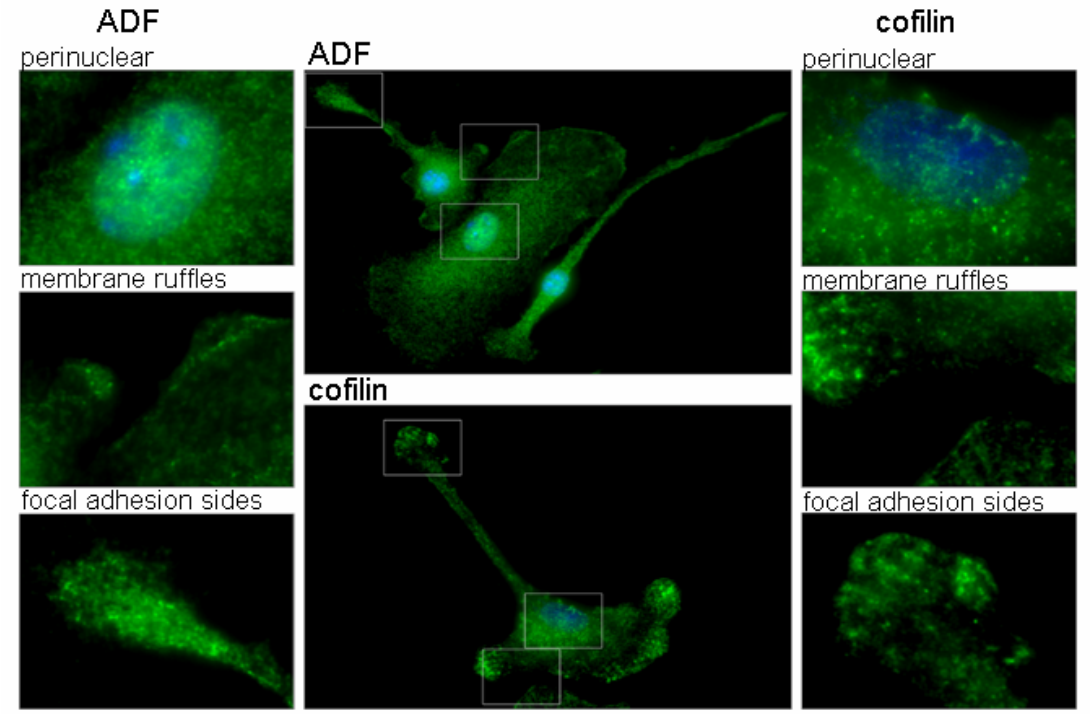

Figure 8: Localization of ADF and cofilin to the leading edge, nucleus and focal adhesions
BMM were fixed and stained with antibodies for ADF (GV-13) and cofilin (KG40). The pictures show the accumulation of the AC proteins in the perinuclear region (DNA visualized with Hoechst), in membrane ruffles and at sites of focal adhesion.

In summary, cofilin and ADF were found enriched in regions at the cell membrane with a high turnover of actin filaments also in macrophages. Both proteins co-localized with F-actin in membrane ruffles and focal adhesions. Diffusely distributed throughout the entire cytoplasma of the cells, AC proteins can be spotted with significant accumulation in the perinuclear region.

2.2 Deletion of ADF and cofilin in murine macrophages

Loss of function studies have proven to be a powerful tool to study the *in vivo* functions of a protein. In the following, I will present the strategy on how I deleted ADF and cofilin in macrophages.

2.2.1 The conventional ADF knockout is viable

The ADF knockout mouse generated in our laboratory and generously provided by C. Gurniak is viable. Consistent with published data on a natural ADF mouse mutant (Smith et al., 1996; Wang et al., 2001), our ADF knockout mouse does not show any gross morphological phenotype, apart from a hyper-proliferation of the cornea.

The ADF knockout mouse was generated by a knock-in of the lacZ cDNA into the second exon of ADF, thus abolishing the expression of a functional ADF protein (Fig. 9). No ADF protein can be detected in this mutant mouse. This ADF knockout mouse was used in the following studies to culture ADF null bone marrow derived macrophages.

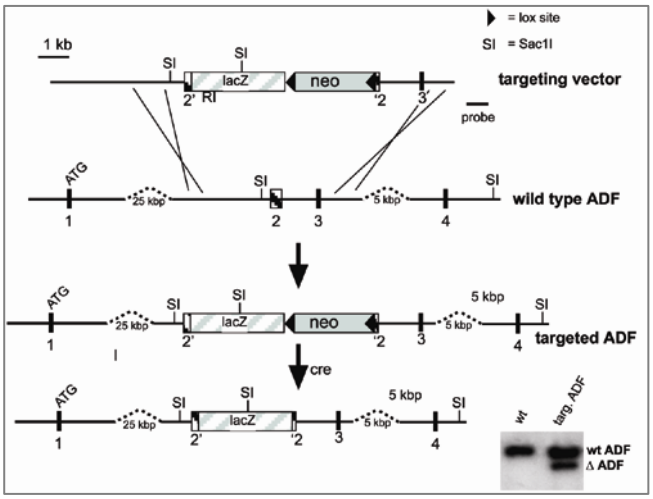

Figure 9: Targeting strategy of the ADF locus
A lacZ gene was recombined into the second exon of ADF, thus abolishing the expression of ADF protein. The genotype of mice carrying the mutant allele was confirmed by Southern blot using an external probe (see insert).

2.2.2 Use of a conditional mouse mutant to delete cofilin in macrophages

In mice the complete knockout of cofilin is embryonically lethal and therefore it is not possible to investigate the role of cofilin in macrophages using these knockout mice (Gurniak et al., 2005). However, conditional cofilin mutant mice generated by C. Gurniak were kindly provided to specifically delete cofilin in macrophages (Fig. 10). The development of the conditional Cre/loxP system (Sauer and Henderson, 1988) allows to delete the gene of interest that in a first step is flanked by two short sequences (loxP sites). These are recognized and excised by the recombinase Cre. Today an entire zoo of mouse strains is available that express Cre-recombinase in a tissue- or cell-type specific manner. In a first strategy, I wanted to create a macrophage specific knockout model for cofilin by crossing the conditional cofilin mouse with a mouse expressing Cre-recombinase under a macrophage specific promoter.

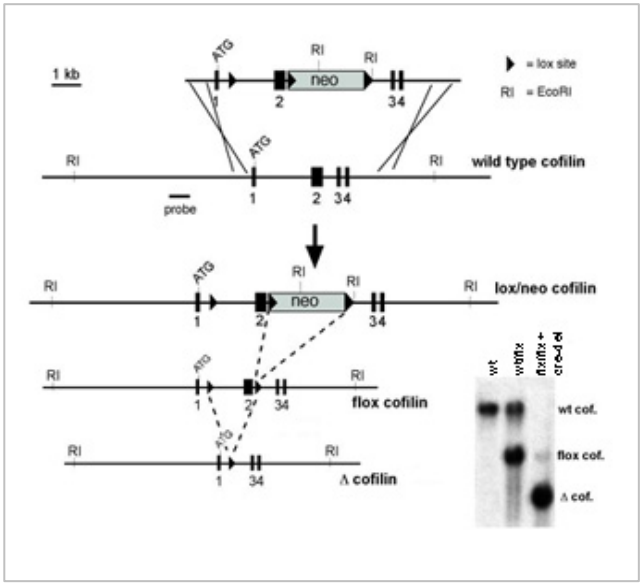

Figure 10: Targeting strategy of the cofilin locus
In the conditional cofilin mouse, the second exon of the cofilin gene was flanked by two loxP sites. Upon Cre recombinase expression this region is excised, resulting in an abolished cofilin expression. The genotype of mice carrying conditional (flox) vs. a deleted (Δ) allele can be detected by Southern blot using an external probe (see insert, here shown for NestinCre deletion).

2.2.3 Macrophage specific deletion of cofilin using the LysMCre strain

Lysozyme M (LysM) is highly expressed in myelomonocytic cells. Thus, its promoter is a good candidate to control Cre-recombinase expression in macrophages and granulocytes (Faust et al., 2000).

Clausen et al. generated a mouse strain that expressed the recombinase Cre under the control of the lysozyme M promoter (Clausen et al., 1999). The authors showed that double mutant mice harbouring both the LysMCre alleles and one copy of a loxP-flanked target gene had a deletion efficiency of 83-98% in macrophages and granulocytes.

I therefore chose the LysMCre mouse to generate macrophages lacking cofilin and crossed the LysMCre strain with cofilin conditional mice to obtain LysMCre/ cof^{flx}/cof^{flx} mice. However, in contrast to the published data, we observed in our system a greater variability of deletion rates in bone marrow derived macrophages, ranging between 20 and 50% on the protein level (Fig 11).

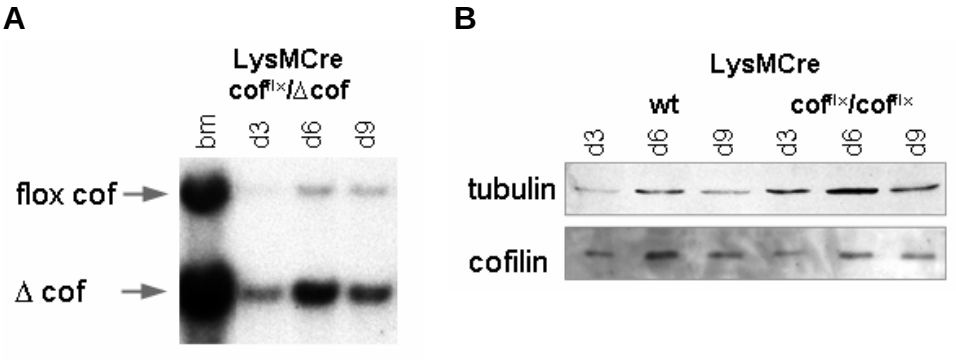

Figure 11: Cofilin deletion under the control of LysMCre in macrophages
Bm of LysMCre wt/cof^{flx} and cof^{flx}/cof^{flx} macrophages was taken into culture. Deletion rates were assessed by Southern blot (A) on day 3, 6 and 9 and by Western blot (B). Cofilin protein levels were detected in mutant vs. wild type cultures on indicated days of culture. Tubulin served as a control.

Such variations might depend on the recombined locus and a similar observation was made in a study using LysM-EYFP showing that “a comparison of individual lysozyme ancestry mice of identical genotype revealed surprisingly large variations in the proportions of EYFP labeled cells in the HSC and B cell compartments” (Ye et al., 2003). Unfortunately, the variations in deletion rates for the cofilin locus were insufficient for my planned studies; why I turned to a different Cre-recombinase expressing mouse strain.

2.2.4 Macrophage specific deletion of cofilin using the CD11bCre strain

CD11b and CD18 together build the Mac-1 integrin heterodimer, an adhesion molecule that is commonly used as a cell surface marker for macrophages. CD11b is up-regulated during myeloid differentiation, reaching its highest expression in mature monocytes, macrophages and neutrophils (Beller et al., 1982; Rosmarin et al., 1989). A CD11bCre mouse mutant was generated by Dr. G. Kollias and generously provided by Dr. M. Pasparakis. According to a recent manuscript, CD11bCre is active in peritoneal macrophages and microglia, whereas no activity could be detected in neurons and astrocytes (Boillee et al., 2006).
I crossed this CD11bCre strain with the cofilin conditional mice, but in my hands, no deletion of cofilin could be detected in bone marrow derived macrophages (Fig. 12).

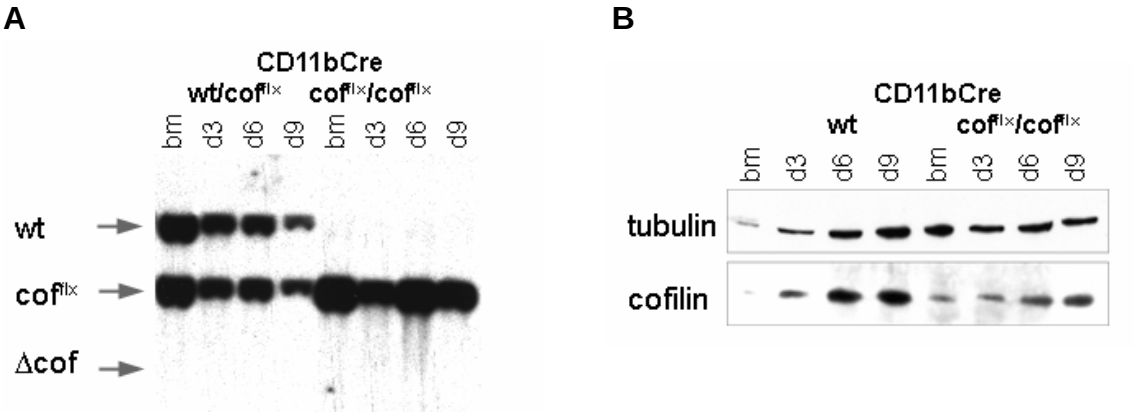

Figure 12: Cofilin deletion does not occur in CD11bCre macrophages
Bm of CD11bCre wt/cof^{flx} and cof^{flx}/cof^{flx} macrophages was taken into culture. Deletion rates were assessed by Southern blot (A) on day 0, 3, 6 and 9 and by Western blot (B). Cell lysates were analyzed for the presence of cofilin, ADF, actin and tubulin on indicated days of culture.

2.2.5 Macrophage specific deletion of cofilin using the Mx1Cre strain

We reasoned that the Mx1Cre system could be a better system to induce cofilin in macrophages. It uses the inducible promoter of the murine Mx1 gene (Hug et al., 1988) to drive expression of the Cre-recombinase transgene. The Mx1 promoter can be transiently activated in many tissues upon application of interferon α (IFN-α) or IFN-β (Staeheli et al., 1986; Sen and Ransohoff, 1993) or of synthetic double-stranded RNA (polyinosinic-polycytidylic acid (polyI:C)) (de Clercq, 1980; Finkelman et al., 1991). PolyI:C mimics a viral infection, during which

an endogenous IFN typeI response is established, thus inducing Mx1 promotor activity.

According to Kühn et al. three polyI:C injections (250 μg i.p.) at a 2-day interval resulted in 100% deletion of the target gene was observed in the liver, 84% in the spleen and low rates in other tissues (Kuhn et al., 1995). Background recombination was also observed in non-treated mice, probably due to endogenous IFN production in these mice, thus making it necessary to use Mx1Cre transgene carrying mice as control animals in the experiments.

The deletion rate in macrophages and bone marrow had not been addressed in the paper, however Jin et al. showed that Mx1 is expressed in macrophages (Jin et al., 1998) and should induce recombination in the bone marrow upon polyI:C injection.

Recently Wells et al. described a Rac1 knockout in bone marrow derived macrophages, which they generated by sequential injections of polyI:C (similar to those described by Kuhn et al.) prior to bone marrow harvest (Wells et al., 2004). Using this approach they obtained deletion rates of 90% in the bone marrow that persisted for 3 month after the last polyI:C injection.

For cofilin, I had to work out a different injection scheme, since several administrations of polyI:C resulted in the death of the animals. Most likely, the deletion of cofilin in the liver and other organs affects vital functions, since *post mortem* analysis of mutant mice suggested systemic organ failure.

In my hands an injection protocol based on a single injection of 300 μg polyI:C i.p. 24 hours prior to bone marrow harvest yielded the best results (Fig. 13).

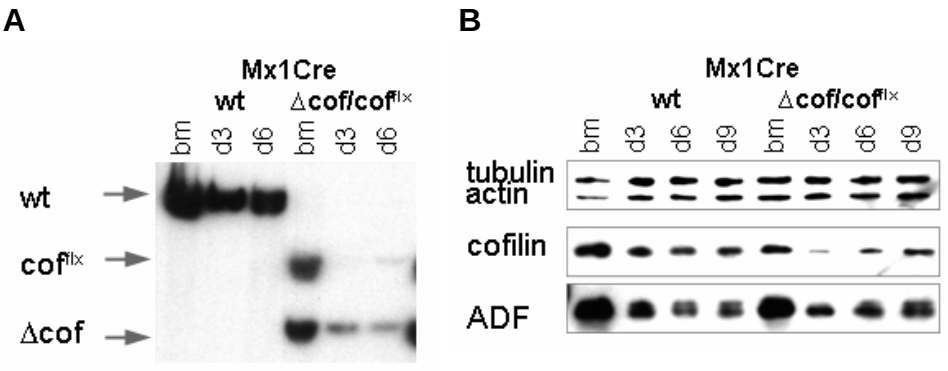

Figure 13: Cofilin deletion upon Mx1Cre induction in macrophages
Bm of Mx1Cre wt and Δcof/cof^{flx} macrophages was taken into culture 24 hours after polyI:C treatment of mice. Deletion rates were assessed by Southern blot (A) on day 0, 3 and 6 and by Western blot (B). Cell lysates were analyzed for the presence of cofilin, ADF, actin and tubulin on indicated days after polyI:C treatment.

As expected, Mx1Cre activity is just increasing after 24 hours and cofilin deletion is negligibly in the bone marrow, as it is in the entire organism. In FACS analysis, normal proportions of cells expressing CD11b, Gr-1, Cd1d, CD43, CD19 and B220 can be found (data not shown). However, on day 3 of culture, the deletion of cofilin is almost complete (>90%) in adherent cells and protein expression reduced to 5-10%. At later time points cofilin levels increase again in the cultures, most likely due to the competition of cells that have escaped deletion in the bone marrow and start overgrowing the mutant cells. At day 9 of culture significant contribution of escaper cells was observed.

I therefore had to compromise between a good representation of mutant cells and sufficient time for differentiation. Consequently, all following experiments were performed with macrophages on day 6 of culture, at which the cells display a macrophage-like phenotype, as displayed by their CD11b/Gr-1 expression profiles in FACS analysis (data not shown) and the significant expression of CapG protein (Fig. 17).

2.2.6 *In vitro* deletion of cofilin using HTNC, a transducible Cre-recombinase

To complement the *in vivo* deletion using Mx1Cre, I also set-up an *in vitro* model to delete cofilin in macrophages. The rational of this approach was to culture bone marrow derived macrophages carrying a conditional cofilin allele and then induce recombination in cultures by adding a cell permeable Cre-recombinase. In this process, known as transduction, Cre-recombinase is used that was fused to the HIV-Tat peptide combined with a nuclear localization signal and a His-tag for purification (HTNC) (Fig. 14, (Peitz et al., 2002)).

Figure 14: Schematic structure of recombinant HTNC recombinase.

HTNC was produced in *E. coli* and purified by FPLC technology (see material and methods). We treated macrophage cultures carrying two floxed cofilin alleles on day 4 for 6 hours with 4 μM HTNC in serum-free media. 24 hours after the treatment (day 1) genomic DNA was prepared and the protein level of cofilin in cell lysates was followed by Western blot on the subsequent days (Fig. 15).

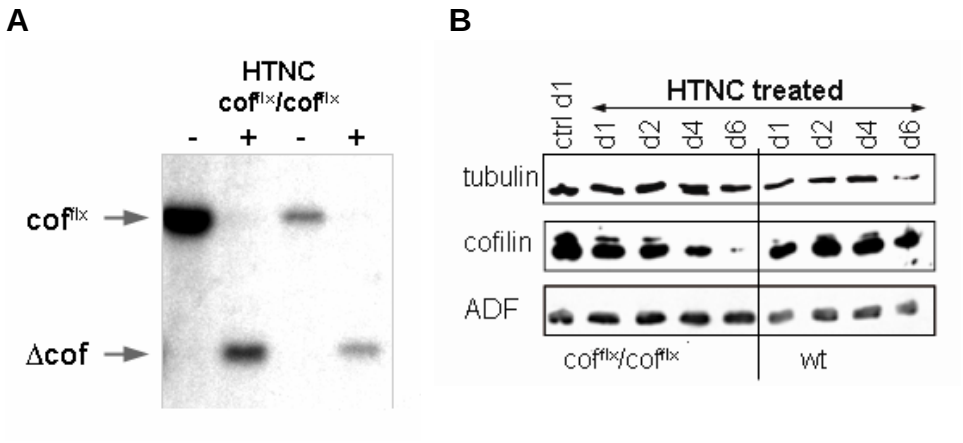

Figure 15: Cofilin deletion upon HTNC treatment of macrophages
A) Cofilin Southern blot of $cof^{flx/flx}$ macrophages 24 hours after mock(-) or HTNC(+) treatment (4 μM). B) Western blot: lysates of cofilin conditional and C57Bl6/J macrophages were probed for cofilin, ADF and tubulin on indicated days after HTNC treatment.

Using this approach, I could show that deletion occurred within 24 hours after HTNC treatment accompanied by a significant reduction of cofilin protein after 4-6 days.

The HTNC deletion allowed me to estimate the half-life of the cofilin in bone marrow derived macrophages and thus to better understand the kinetics of cofilin protein regulation. I considered the time point of HTNC addition as t_0 and followed cofilin protein levels on subsequent days by Western blotting (Fig. 11). Cofilin peak intensity was normalized using the measured peak intensity of tubulin. Ratios from control and treated macrophages were plotted on a semi-logarithmic scale. The half-life of cofilin was determined graphically; as it is the time, it takes before only half of the protein pool for that particular protein is left (Fig. 16).

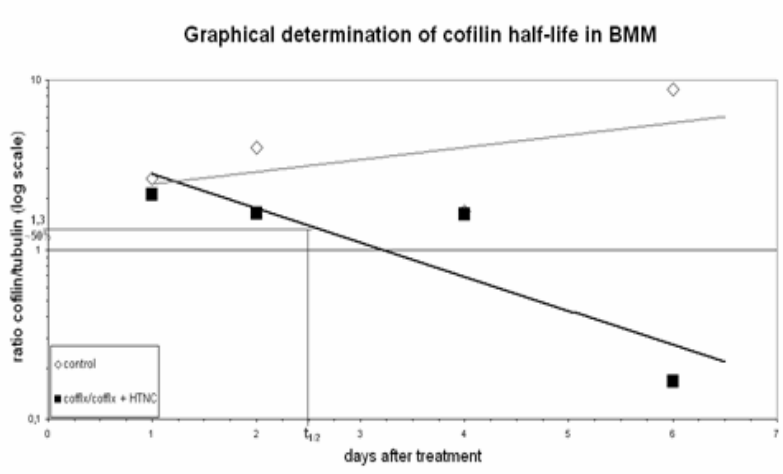

Figure 16: Graphical determination of cofilin half-life in BMM
Protein samples of cofilin conditional and wt macrophages treated with HTNC were prepared at indicated time points and protein levels were determined by Western blotting. Peak intensities of cofilin were normalized using the respective tubulin peak intensity. Cofilin/tubulin ratios were plotted against the time and cofilin half-life was assessed graphically.

Graphical evaluation HTNC induced cofilin reduction lead to the result that the half-life of cofilin is about 60 hours in bone marrow derived macrophages. This is in concordance with the observation of cofilin reduction in other systems, like the Mx1Cre induced deletion. Using the Mx1Cre system, I showed that cofilin is significantly reduced four days after polyI:C injection. However, the excision of the floxed allele is delayed in the model and occurs at some point within the first 24 hours after polyI:C injection: This is due to the fact that Mx1Cre has to be induced and expressed before it can act on the genome.

2.2.7 Efficacy of different approaches to delete cofilin in macrophages

The table below summarizes the results I obtained using the different approaches to delete ADF and cofilin in bone marrow derived macrophages:

Table 1: List of approaches used to delete AC proteins in macrophages

AC mutation	Cre-recombinase	Deletion efficiency	Deletion
ADF$^{-/-}$		100%	*in vivo*
cofilin conditional	**Lysozyme M**	20-50% in bm/BMM	*in vivo*
cofilin conditional	**CD11b**	0% in bm/BMM	*in vivo*
cofilin conditional	**Mx1**	Depends on injection protocol and time point, up to 90%	*in vivo* or in culture
cofilin conditional	**HTNC**	90%	in culture

The different deletion protocols highlight potential problems of certain “macrophage specific Cre-lines and the general problem of using conditional mutagenesis in hematopoietic cells for essential proteins such as cofilin. The Mx1Cre system offered the best compromise and allowed us to generate cofilin mutant macrophages suitable for further analysis.

If not mentioned otherwise the following experiments were performed with mice of the following genotypes: ADF$^{-/-}$, Mx1Cre cofilin conditional (from here on referred to as Mx1Cre cof^{flx}/cof^{flx} or cof$^{-/-}$). If required the double mutant ADF$^{-/-}$. Mx1Cre cof^{flx}/cof^{flx} was included in certain experiments. For the interpretation of the following results one has to keep in mind that the deletion rate in Mx1Cre cofilin conditional cultures usually was around 80-90% and was controlled in each experiment by Western blot.

2.3 Role of ADF/cofilin in bm cultures

2.3.1 ADF/cofilin deletion does not affect the expression other actin binding proteins

Redundancy is a widespread strategy to counteract a mutation in an essential gene. In protein families, the effect of a deletion sometimes only becomes detectable, when several proteins of a family are depleted.

It is also conceivable that the deletion of a protein results in the up-regulation of proteins that have similar activities. Thus, I tested if the deletion of ADF and cofilin led to the up-regulation of other related actin binding proteins (Fig. 17).

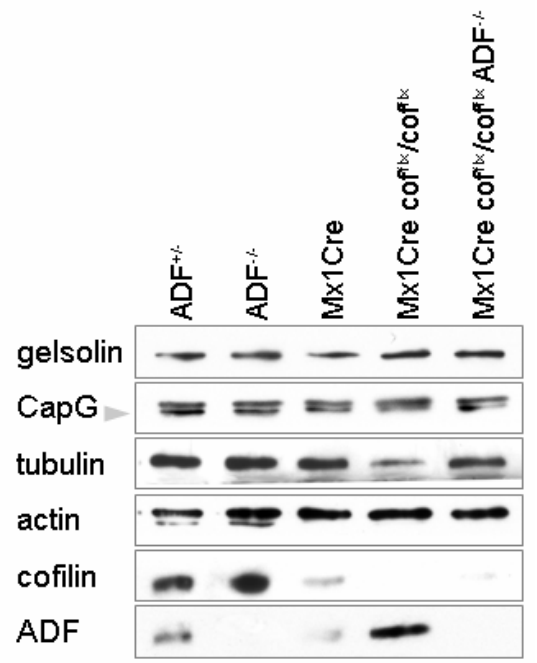

Figure 17: Actin binding proteins in bone marrow macrophages
BMM of mutant mice were analyzed by Western blotting for the presence of gelsolin, CapG, tubulin, actin, cofilin and ADF.

The expression of neither gelsolin nor CapG was altered by the depletion in AC mutants. This is remarkable as gelsolin has very similar biochemical properties as ADF and cofilin and CapG is a very abundant protein in macrophages required for actin dependent processes (Witke et al., 2001).

However, ADF is induced upon cofilin deletion, suggesting a mechanism by which the cell tries to counteract the loss of actin depolymerizing factor. The same is true in the case of a depletion of ADF, upon which cofilin is somewhat induced.

Interestingly, not even the depletion of both ADF and cofilin alters the expression of any of the tested proteins, thus indicating that ADF and cofilin are part of a separate pathway, which does not cross-talk to other actin binding proteins.

2.3.2 Morphology of macrophages lacking ADF and cofilin

Cell shape is largely determined by the re-arrangement of the actin cytoskeleton. Consequently, I first analyzed the overall morphology of macrophages lacking ADF/cofilin.

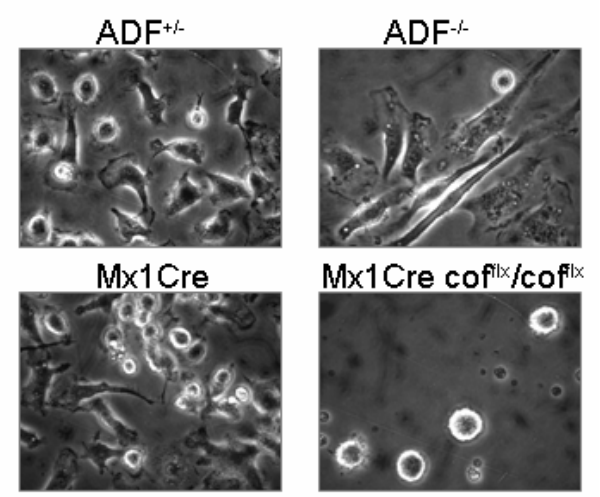

Figure 18: Morphology of BMM on day 6 of culture
BMM were cultivated in the presence of M-CSF; pictures were taken under phase contrast microscope with a digital camera.

Microscopic inspection of bone marrow cultures using phase contrast showed that compared to control macrophages, $ADF^{-/-}$ BMM were more elongated, while Mx1Cre cof^{flx}/cof^{flx} cultures mostly consisted of round cells (Fig. 18).

Round cell morphology was also observed in BMM cultured from LysMCre and in cultures, where cofilin was deleted by treatment with HTNC (data not shown).

2.3.2.1 Electron microscopy of cofilin mutant macrophages

To better analyze the morphology of macrophages lacking cofilin, we performed scanning electron microscopy (SEM, Fig. 19).

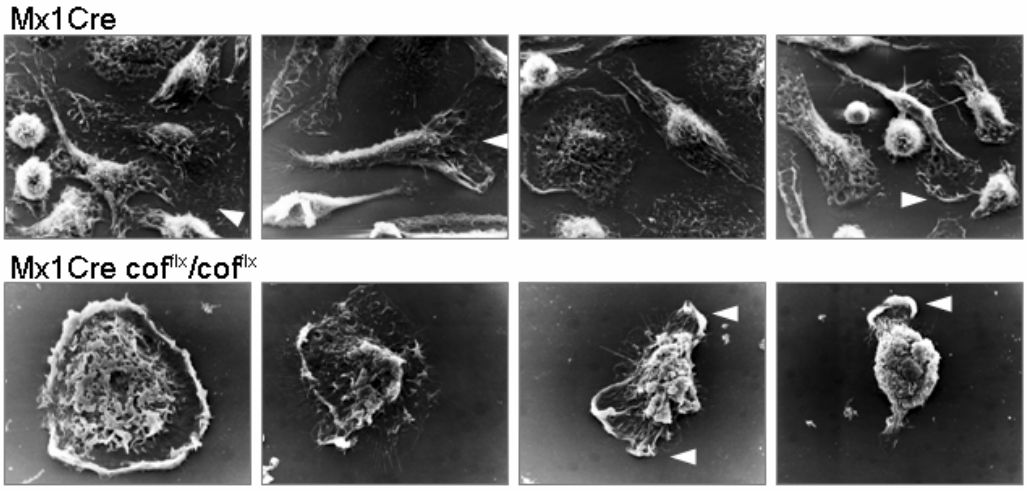

Figure 19: Scanning electron microscopy on BMM
On day 6 of culture BMM were fixed in glutharaldehyde and are subsequently dehydrated. Gold spattering allows analysis with the electron microscope. Arrowheads indicated lamellipodia. All pictures were taken at a magnification of 5000x.

Wild type macrophages showed the expected diversity in morphology and shape. Both, pancake-like flat cells and polarized migrating cells with a defined leading edge and a tail can be found. The small fraction of round cells are likely to undergo cell division, as it is essential for the cell to reduce substrate contact prior to cytokines. Furthermore, the surface of wild type macrophages appears thin and covered by membrane ruffles.

Instead, in Mx1Cre cofilin conditional cultures the large majority of cells showed an increased cell elevation with an apparently thick and rigid cell cortex. Instead of even membrane ruffling the mutant cells showed exaggerated lamellipodia (see arrowheads) or pseudopodia. Rarely polarized cells were observed. In summary, macrophages lacking cofilin seem to have a very rigid cell shape pointing to a lack of cytoskeletal dynamics.

2.3.3 Use of ADF/cofilin antibodies to discriminate mutant and wild type BMM

To discriminate between knockout and wild type macrophages in the mixed culture of Mx1Cre cof^{flx}/cof^{flx} macrophages, I used immunofluorescent labeling with ADF/cofilin specific antibodies (described in chapter 2.1.2).

In order to test my hypothesis that the alterations observed in the morphology and appearance of the macrophages were due to impaired F-actin turnover, I stained the macrophages for actin visualizing the structure and appearance of the actin cytoskeleton in the cells (Fig. 20).

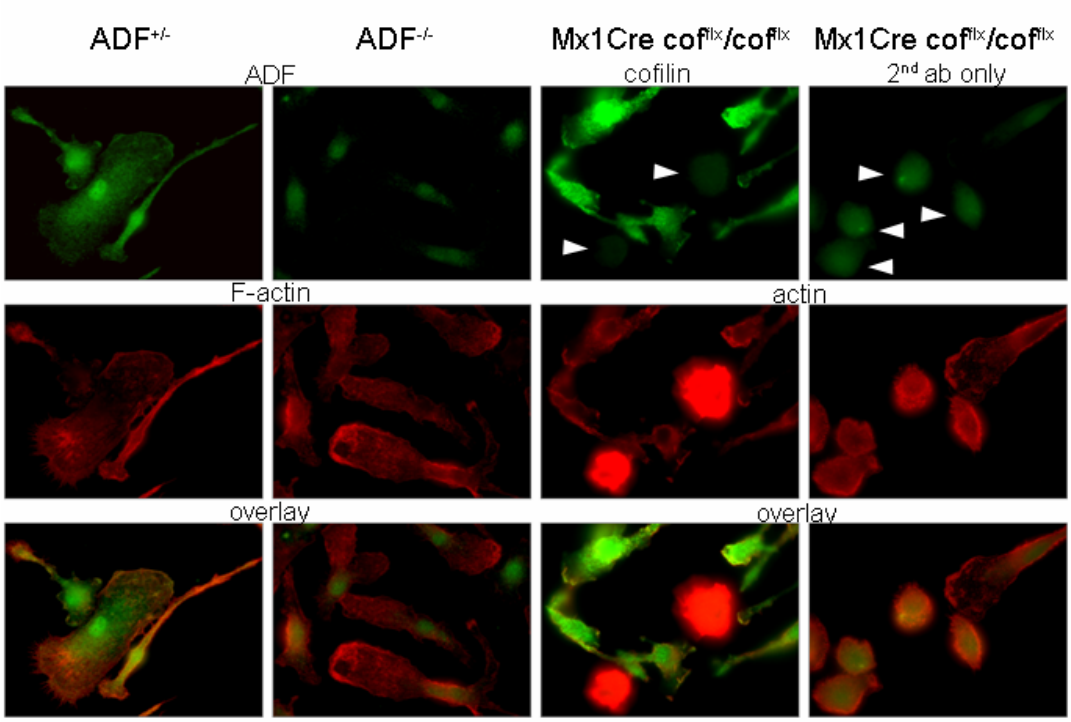

Figure 20: Staining of mutant macrophages
BMM with indicated genotypes were fixed and stained for the respective AC protein (ADF:GV13, cofilin:KG40). Specificity of staining was confirmed using macrophages that lack ADF or cofilin. Cultures of Mx1Cre cof^{flx}/cof^{flx} mice contain cofilin null macrophages as well as cofilin positive escaper cells (mutants indicated with arrowheads). Actin was used for counterstaining (phalloidin for ADF/ C-4 antibody for cofilin staining).

As expected, ADF could not be detected in BMM generated from $ADF^{-/-}$ bone marrow, thereby serving as a good control for the specificity of the ADF antibody. The mutant macrophages do not show any striking phenotype. The actin cytoskeleton appears normal as judged by the F-actin distribution. In contrast to this, we could confirm that the $cofilin^{-/-}$ macrophages display a round phenotype and that the actin cytoskeleton was altered. Background staining of the anti-cofilin antibody (KG40), but also of the anti-ADF antibody (GV13), can be explained with the high autofluorescence that is a well known feature of macrophages. The control staining with just the secondary antibody showed a low background label in knockout macrophages. A hallmark of cofilin null macrophages was the strong actin signal, which suggested increased levels of F-actin compared to control cells. Using confocal microscopy, the enrichement of cortical actin in cofilin mutant macrophages was confirmed (see cover, Fig. 47 appendix A)

2.3.4 Actin filament turnover is reduced in cofilin$^{-/-}$ macrophages

To quantitate the accumulation of F-actin inside the cells, I stained mutant and control macrophages with phalloidin that selectively binds to F-actin. Then I determined the intensity of the F-actin signal (Fig. 21).

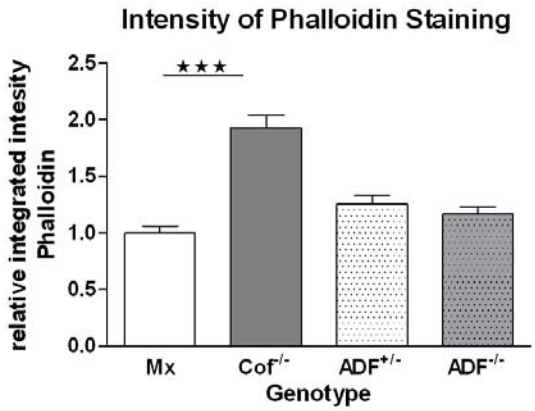

Figure 21: F-actin staining of BMM
BMM grown on cover slips were stained with phalloidin and F-actin signal intensities were determined using MetaMorph regional (n>100 cells each, p-value Mx1Cre: Cof-/- <0.0001).

Macrophages lacking cofilin showed a doubling in F-actin signal intensity, whereas ADF$^{-/-}$ macrophages displayed the similar signal intensities compare to control macrophages. This suggested an impaired actin filament turnover in cofilin mutant macrophages that leads to an accumulation of F-actin in cultured cells (see also Fig. 47, appendix A). To confirm this hypothesis, I employed a biochemical assay to determine the F-actin content. When cells are lysed using a buffer that stabilizes existing actin filaments (PHEM buffer), the F-actin can be collected by a simple centrifugation step. The supernatant contains the monomeric G-actin, whereas the heavier F-actin pellets during this centrifugation (Fig. 22).

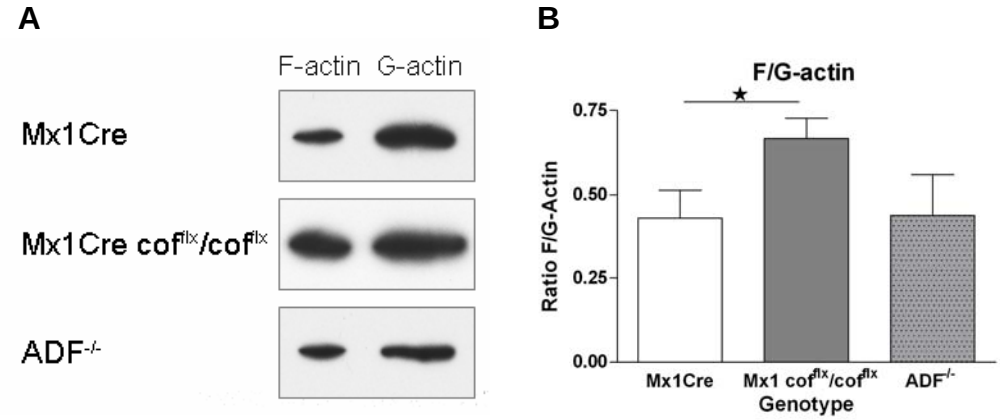

Figure 22: Ratio of F/G-actin in BMM
BMM were lysed in PHEM buffer and G- and F-actin were separated by centrifugation. Actin content in soluble and precipitated fraction were analysed by Western blotting (A). B) Statistical analysis of F-/G-Actin ratio (number of experiments of n=6, for ADF$^{-/-}$ n=2, p-value Mx1Cre:Mx1Cre cof^{flx}/cof^{flx} = 0.0443).

In summary, I could show that cofilin$^{-/-}$ macrophages contain significantly more F-actin than control macrophages. This result is consistent with my data obtained from the immunofluorescent labelling of actin in the cells. Thus, F-actin accumulation allows to easily distinguish between cofilin$^{-/-}$ and wild type macrophages in mixed cultures.
Interestingly, actin filament turnover is not impaired in ADF$^{-/-}$ macrophages. The ratio between G- and F-actin was comparable to those of control macrophages (Mx1Cre or ADF$^{+/-}$, Fig. 22).

2.3.5 Microtubulus in AC mutant macrophages

The finding that the actin cytoskeleton is severely modified in cofilin$^{-/-}$ macrophages raised the question if the microtubular network is altered in a similar fashion. Like actin, microtubules can be visualized for microscopical analysis. An antibody against α-tubulin served as a probe to label microtubules, while phalloidin was used to stain actin in the cells and thus, to discriminate between wild type and cofilin mutant cells (Fig. 22).

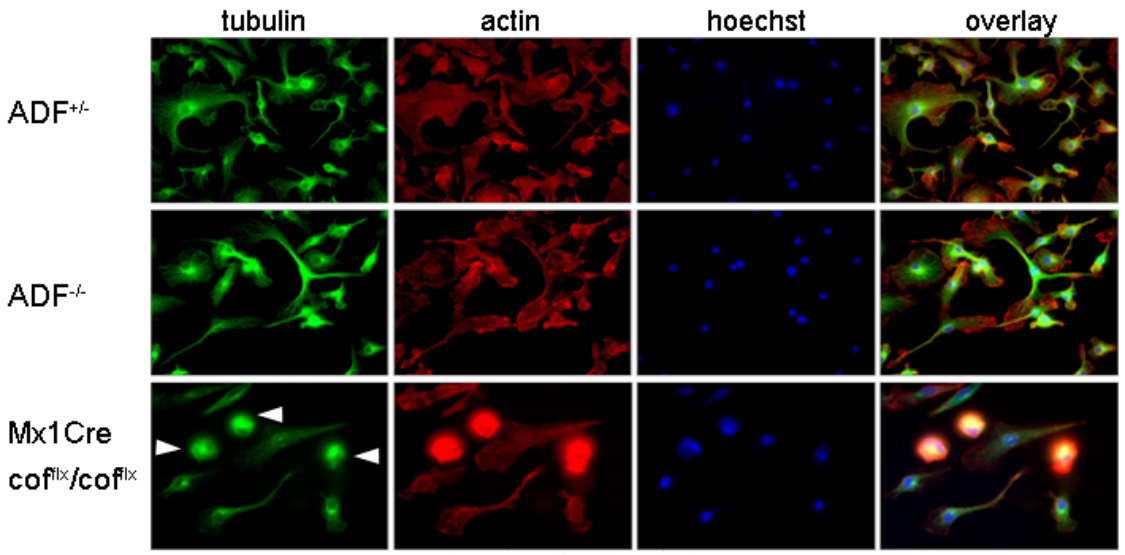

Figure 23: Microtubular system in mutant macrophages
Microtubules of BMM were stained with antibody against α-tubulin, F-actin with Phalloidin-Red and the DNA with Hoechst dye. Pictures were taken at different magnifications (40x ADF/ 63x cofilin).

The examination of the α-tubulin staining revealed no obvious differences concerning the organization and appearance of the microtubular network in ADF mutant macrophages. However, it is difficult to judge the structure of microtubules in cofilin mutant cells, due to the strong F-actin signal and their abnormal morphology.

2.3.6 Morphometric analysis of AC mutant macrophages

To analyze the morphological alterations in detail at least 100 macrophages were analyzed for every genotype using the regional measurement tool of the MetaMorph program. In Mx1Cre cof^{flx}/cof^{flx} cultures, F-actin staining was used as a discriminator between mutant and wild type cells.

2.3.6.1 Spreading area

Macrophages are cells that normally attach very tightly to their substrate through foal adhesions that contain F-actin to connect the cell membrane to the cytoskeleton. We were interested if the mutant macrophages differed in the way the cells spread on their substrate (Fig. 24).

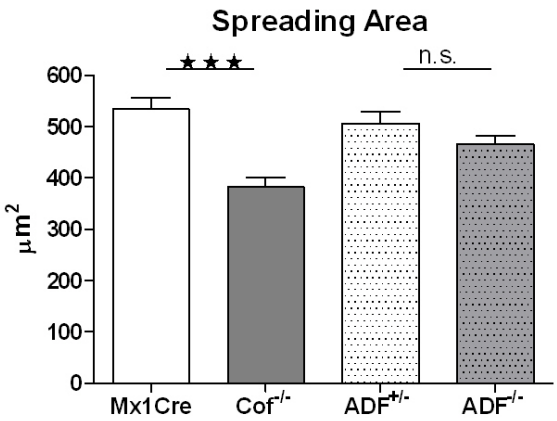

Figure 24: Spreading area of macrophages
BMM were grown on cover slips and analyzed on day 6 of culture. Regional measurements were performed to calculate the spreading area (A) of the macrophages; n>100 for each genotype (p-values Mx1Cre:$Cof^{-/-}$ <0.0001, $ADF^{+/-}$:$ADF^{-/-}$ = 0.15).

$Cofilin^{-/-}$ macrophages fail to flatten and therefore occupy on average about 30% less area. Instead, the $ADF^{-/-}$ macrophages showed almost no effect on their spreading area, although their shape looked distinct.

2.3.6.2 Shape

In order to obtain an unbiased statistical analysis of the cell shape we analyzed the shape factor (sf) of more than 100 macrophages per genotype. The shape factor was assessed by putting the spreading area (A) in relation to the perimeter (P) of the cell, following the formula:

$$sf = 4\pi A/P^2$$

A spreading factor of 1 would represent a perfect circle, while a factor close to 0 reflects an irregular and elongated object (Fig. 25).

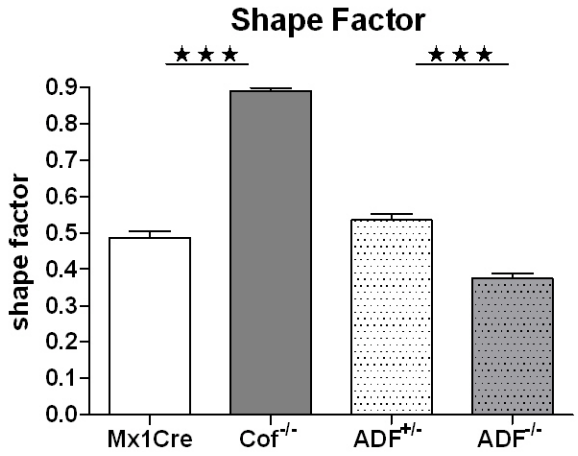

Figure 25: Shape factor of macrophages
BMM were grown on cover slips and analyzed on day 6 of culture. Regional measurements were performed using the MetaMorph program. The shape factor (sf) was calculated as $sf = 4\pi A/P^2$ (with A: area and P: perimeter); n>100, p-values Mx1Cre:$Cof^{-/-}$ <0.0001, $ADF^{+/-}$:$ADF^{-/-}$ <0.0001

Almost all cells in cofilin conditional cultures have a circular phenotype, while in cultures of control macrophages, like Mx1Cre and $ADF^{+/-}$ the shape of the cells vary much more. Interestingly, this statistical analysis showed that indeed the $ADF^{-/-}$ macrophages are significantly more elongated than control cells.

2.3.6.3 Polarization

Macrophages need to polarize the cell body to fulfil many of their cellular functions. For instance, directed migration along a chemokine gradient can only occur once a cell orientates itself in the direction of the chemokine source. Also antigen presentation can only be performed properly if the macrophage is able to polarize and thus can form a stable immunological synapse. Cells were scored visually using three different criteria: apolar, bipolar and multipolar (Fig. 26).

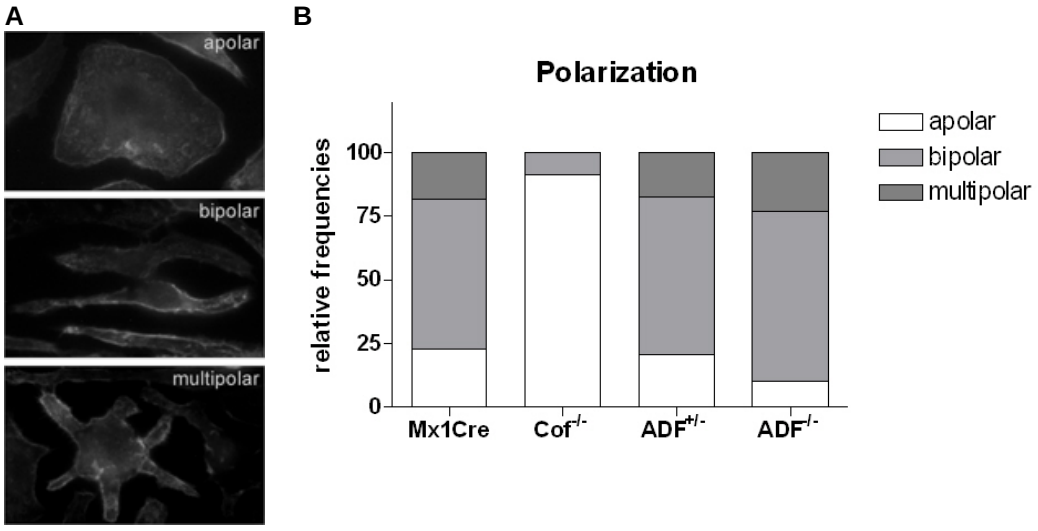

Figure 26: Polarity of macrophages
On day 6 of culture the polarity of macrophages was assessed microscopically. At least 130 cells per genotype were scored according for polarization. **A**) Examples for the scoring parameters (apolar, bipolar, multipolar), **B**) shows the relative frequencies of phenotypes found in the cultures.

In control cultures around 20% of the control macrophages are spread out and do not show a polarization while more than 75% of the cells are polarized and have at least one lamellipodium. One third of those cells have a multipolar appearance, which is due to multiple external cues or a reorientation of the cell.

Instead almost all macrophages lacking cofilin were apolar. Only very few cells showed a slight bipolar phenotype, suggesting that the accumulation of F-actin under the cell membrane is not directed. ADF$^{-/-}$ macrophages showed a larger degree of polarized cells than in the control cells.

2.3.7 Cofilin is essential for macrophage proliferation

Cell shape and F-actin turnover are impaired in macrophages lacking cofilin and one important question is how this affects the physiology of BMM, such as cell division and proliferation. First evidence that the cell cycle progression of cofilin null macrophages is disturbed resulted from the observation of bone marrow cells in culture. Harvest of BMM on day 6 of culture showed significant differences in the yield of cofilin$^{-/-}$ macrophages compared to control or ADF$^{-/-}$ macrophages. Thus, I designed an experiment to study proliferation kinetics (Fig. 27).

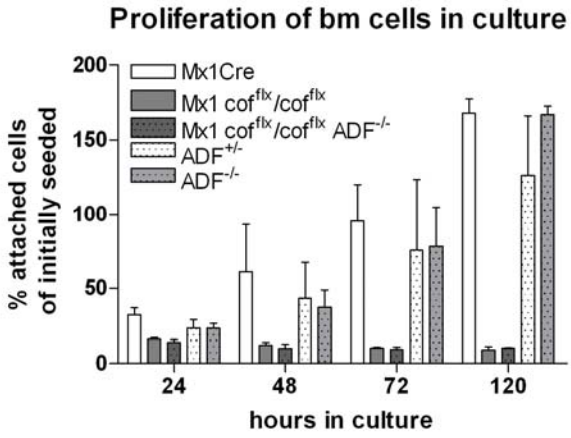

Figure 27: Proliferation of bone marrow cells in culture
$1x10^5$ bone marrow cells were taken into culture in 96 well flat bottom plates after indicated time period plates were washed thoroughly and the DNA content per well was assessed by CyQuant analysis. All values were prepared in quadruples. The graph shows the average of three independent experiments.

Cells were flushed from the bone marrow and plated at the same density. Proliferation was followed up to 120 hours (see materials and methods, Fig. 27). While control cells as well as $ADF^{-/-}$ bone marrow cells start to proliferate after 48 hours, cells lacking cofilin or both, cofilin and ADF, fail to propagate completely. Two possible explanations could account for this finding: Either the mutant cells do not proliferate or more cells undergo programmed cell death. In order to discriminate these two different possibilities I analyzed the proliferation rate by BrdU incorporation and the proportion of apoptotic cells by TUNEL assay (Fig. 28).

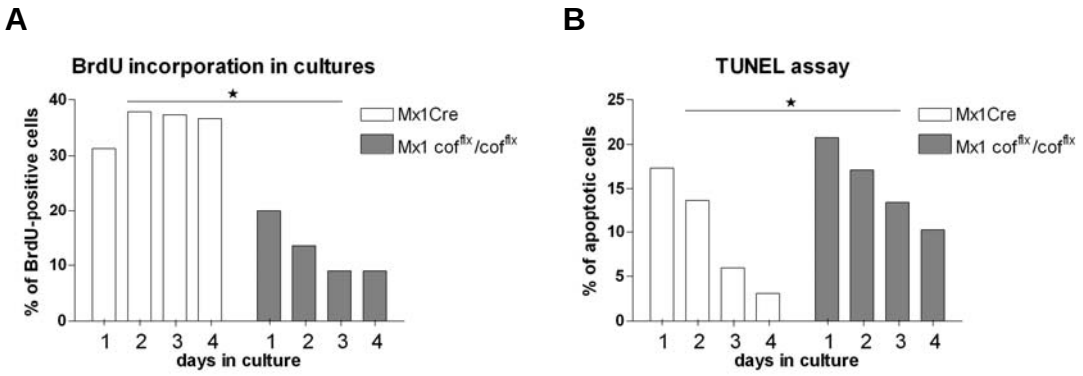

Figure 28: Proliferation and apoptosis in bm cultures
A) Bm cells were plated on cover slips and pulsed with BrdU 1 hour before fixation and subsequent BrdU staining. At least 200 cells were counted for each time point (p-value = 0.0108, two-way ANOVA). **B**) Bm cells were plated on cover slips and analyzed every subsequent day for the presence of apoptotic cells by TUNEL staining (n>100, p-value = 0.0175, two-way ANOVA).

As shown in Fig. 28 cofilin mutant macrophages proliferate less than control cells throughout the entire period of cell culture. At later time points also the control cells run into a proliferation arrest (data not shown). This is a common finding in cells that become confluent.

The proportion of apoptotic cells was slightly increased in macrophage cultures lacking cofilin compared to control cultures. In general, apoptotic cell death is highest in fresh bm cultures (15-20%), however after adaptation of the bm cells to the environmental conditions less dying cells can be found in the cultures. This was true for both tested genotypes, Mx1Cre and Mx1Cre cof^{flx}/cof^{flx}.

Taken together, we can conclude that mainly the lack of proliferation accounts for the reduced number of macrophages found in cofilin conditional cultures.

2.3.7.1 Cofilin mutant macrophages have a cytokinesis defect

The BrdU incorporation showed that cofilin mutant macrophages have a severe proliferation defect. Next, I was interested which step of cell division was affected by deletion of cofilin. ADF1 has been found in fission yeast to be important in the regulation of the contractile ring (Nakano and Mabuchi, 2006) and cofilin dysregulation lead to the appearance of multi-nucleated cells in several model systems (Nagaoka et al., 1995; Kaji et al., 2003; Nagata-Ohashi et al., 2004), suggesting a role of cofilin in cytokinesis.

To examine defects in cytokinesis, I stained the nuclei of macrophages with Hoechst dye and determined the degree of multi-nucleated cells on day 6 of BMM culture (Fig. 29).

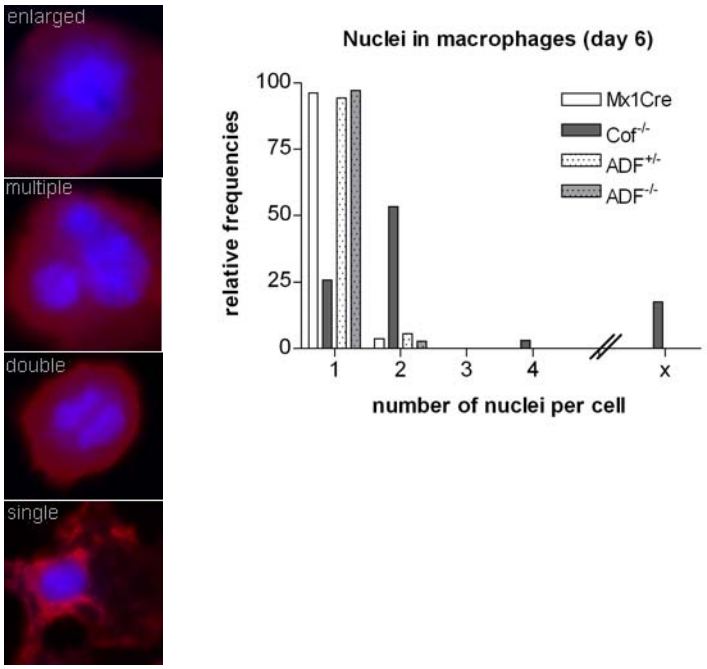

Figure 29: Percentage of polynucleated cells
The DNA (Hoechst) and the actin cytoskeleton (Red-Phalloidin) of BMM was stained and analyzed by microscopy. Left side: criteria used to discriminate between different states. Single (1), double (2), multi-nucleated (3) and enlarged (4). Right side: Number of nuclei in cultured macrophages (n>150). X summarizes a population with an enlarged, fuzzy nucleus. (ANOVA analysis: Mx1Cre:$Cof^{-/-}$ $p<0.0001$)

I found that a high proportion of cofilin mutant macrophages contain multiple nuclei. Over 50 % of cofilin$^{-/-}$ macrophages contained two nuclei and in addition, I found a fraction of mutant cells in the cultures that contained enlarged and fuzzy nuclei, which were clearly distinct from nuclei found in quiescent control cells. Enlarged nuclei can be found in cells either replicating or undergoing cell death; and most likely this finding points towards an increased apoptotic rate in cells lacking cofilin (see Fig. 28). The ADF$^{-/-}$ BMM did not accumulate nuclei and were indistinguishable from the control genotypes.

2.3.7.2 Cofilin is required for G2/M-phase progression

The cell cycle is a complex progress that is characterized by site specific phosphorylation of regulatory molecules. Chromatin condensation is a pre-requisite for cell division and phosphorylation at Ser10, Ser28 and Thr11 of histone H3 is tightly linked with chromosome condensation during mitosis and meiosis (Hendzel et al., 1997; Goto et al., 1999; Preuss et al., 2003). Immunostaining with phospho-specific antibodies in mammalian cells reveals mitotic phosphorylation of H3 Thr3 in prophase and its dephosphorylation during anaphase (Dai et al., 2005).

We used here a H3 Thr3 phospho-specific antibody to further investigate the proliferation defect in cofilin mutant cells (Fig. 30).

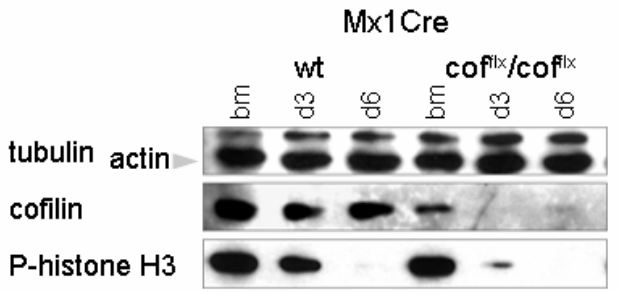

Figure 30: Cell cycle markers in BMM cultures
Cell lysates of mutant and control BMM were tested at indicated time for the cell cycle marker phospho-histone H3 (Thr3) by Western blotting. As loading controls actin and tubulin are shown. Cofilin deletion was verified by the antibody KG60.

On day 3 of culture, cells lacking cofilin contain less phosphorylated histone H3, suggesting that less cells progress through the G2/M checkpoint. Control macrophages contain more phosphorylated histone H3 on day 3 of culture, however on day 6 hardly any protein was detectable. This observation is in agreement with the reduced number of BrdU positive cells at this time point (Fig. 28) and a proliferation stop upon reaching confluence.

2.4 Functional analysis of AC mutant cells

To discriminate, prior to the functional analysis, between live and dead cells we performed a double staining with calceinAM and ethidium bromide homodimer (EthD). CalceinAM is an ester that freely enters the macrophages where it is cleaved by cellular esterases. Upon cleavage fluorescent calcein can not leave the live cells anymore. EthD on the other hand can not pass the membrane of living cells, but intercalates with the DNA of dead cells. The proportion of living cells on day 6 of BMM culture was determined by FACS analysis (Fig. 31).

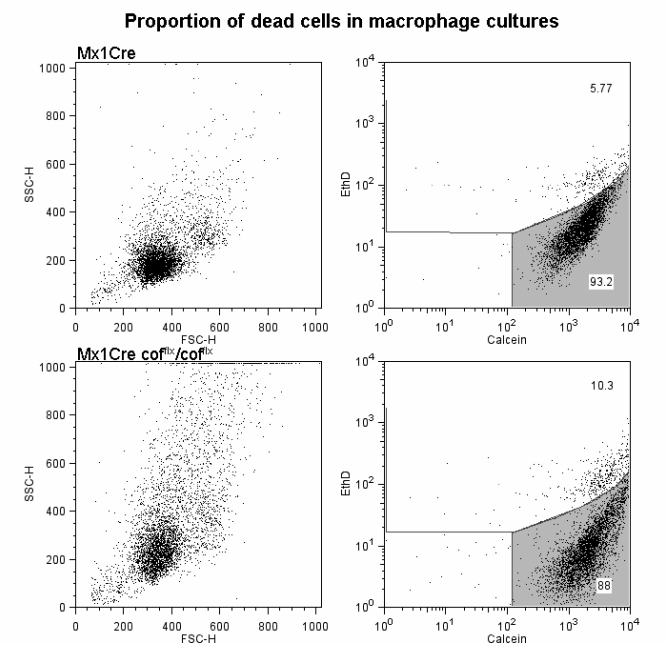

Figure 31: Proportion of dead cell in BMM cultures
On day 6 bone marrow derived macrophages were harvested and incubated with ethidium bromide homodimer and CalceinAM for 15 min prior to immediate analysis by flow cytometrie. Viable cells are Calcein positive and EthD negative.

On day 6 of culture we found in control macrophages about 93% of live cells, while in macrophage cultures lacking cofilin we found slightly less viable cells (88%). This result confirms that the round mutant cells are in fact viable which is important for the following functional analysis I performed.

2.4.1 ADF and cofilin are not required for bm cell attachment

An important functional criteria of macrophages is their tight attachment to the substrate. Several studies suggested the involvement of ADF/cofilin in the attachment behaviour of cells (Djafarzadeh and Niggli, 1997; Muller et al., 2006). This was further supported by my finding that ADF and cofilin localize to focal contacts of macrophages. I therefore performed an attachment assay for which I used freshly isolated bone marrow from control and mutant mice (Fig. 32).

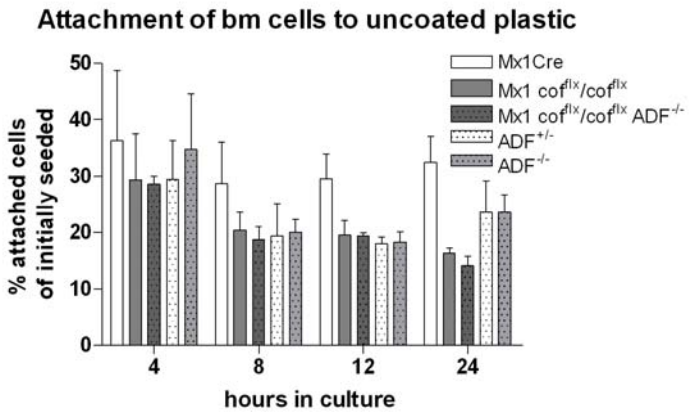

Figure 32: Attachment of bone marrow cells in culture to uncoated plastic
$1x10^5$ bone marrow cells were allowed to attach to 96 well flat bottom plates. After indicated time periods plates were washed thoroughly and the cell number was assessed using the CyQuant kit. All values represent quadruple experiments. The graph shows the average of three independent experiments.

Interestingly, we found that the deletion of ADF and/or cofilin does not effect the attachment of cells during a period of 12 hours. Similar results were obtained with different substrates, like laminin, poly L-lysin or gelatine (data not shown). This result suggests that cofilin and ADF dependent actin cyto-skeleton remodelling is dispensable for cell attachment.

2.4.2 Cofilin, but not ADF is required for cell migration

2.4.2.1 Random migration *in vitro*

The importance of ADF/cofilin proteins for migration has been the focus of many studies. Dawe et al. proposed that cofilin is essential for fibroblasts to maintain polarity during directed migration using LIMK overexpression to inactivate cofilin (Dawe et al., 2003). Consistent with this publication, it has been shown that cofilin is required for the correct homing of haematopoietic stem/progenitor cells into haematopoietic microenvironments in the bone marrow; a process that depends on a signalling cascade from the integrin CD29 over LIMK1/cofilin to actin (Konakahara et al., 2004). Additionally the description of the cofilin null deletion in mouse suggests that it could be a migratory defect of neural crest cells that causes the embryonic lethality of these mice (Gurniak et al., 2005).

The enrichment of cortical actin, I observed in cofilin$^{-/-}$ macrophages (see 2.3.1.2) suggested that these cells are less motile than wild type BMM. To study a potential migratory defect, BMM (day 5) were seeded in tissue culture treated chambers (Ibidi, *Integrated BioDiagnostics*) 24 hours before analysis in normal bone marrow macrophage medium. The next day macrophages were analyzed by video microscopy. Pictures were taken with a time lapse of 15 sec for 20 minutes and the nuclei of the macrophages were tracked with the MetaMorph tracking objects tool in order to calculate the average velocity of cells (Fig. 33).

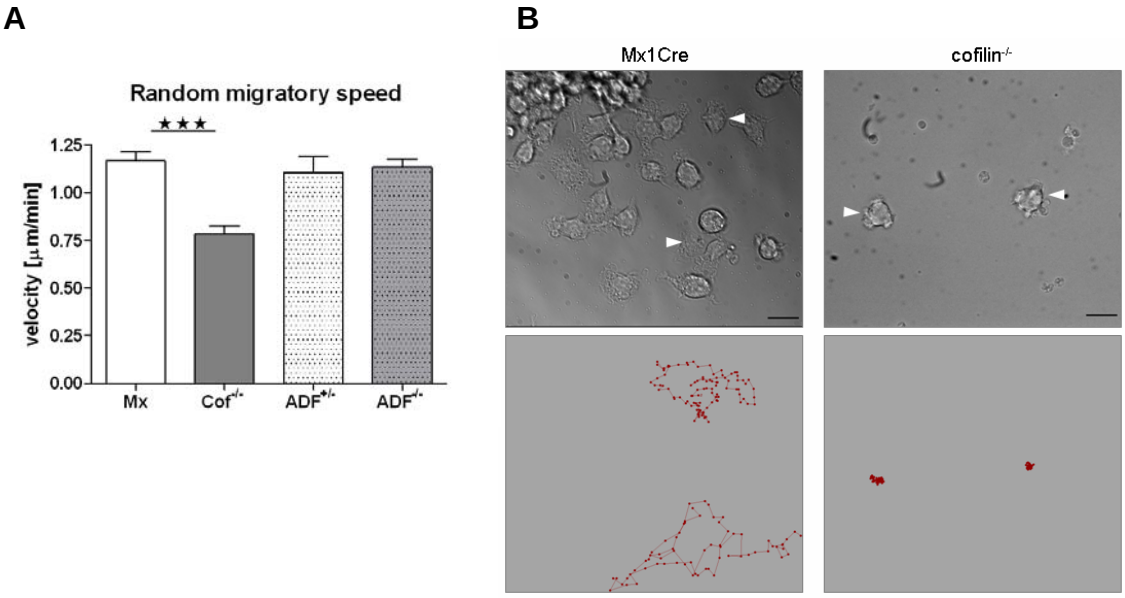

Figure 33: Random migration of BMM

A) After 6 days in culture random migration of macrophages was determined by time lapse video microscopy. Videos were taken at a frame rate of 4 pics/min. For every genotype at least 60 macrophages were tracked for 20 min (p-value Mx:Cof$^{-/-}$ <0.0001). **B)** Bm cells from Mx1Cre (left side) and Mx1Cre cof^{flx}/cof^{flx} mice were followed for eight hours under the microscope (DIC, 40x; time lapse: 5 min, scale bar: 20 μm). The starting frame is shown in the upper part, with the tracked cells indicated by arrowheads. In the lower panel the tracking paths of the indicated cells are shown.

I found that the migratory velocity of cofilin null BMM is reduced compared to wild type or ADF lacking macrophages (Fig. 33A). In fact, it seemed that cofilin$^{-/-}$ macrophages completely failed to reorganize their actin cytoskeleton in order to migrate into one direction. It appeared as if the round cell body wiggles from one side to the other, but never pushed into one direction (Fig. 33B). A likely explanation is the missing actin depolymerization that is in cell orientation as important as the polymerization. ADF$^{-/-}$ macrophages did not show differences in their migratory speed although their cell morphology is different from wild type cells (see 2.3.1.5).

Studying cell migration in a 2D environment is limited and therefore, I wanted to employ a migration assay that is closer to an *in vivo* situation.

2.4.2.2 Recruitment of AC mutant cells *in vivo* to sites of inflammation

A simple way to induce neutrophil and macrophage transmigration *in vivo* is the injection of thioglycolate (TG) into the peritoneum of a mouse, which elicits an immediate inflammatory response. Upon this stimulation, myeloid cells are recruited into the abdominal cavity, where they can be easily collected by peritoneal lavage. During the first 24 hours mainly the fast migrating neutrophils enter the peritoneum, while macrophages migrate slower and contribute 90 % of the peritoneal exsudate cells 5 – 7 days after injection.

6 hours after TG injection the lack of ADF had no effect on cell recruitment (Fig. 34). At this early time point most cells are neutrophils, but very similar results were obtained in experiments with longer induction periods (5 days, data not shown).

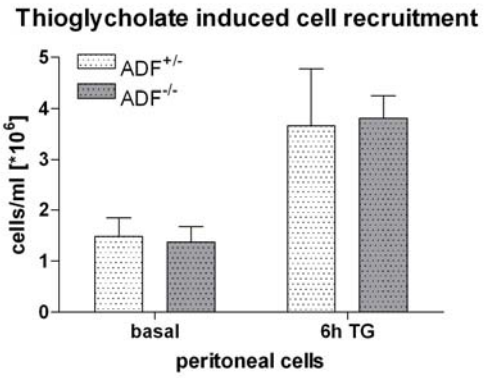

Figure 34: Thioglycholate induced cell recruitment *in vivo*
500 µl of 3% Thioglycholate were injected i.p. to induce migration. 6 hours later, peritoneal cells were collected in 5 ml and counted. As a control uninduced peritoneal cells were assessed as well (n=5).

Studying the *in vivo* migration of cofilin$^{-/-}$ macrophages was complicated by several parameters. As described in chapter 2.2.5, Mx1Cre cof^{flx}/cof^{flx} mice die, if the systemic induction of deletion is too strong. Thus, we set up an injection protocol in order to obtain PEC lacking cofilin. Five days prior to the experiment, the mice received a single injection of 250 µl polyI:C. 48 hours later PEC recruitment was induced with an injection of 500 µl TG. After another three days bm and PEC were collected (Fig. 35).

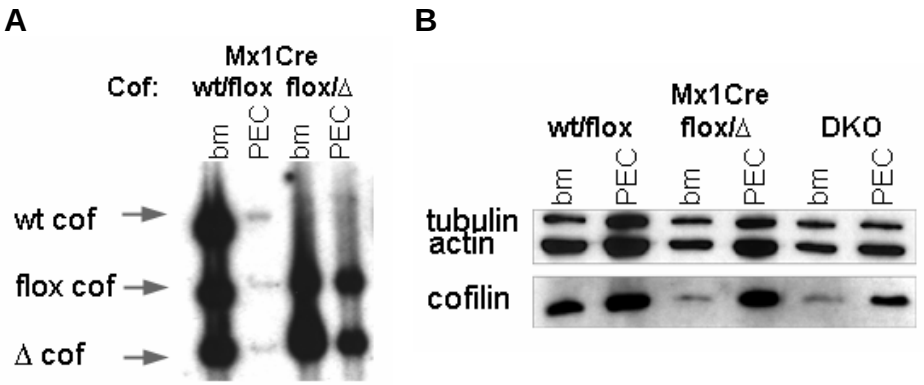

Figure 35: *In vivo* recruitment of cofilin mutant cells
Bm and PEC were analyzed by Southern blot (**A**) and Western blot (**B**) for the presence of cofilin. 5 days prior to harvest deletion was induced by a single administration of 400 μg polyI:C, 2 days later 500 μl TG was injected to recruit cells into the peritoneum.

However, I was unable to isolate significant numbers of PEC from mice that showed a very good deletion in the bone marrow; a finding that clearly indicated that cofilin is essential for *in vivo* recruitment of cells to the peritoneal cavity. In mice showing a medium deletion rate, we observed that the cells that actually arrive in the peritoneum were escapers, which contained cofilin (Fig. 35).
Taken together we can conclude that cofilin but not ADF is essential for migration *in vitro* and *in vivo*.

2.4.3 Role of ADF/cofilin in phagocytosis

Rearrangement of the cortical actin meshwork is believed to be involved in endocytosis, since actin sequestering agents like thymosin β4, DNaseI and latrunculin A have been shown to interfere with early steps in the endocytotic process (Lamaze et al., 1997). Concerning the role of cofilin in this process some studies addressed its role during phagocytosis. In J774.1 cells, the use of cofilin antisense oligonucleotids lead to an increase in phagocytotic activity of opsonized zymosan in the population (63% instead of 44% of controls) (Adachi et al., 2002). However, cofilin was not absent in these cells but reduced to 30%. A similar experiment was performed with U937 cells in which the overexpression of LIMK led to an increase in phagocytic activity of these cells (Matsui et al., 2002).

Since phagocytosis is an important cellular function of macrophages we were interested, if ADF and cofilin play an essential role during this process. I performed two different experiments to address this question: First, I analyzed the phagocytotic activity of the entire population of cells, using labelled *E. coli*

particles; and second FITC-labeled zymosan uptake was followed on a single cell level using fluorescence microscopy (Fig. 36).

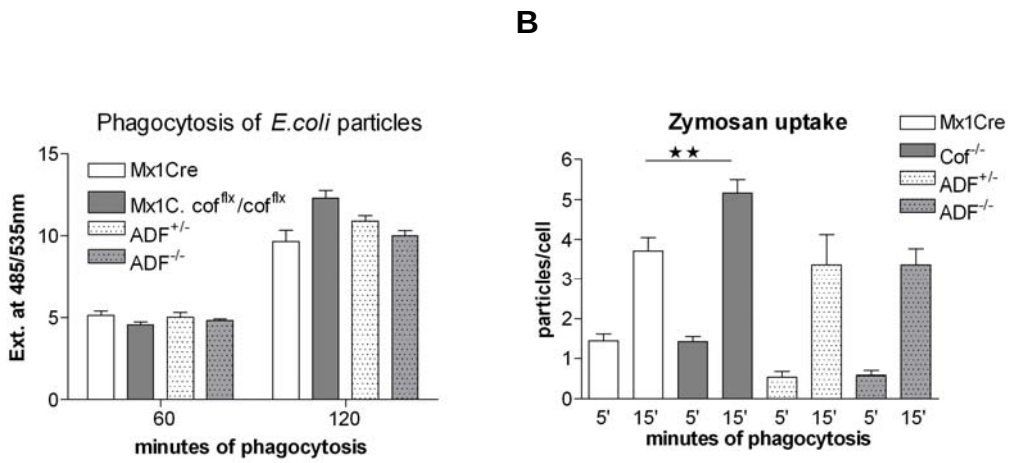

Figure 36: Phagocytosis of BMM
After 6 days in culture macrophages were tested for their capability to phagocytose bacteria and yeast particles. **A**) BMM were incubated with FITC labeled *E. coli* particles for 1 or 2 hours. Not internalized particles were quenched prior to measurement. **B**) BMM were offered FITC-zymosan for the indicated times and cells were additionally stained with phalloidin, before internalized particles were scored (n=100, p-value 15´ Mx1Cre: $Cof^{-/-}$ = 0.0019).

Using florescent *E. coli* particles, I studied the phagocytotic activity of BMM cultures. In this approach, attached but not internalized particles were quenched with trypan blue. Macrophages of all genotypes were indistinguishable for their phagocytotic activity after 60 min of phagocytosis; only after 120 min macrophages lacking cofilin contained slightly more particles (Fig. 36, p=0.84).

The uptake of FITC-zymosan was assessed on a single cell level using microscopy. Using this approach it was possible to determine the contribution of cofilin mutant macrophages to the overall phagocytotic activity. F-actin in macrophages was again visualized using phalloidin. After 5 minutes of phagocytosis similar numbers of particles could be detected in all experiments. However, macrophages lacking cofilin internalized significantly more particles after 15 minutes of particle up-take compare to macrophages of the other genotypes. This is in concordance with a previous report that showed that cofilin depletion by antisense oligonucleotids leads to an increase in the phagocytotic activity of J774.1 cells (Adachi et al., 2002).

A hallmark of phagocytosis is the formation of the phagocytic cup, an F-actin rich structure that is formed around the vesicle upon endocytosis. I therefore asked the question, if a phagocytic cup can be established by cells lacking cofilin. Upon FITC-zymosan uptake, cup formation was visualized with phalloidin (Fig. 37).

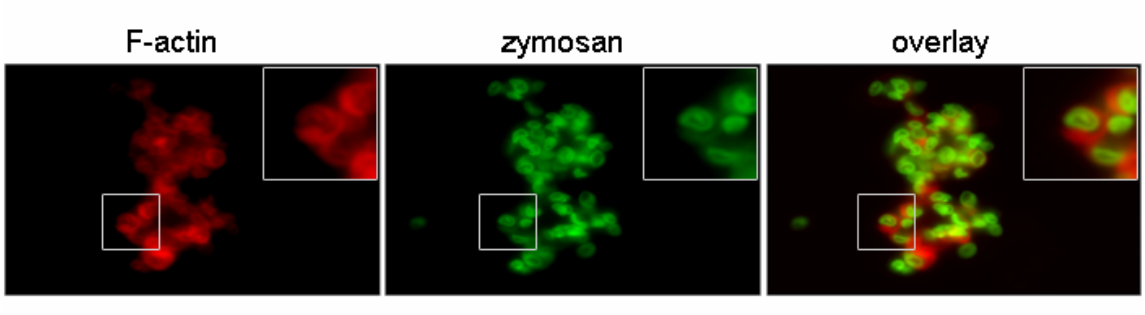

Figure 37: Actin cup formation during phagocytosis in cofilin$^{-/-}$ BMM
Cofilin$^{-/-}$ macrophages were fixed after 15 minutes incubation with FITC-labeled zymosan and F-actin was stained with Red-Phalloidin. The inlays show a 2x magnification of the indicated areas.

The phalloidin staining showed that the formation of a phagocytic cup is not impaired in macrophages lacking cofilin.

Taken together we can conclude that phagocytosis was not impaired in macrophages lacking AC proteins. On the contrary, macrophages lacking cofilin showed an increased rate of phagocytotic activity. The formation of the phagocytic cup indicates that the underlying F-actin rearrangement is not impaired in these cells.

2.4.4 Role of ADF/cofilin in antigen presentation

A key switch during immune reaction is the shift from an innate to an adaptive immune response. For this step, professional antigen-presenting cells (APC) have to present peptide antigens bound in their MHC molecules to lymphocytes in order to activate them. If this process occurs in the presence of co-stimulatory signals, specific B and T cells are activated and undergo clonal expansion.

The actin cytoskeleton is an important platform for these events. Antigen presentation requires the formation of the immunological synapse (IS); a highly structured contact zone between the APC and the T cell that allows a stable contact between the two cell types. To establish the IS both cells have to polarize and direct signalling molecules to this area. It recently becomes more and more evident that the actin cytoskeleton is not only involved in the stabilization of the IS, but also in the active transport of signalling molecules towards this zone. Thus, we hypothized that antigen presentation might be disturbed in cofilin mutant cells, since they fail to polarize and display a different membrane structure.

An elegant way to test the ability of APC to present antigens to T cells is the use of T cell receptor (TCR) transgenic mice. We used transgenic mice that

express the mouse alpha-chain and beta-chain T-cell receptor on $CD4^+$ T cells that is specific for the chicken ovalbumin peptide $OVA_{323-339}$ in the context of a MHC class II molecule of the haplotype $I\text{-}A^b$ (Barnden et al., 1998).

Instead of BMM that have only a weak presentation capability, we used for these experiments bone marrow derived dendritic cells (DC). Using the Mx1Cre driven cofilin depletion DC behave like BMM, their kinetics as well as the amount of living cells in the culture equals the data obtained from BMM (data not shown). After 24 and 48 hours of antigen presentation the supernatant was collected and assayed by ELISA for the cytokines IL-2 and IFN-γ, which are a measure for the efficiency of stimulation (Fig. 38).

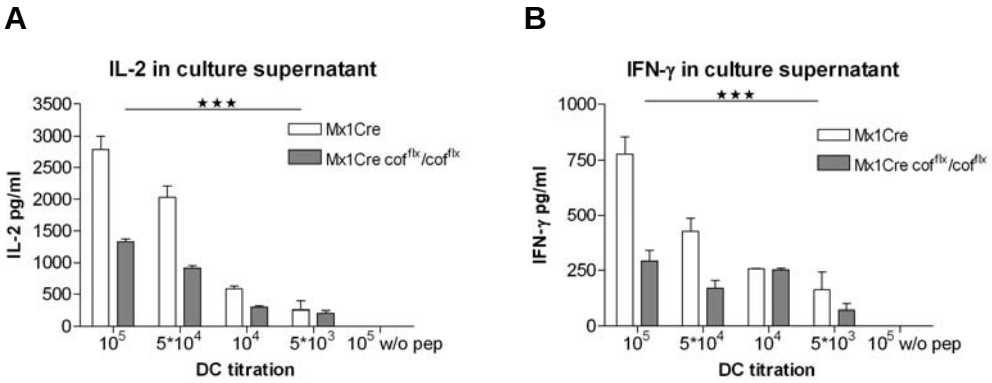

Figure 38: *In vitro* OT-II T cell stimulation by antigen presenting cells
Control and cofilin null dendritic cells were titrated from 10^3 - 10^5 cells and allowed to present externally added $OVA_{323-339}$ peptide to purified OT-II T cells. Culture supernatants were collected after 24 hours and cytokine levels of IL-2 (**A**) and IFN-γ (**B**) were determined by ELISA. Note that antigen presentation and activation of T-cells was consistently reduced by up to 70% with cofilin null dendritic cells. Shown is one repesentative experiment out of three. P-values for IL-2 and IFN-γ Mx1Cre: Mx1Cre cof^{flx}/cof^{flx} <0.0001.

Dendritic cells lacking cofilin are strongly impaired in their T cell activating capacities compared to control DC. In all experiments IL-2 and IFN-γ production of T cells was significantly reduced. $ADF^{-/-}$ dendritic cells were perfectly capable of antigen presentation and no difference in cytokine expression of IL-2 and IFN-γ was observed (data not shown).

2.4.5 Conclusions from AC functional analysis in macrophages

Using a genetic approach, I was able to generate macrophages lacking ADF and/or cofilin. Cofilin$^{-/-}$ macrophages were severely impaired in actin remodelling, resulting in the accumulation of F-actin in the cell (2.3.4) and a round, elevated and unpolarized phenotype of the cells (2.3.6/2.3.3). Interestingly, cells lacking cofilin can still attach to plastic surfaces upon plating (2.4.1); however they fail to spread and flatten. Macrophages lacking cofilin were impaired in the cell cycle progression (2.4.3.3) and cytokinesis, which explains the high proportion of poly-nucleated cells in the culture and the strong proliferation defect (2.3.7).

The defect of macrophages lacking cofilin in polarization might also account for the observed defects in migration (2.4.2) and antigen presentation (2.4.4). Cofilin$^{-/-}$ macrophages are not impaired in their phagocytotic activity (2.4.3) but show an increase compared to control cells.

In complete contrast to the functional alterations observed in cofilin mutant macrophages, cells lacking ADF did not show any gross functional defects. They attached (2.4.1), proliferated (2.3.7) and phagocytosed particles (2.4.3) at the same speed as control cells. The slightly elongated phenotype of macrophages lacking ADF (2.3.6.2) affected neither their migratory speed (2.4.2) nor their ability to present antigens to T cells (2.4.4).

Thus, I can conclude that ADF and cofilin play distinct roles in macrophages. However, the up-regulation of the other respective protein in mutant macrophages (2.3.1) suggests that the molecules can complement somewhat a defect in their counterpart.

Macrophages lacking both ADF and cofilin are even more impaired in their cellular functions and in general, I was unable to obtain enough double mutant macrophages for functional analysis.

Based on these results, I wanted to test if ADF could counteract a cofilin deletion, when it is expressed and regulated exactly like cofilin. Therefore, I developed a strategy to replace cofilin with ADF in a transgenic mouse.

2.5 Replacement of cofilin by ADF using a genetic approach in mouse

In order to generate a mutant mouse that expresses ADF instead of cofilin (see material and methods) a targeting construct carrying the cofilin gene with the exons 2-4 flanked by loxP sites was generated as shown in Fig. 40. The neomycin resistance cassette (neo) was flanked by FRT sites, which should allow its removal upon FLP recombination. Downstream of the neomycin cassette, exons 2-4 of the wild type ADF gene were introduced into the vector (a). Upon cofilin deletion the first exon, encoding just the starting Methionine should be spliced to the second exon of ADF. This is possible as ADF and cofilin show exactly the same genomic organisation (see introduction).

The targeting construct contained a 1.5 kb 5' homology arm and a 5 kb 3' homology arm for the recombination in the genomic locus of mouse cofilin, as shown in Fig. 39. Upon recombinase Cre expression, exon 2-4 of the cofilin gene will be removed, so that the first exon of cofilin should then be spliced to exon 2-4 of ADF. Thus, the induction of Cre-recombinase serves as a conditional switch to change from cofilin to ADF expression.

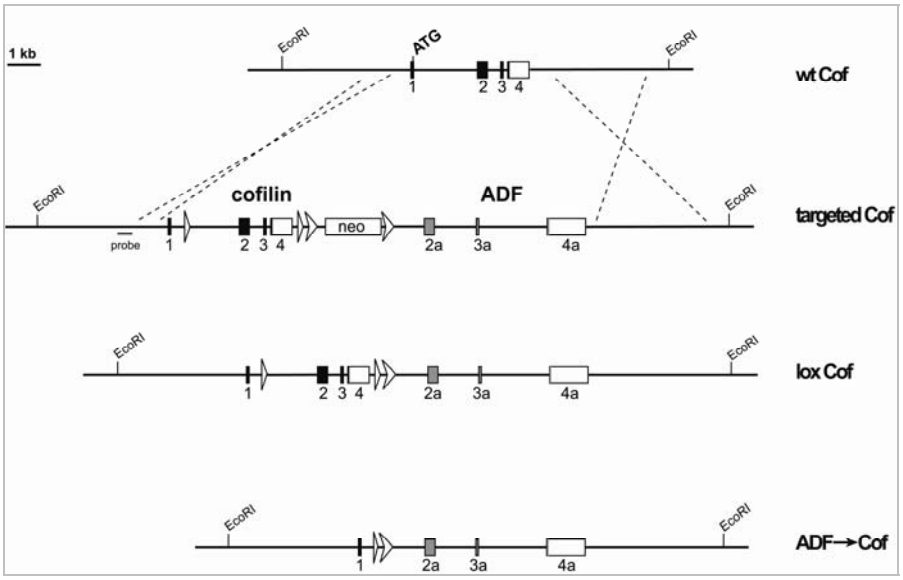

Figure 39: Targeting construct: cofilin replacement by ADF
Schematic drawing representing the cofilin wild type region, the targeting construct and the targeted locus where cofilin is flanked by loxP sites and carries a neomycin resistance flanked by FRT sites and exon 2-4 of wild type ADF(a), downstream of its 3' UTR. The targeted locus after Cre and Flip recombination is displayed as well. Cofilin exons are indicated by black, ADF exons by grey boxes, the *Eco*RI sites and the probe used for the Southern blot are indicated as well.

ES cells were electroporated with the linearized targeting vector, 300 neomycin resistant clones were picked, and analyzed by Southern blot, using an *Eco*RI restriction digest and the external probe, as shown in Fig. 40. A band of 13 kb was expected from the wild type allele and a band of 20 kb in case of a homologous recombination event due to the presence of the insertion of the 2 kb neomycin cassette and the 5 kb ADF fragment downstream of the gene (see Fig. 40). Single copy integration was subsequently confirmed using a neomycin probe (data not shown).

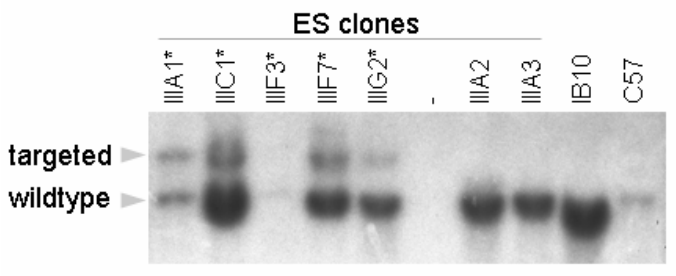

Figure 40: ES cell screening
Southern blot analysis of genomic DNA from homologous recombinant ES cell and wild type clones digested with *Eco*RI. Targeted ES clones are marked with a *.

Although the *Eco*RI digest identified the clones in which homologous recombination had occurred upstream of the neo resistance gene, it does not distinguish whether recombination had occurred in the 5' homology arm or between the loxP sites, in which case the 5' loxP site would have been lost.

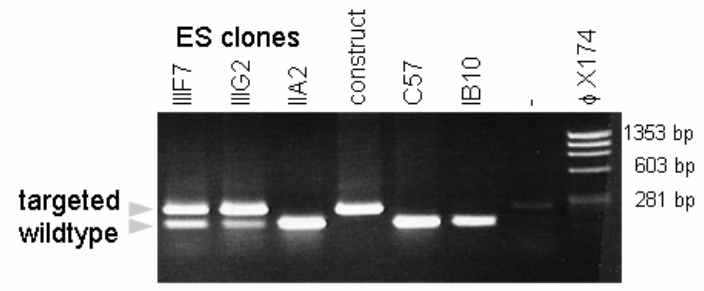

Figure 41: LoxP spanning PCR
To verify the presence of the 5' loxP side a PCR protocol was established that spans the loxP side. The wild type allele produces a 100 bp fragment (lane 5, 6), whereas the targeted allele yields a 130 bp fragment (lane 4). Two of the three tested ES clones (lanes 1-3) carried the targeted allele.

The presence of the second loxP site was verified by a specific PCR that was designed to span the 5' loxP site. I obtained 20 clones out of 300, in which homologous recombination had occurred (percentage of recombination events > 15%). Six clones out of these 20 contained both loxP sites (Fig. 41, lane 1 and 2). All six correctly targeted ES cell clones (IIIA1, IIIC1, IIIF3, IIIF7, IIIG2 and IIIG6) were subsequently expanded, and four of them were injected into C57Bl/6 blastocysts. Six male and four female chimeras were obtained and are currently tested for germline transmission of the targeted allele.

2.6 Studies on AC complexes from mouse tissues

The strong effect on migration tells us that ADF and cofilin must be regulated in a tight temporal and spatial manner. Apart from phosphorylation of Ser-3, which was shown to regulate AC activity (Morgan et al., 1993; Moriyama et al., 1996), interaction of AC with other proteins might have regulatory functions. For example, Cap1 and 2 and the protein 14-3-3ζ have been shown to interact with AC proteins. It is not clear yet whether cofilin/ADF have *in vivo* additional functions apart from regulating actin depolymerization. The role of the nuclear localization signal is unclear and one can speculate about a possible involvement of AC in the translocation of actin into the nucleus, where an involvement of actin in transcription regulation has been suggested.

We were interested in shedding some light on ADF and cofilin interactions, by characterizing novel components of ADF/cofilin complexes. As it has been shown before ADF and cofilin have a tissue-specific expression (see 2.1.1, and (Gurniak et al., 2005)). Thus, we wanted to compare isolated complexes from different tissues, using ADF/cofilin affinity chromatography. For this, it was necessary to generate recombinant proteins in good quantities, which then were coupled to a resin.

2.6.1 Use of GST-fusion molecules to purify ADF and cofilin complexes

A vector that expresses cofilin N-terminally linked to a GST-fusion molecule was already generated in the lab and generously provided by C. Gurniak (plasmid # 101). To generate an equivalent expression vector for ADF, I cloned the cDNA of ADF into the pGEX2T vector. The cDNA was obtained by reverse transcription of brain RNA. The DNA sequence was verified by sequence analysis. In order to have a valid control that points out unspecific binding, the empty vector pGEX2T was used, that expresses the GST protein alone.

Recombinant cofilin, ADF and GST were expressed by IPTG induction (see materials and methods).

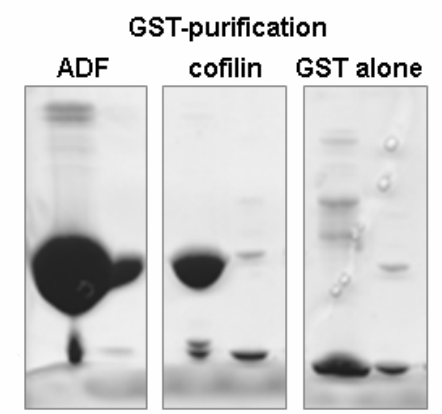

Figure 42: Purification of recombinant ADF, cofilin and GST from bacteria
The recombinant proteins were expressed in *E. coli* as GST fusion proteins. Proteins were purified from bacterial lysates using a Glutathione-sepharose column; Elution occurred in 15 mM glutathione/ 50 mM TRIS pH 8.0.

The recombinant proteins were prepared as fusion molecules, containing an N-terminal glutathione-S-transferase (GST) part. Using this feature, bacterial lysates were prepared and passed over a column with immobilized glutathione. Fusion proteins bound to the column were washed several times before elution with an excess of glutathione, competing for GST binding (Fig. 42).

To identify novel cofilin/ADF interaction partners, purified GST-proteins were immobilized with fresh glutathione sepharose. Lysates from thymus, brain and uterus were prepared and passed over the columns. Proteins with an affinity to ADF or cofilin bound to the column while other proteins passed through. After excessive washing, the resin was boiled in SDS sample buffer to elute all bound proteins that were then separated by gel electrophoreses (Fig. 43). Gel bands were excised and analyzed by mass spectrometry. To exclude unspecific binding to a resin or GST, a column with GST alone bound to it was used as a control.

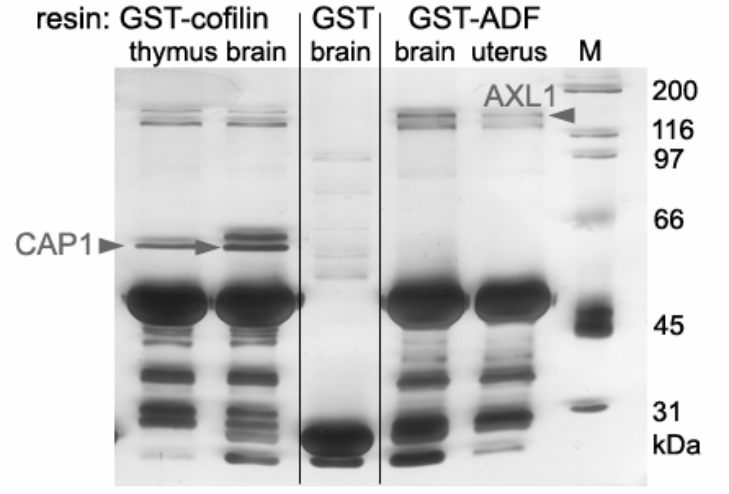

Figure 43: GST-Complexes of ADF and cofilin
Silver-stained protein gel showing GST-ADF and GST-cofilin complexes from brain, thymus and uterus. Ligands were identified by mass spectrometry.

The first experiment to identify new binding partners of ADF and cofilin yielded only two proteins in the complexes - CAP1, which had been already described to interact with cofilin (Moriyama and Yahara, 2002) - and AXL1, a putative protease that has not been characterized yet. In a second experiment I detected tubulin-β5 and a heterogeneous nuclear ribonucleoprotein (type M) in GST-cofilin complexes of the thymus and a serine/threonine-protein kinase, called PRP4m, and vimentin in GST-ADF complexes of the spleen. However, one main difficulty with this approach was the ubiquitous presence of GST fusion molecules that masks other proteins in the mass spectrometry analysis.

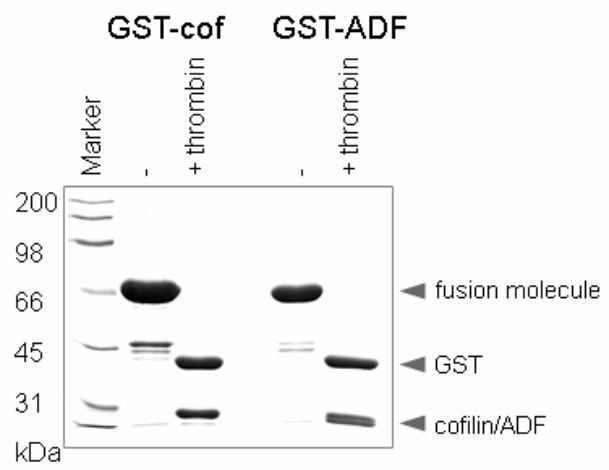

Figure 44: Thrombin cleavage of AC fusion molecules
Coomassie protein gel showing the cleavage of GST fusion. After the incubation of fusion molecules with thrombin, whereas two bands corresponding to the GST part and to ADF/cofilin were generated.

Therefore, I changed the strategy to purify the complexes by cleaving the GST-fusion molecules followed by purification of the authentic ADF and cofilin (Fig. 44). The cleaved proteins were purified using a cation exchange column (Macro S) (see materials and methods). ADF/cofilin was subsequently chemically linked to CNBr activated sepharose. In this nucleophilic substitution a covalent bond is established between the sepharose and primary amines of protein side chains, thus immobilizing the protein in different orientations on the sepharose. Again lysates of brain and thymus were passed over the columns. After washing, ligands were eluted directly in SDS sample loading buffer and separated by gel electrophoresis (Fig. 45).

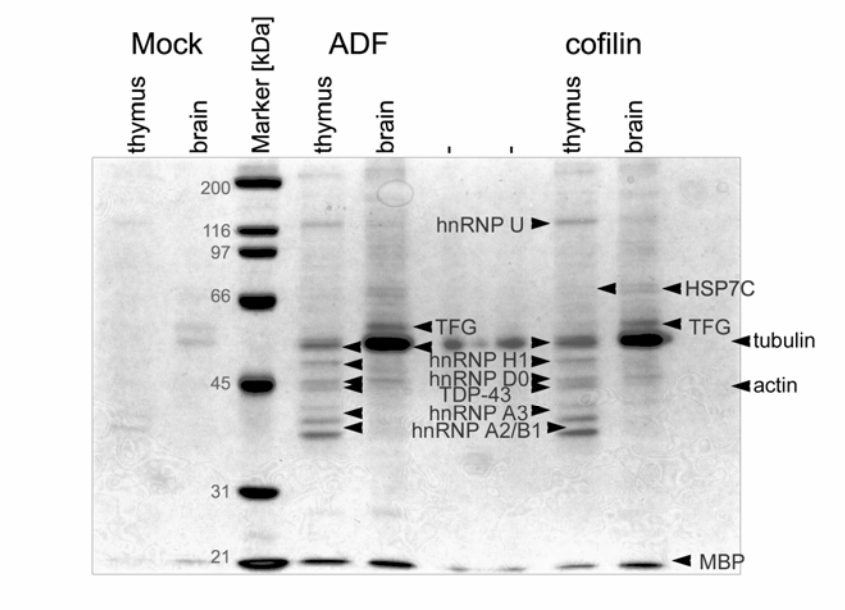

Figure 45: Covalent complexes of ADF and cofilin
Coomassie-stained protein gel showing ADF and cofilin complexes from mouse brain and thymus. Ligands were identified by mass spectrometry.

Following this approach, more potential interaction partners of cofilin and ADF could be identified. Interestingly, we detected a class of heterogeneous nuclear ribonucleoproteins (A2/B1, A3, D0, H1 and U) that were found in complexes, called ribonucleosomes and provide the substrate for the processing events that pre-mRNAs undergo before becoming functional, translatable mRNAs in the cytoplasm. Additionally we found another nuclear protein, named TAR DNA-binding protein-43 (TDP-43). TDP-43 binds to DNA and RNA and is probably involved in transcriptional repression (Ayala et al., 2005).
Moreover we could detect a heat shock cognate protein of 71 kDa, myelin basic protein (MBP) in cofilin complexes from the brain and a so far not characterised Trk-fused gene protein (TFG). Apart from this, I found proteins of the cell cytoskeleton, like β,γ-actin and α,β-tubulin.
The complete list of identified AC ligands is depicted in the following table. It lists the name of the protein, their accession number as well as the approach, by which the proteins were isolated (GST or covalent). In addition, I listed the score in mass spectrometry and the complex, in which the proteins were detected:

Table 2: List of proteins identified in ADF/cofilin complexes

Gene name	Accession number	Approach	Score	Complex	Tissue	Detected at [kDa]
CYTOSKELETON:						
Adenylyl cyclase associated protein 1						
CAP1	P40124	GST	81	cof	brain/thymus	~ 50
β-Actin						
ACTB	P60710	GST/cov.	36/73	cof/ADF	brain/thymus	~ 45
γ-Actin						
ACTC	P63260	cov	36/74	cof/ADF	brain/thymus	~ 45
Tubulin-α						
TBA1	P68369	cov	209	cof/ADF	brain	~ 50
Tubulin-β3						
TBB3	Q9ERD7	cov	317/400	cof/ADF	brain/thymus	~ 50
Tubulin-β5						
TBB5	Q91575	GST	90	cof	thymus	~ 50
Vimentin						
Vimentin	P20152	GST	6.7	ADF	thymus	~ 50
NUCLEAR:						
Heterogeneous nuclear ribonucleoprotein M						
hnRNP M	Q9D0E1	GST	42	cof	thymus	~ 78
Heterogeneous nuclear ribonucleoprotein H1						
hnRNP H1	Q8C2Q7	cov	919	cof/ADF	thymus	~ 48
Heterogeneous nuclear ribonucleoprotein D0						
hnRNP D0	Q60668	Cov	69	cof/ADF	thymus	~ 46
Heterogeneous nuclear ribonucleoprotein A3						
hnRNP A3	Q8BG05	cov	45	cof/ADF	thymus	~ 38
Heterogeneous nuclear ribonucleoprotein A2/B1, isoform 2						
hnRNP A2/B1	gi|32880197	cov	75	cof/ADF	thymus	~ 37
Heterogeneous nuclear ribonucleoprotein U						
hnRNP U	Q8C290	cov	152	cof	thymus	~ 140
Serine/Threonine-proteine kinase PRP4m						
PRP4m	gi|1399464	GST	46	ADF	spleen	~ 130
TAR DNA-binding protein-43						
TDP-43	Q921F2	cov	381	cof/ADF	thymus	~ 43
MISCALLANEOUS:						
Trk-fused gene						
TFG protein	Q9Z1A1	cov	129	cof/ADF	brain	~ 54
Myelin basic protein						
MBP	P04370	cov	63	cof	brain	~ 22
Heat shock cognate 71 kDa protein						
HSP7C	P63017	cov	77	cof	brain/thymus	~ 71
Putative protease						
AXL1	gi|728939	GST	1	ADF	uterus	~ 130

3 DISCUSSION

20 years after the discovery of the first actin-depolymerizing factor, the distinct *in vivo* functions of these proteins in mammels are poorly understood. Their essential role has been demonstrated by the lethal phenotype of the cofilin gene deletion in mice (Gurniak et al., 2005).

Interestingly, ADF, the biochemically more active actin depolymerizing factor, seems to play a distinct role *in vivo*. The rather mild phenotype of ADF mutant mice (Smith et al., 1996; Wang et al., 2001) and my results presented here indicate that these two highly conserved AC proteins are involved in distinct pathways. Together with the developmental- and tissue-specific expression, these findings nourish the idea that different actin depolymerizing factors may perform specific tasks, which are controlled by distinct protein ligands.

3.1 Cofilin, to be or not to be?

In my thesis I had to first develop a strategy to circumvent a common problem using conditional mutagenesis in the myeloid system of the mouse. Cre-models that had been described to be efficient in the deletion of floxed alleles in macrophages, like LysMCre or CD11bCre, proved to be unsuitable in the case of the conditional cofilin allele. Neither of these two strains yielded efficient deletion of the cofilin allele.

There are several explanations that could explain these findings. First, the cofilin locus might not be easily accessible for the Cre-recombinase. Several studies have shown that gene excision depends on the accessibility of the loxP-flanked locus. In a comparative study using two differentially regulated Cre-recombinases in combination with five different Cre responder strains, Hara-Kaonga et al. convincingly showed that Cre-recombination is highly variable and strongly depends on the locus of the target gene (Hara-Kaonga et al., 2006). Variances in recombination might be caused by the distance between the two loxP sides, the transcriptional activity of the locus or the overall chromatin structure. However, several findings argue against this explanation in the case of cofilin: First, cofilin is strongly expressed (see 2.1.1), thus a constant transcriptional activity is expected at the cofilin locus. Secondly, the use of other Cre-expressing strains, like NestinCre or CD4Cre (personal communication, C. Gurniak and W. Witke), showed that cofilin can be deleted with a high efficiency, arguing against the inaccessibility of the locus.

Another explanation for this phenomenon could be counter-selection upon deletion of an essential gene. In general, reporter lines, like ROSA26 or reporter EYFP strains are being used to verify deletion efficiency; and activation of LaqZ or YFP expression does not affect cell homeostasis. Contrarily to this, cofilin deletion has severe effects on the cell physiology. One can expect that there is great selective pressure against the deletion of this gene, while in the case of reporter lines the recombination can occur freely leaving the cell almost unaffected. This hypothesis is supported by the finding that cofilin depletion (by the use of CD4Cre or CD19Cre) in developing T and B lymphocytes results in an almost complete block in lymphocyte development in the thymus and bone marrow. However, in the periphery of these mice populations of wild type B and T cells can be found (personal communication, Witke group). The disadvantage of cells lacking cofilin is so severe that only cells that escaped deletion contribute to the lymphocyte pool.
The same could be true for the deletion of cofilin in macrophages using LysMCre and CD11bCre.

Taken together, it has become clear that the success of a Cre/loxP-mediated approach does depend on the recombination of a locus that does not negatively affect the cellular homeostasis. In the case of LysMCre and CD11bCre cofilin conditional mice this selection occurs continuously as hematopoetic stem cells (HSC) develop into macrophages, so that the pool of differentiated macrophages consists of many cells that “escape” recombination.
To circumvent problems related to the adaptation the use of an inducible system, like Mx1Cre, was a logical consequence. In this model, the sudden induction of type I interferons acts on all cells, boosting the expression of Cre-recombinase. Also in this model, I observed “escaper” cells, which become more and more dominant in bone marrow cultures over time (see 2.2.5). However, initial synchronised deletion of cofilin in more than 90% of macrophage precursor cells allowed me to set up a system to study the role of cofilin in macrophages. One draw-back of the Mx1Cre-driven gene recombination is that deletion also occurs with good efficiency in the liver, spleen and the gut (Schneider et al., 2003). As it was shown for the complete cofilin knockout, systemic deletion of cofilin results in the death of the animal (Gurniak et al., 2005). Also in Mx1Cre cofilin conditional mice the systemic deletion of cofilin was lethal, so that this approach could not be used for immunological experiments in the mouse. Once more these results underline the essential function of cofilin in cells as other studies showed that long term gene ablation mice of genes that are dispensable for the survival and homeostasis of cells, such as Rac1 or BMK/ERK5 is tolerated using the Mx1Cre conditional approach (Hayashi et al., 2004; Wells et al., 2004).

It should be noted that the use of recombinant HTNC was another successful approach to deplete cofilin in macrophages (see 2.2.6). This method yielded high deletion efficiencies, but HTNC treatment strongly activated macrophages and showed cytotoxic effects at high concentrations (Peitz et al., 2002). Therefore, in this study HTNC-driven deletion was only used as a tool to independently confirm results obtained with other deletion approaches.

3.2 Actin-depolymerizing factors and macrophage function

For the first time, it was possible to study cofilin$^{-/-}$ and ADF$^{-/-}$ bone marrow derived macrophages and one unexpected outcome of my experiments was that ADF and cofilin play distinct roles in regulating macrophage morphology and cytoskeletal rearrangement. While ADF$^{-/-}$ macrophages were slightly elongated, cofilin depleted macrophages accumulated filamentous actin and failed to polarize. Wild type macrophages express cofilin about 8-fold higher than ADF (see 2.1.1). However, a publication by Pope et al. showed that ADF is the more active actin depolymerizing factor *in vitro* (Pope et al., 2004). Therefore, it was unexpected that cofilin but not ADF played an essential role in modulating macrophage morphology (see 2.3.2).

The depletion of F-actin modulating proteins has been shown before to affect macrophage morphology, suggesting that the actin cytoskeleton is the major structure to determine cell shape. For instance, the depletion of gelsolin, an actin severing protein, in osteoclasts renders the cells incapable of establishing podosomes (Chellaiah et al., 2000). In macrophages lacking the actin filament capping protein CapG a decrease in spontaneous membrane ruffling was observed (Witke et al., 2001).

Moreover, molecules that act in signalling cascades upstream of AC proteins were found to alter macrophage morphology. A dominant negative mutant of LIMK1 leads to an increase in F-actin levels in macrophage-like U937 cells (Matsui et al., 2002). And BMM from mice lacking Rac molecules, which belong to the family of Rho-GTPases, show a different morphology compared to wild-type macrophages. Rac1$^{-/-}$ BMM have a smaller adhesive area and appear more elongated, while Rac2$^{-/-}$ BMM display a normal spreading but are also elongated. Interestingly, double knockout BMM that lack Rac1 and Rac2 show multiple thin protrusions rich in microtubular bundles but with few F-actin (Wheeler et al., 2006), suggesting that some effects caused by the single knockouts can be counteracted by the respective other Rac molecule. One could speculate that the effects on

macrophage morphology seen in the previously described studies might be caused by a disturbed regulation of cofilin. However, such conclusions are generally difficult to prove as these signalling molecules affect an array of downstream proteins that modulate the cytoskeleton.

BMM lacking ADF showed very mild morphological changes, which suggests that either ADF is dispensable for macrophages, or that cofilin attenuates possible consequences. Evidence for the second hypothesis comes from the finding that cofilin was up-regulated in $ADF^{-/-}$ macrophages (see 2.3.1). This indicates that the cells try to overcome their physiological disadvantage by counter-regulation of a similar protein. This behaviour can be found even more pronounced in macrophages lacking cofilin. These BMM strongly induced ADF. Nevertheless, ADF failed to ameliorate the effects caused by the ablation of cofilin. The high F-actin content observed in cofilin mutant macrophages suggests that cofilin is the main actin depolymerizing factor controling actin filament severing. This is in agreement with studies using cofilin antisense oligonucleotides that also induced F-actin formation (Adachi et al., 2002). These findings lead to the conclusion that cofilin can probably buffer some of the effects of the ADF deletion; however, even a strong ADF up-regulation does not make-up for the lack of cofilin. Also macrophages lacking both ADF and cofilin strongly resemble the phenotype of cofilin mutant cells. They also contained high levels of F-actin, failed to polarize and did not spread to a normal area.

Interestingly, I could show that none of the other tested actin-binding proteins, like CapG or gelsolin, was up-regulated upon AC protein deletion. This indicates that AC proteins are regulated in an independent pathway that does not involve CapG or gelsolin.

Cofilin and ADF are known to exclusively enhance the turnover of actin filaments and an interaction of AC proteins with microtubules has not been described. However, an alteration of the actin network could result in the modification of other cytoskeletal structures in the cell, as these structures are strongly interwoven. Microtubules, for instance, help establish and maintain cell polarity by promoting actin-dependent membrane protrusion at the leading edge of the cell, but the molecular mechanisms that mediate cross-talk between actin and microtubules during this process are unclear (Bershadsky et al., 1991; Vasiliev, 1991). Indeed, disruption of microtubules perturbs the polarity of the actin cytoskeleton (Omelchenko et al., 2002; Palazzo and Gundersen, 2002), whereas actin depolymerization does not affect the polarization of the microtubule cytoskeleton (Etienne-Manneville and Hall, 2001; Palazzo et al., 2001; Magdalena et al., 2003). The abnormal morphology and the accumulation of nuclei in cofilin

mutant macrophages made it difficult to judge the integrity of the microtubular network in macrophages lacking cofilin. Cofilin$^{-/-}$ macrophages often contained two or more kinetochores due to the cytokinesis defect. The microtubular network of macrophages lacking ADF was not altered (see 2.3.5).

The effect of AC protein depletion on the cytoskeletal network built from intermediate filaments was not assessed in this thesis. Intermediate filaments are tissue specific and not as conserved as the actin cytoskeleton or the microtubules. They are known to be more independently regulated, thus we did not expect a direct effect of AC protein deletion on this structure. To verify this speculation, additional experiments have to be performed that investigate the functionality of intermediate filaments in mutant macrophages.

3.3 Cell shape determines cell function?

Macrophages lacking cofilin showed several defects in essential cellular functions that could be due to an abnormal cell shape. These included proliferation, migration and antigen-presentation. Common for all these functions is the ability of a cell to polarize in a coordinated way and to establish an asymmetric distribution of membrane proteins. Polarization can be followed by the re-orientation of the cytoskeleton in the cell cortex. Actin filaments have to be nucleated or extended in a directed way (Wedlich-Soldner and Li, 2004). My results show that cofilin is a key regulator for cells to become polarized and that the lack of polarization is directly linked to cellular defects in cofilin mutant macrophages. Interestingly, cellular functions that do not require polarization were not impaired in macrophages lacking cofilin; for instance, the attachment of bone marrow cells and macrophages to plastic surfaces or the phagocytosis of particles.

3.3.1 Role of AC proteins in cell migration

Migration requires the continuous treadmilling of the filaments in order to push the membrane forward and to translocate the cell body (Borisy and Svitkina, 2000). Using caged cofilin that can be photo-activated Ghosh et al. showed that cofilin acts as a “steering wheel” of the cell. Local cofilin activation generates cell surface protrusions and sets the direction of cell motility (Ghosh et al., 2004).

ADF$^{-/-}$ macrophages contained a high proportion of polarized cells in cultures. On the contrary, macrophages lacking cofilin completely failed to polarize, which correlated with undirected accumulation of cortical F-actin underneath the

plasma membrane. A similar observation was made in the case of Wiskott-Aldrich Syndrome (WAS), an X-linked recessive disorder, caused by a mutation in the WAS protein (WASP, (Derry et al., 1994)). WAS is characterized by low platelet counts and immunodeficiencies (Kirchhausen, 1998), caused by defects in migration of myeloid cells (Ochs et al., 1980; Binks et al., 1998). Different to the phenotype observed in macrophages lacking cofilin, WASP mutant macrophages migrate at normal speed, but fail to orientate in a chemotactic gradient (Badolato et al., 1998; Zicha et al., 1998). This defect in chemotaxis of $WASP^{-/-}$ macrophages in response to a stimulus is probably due to a lack of new actin filament nucleation (Linder et al., 2000). This example shows that a dysfunction in polarization contributes to a defective chemotactic response. However, in contrast to the cofilin mutants, WASP mutant macrophages are not affected in their random migration. This might be explained by the fact that the cytoskeleton and morphology of WASP mutant cells as such is not affected, whereas macrophages lacking cofilin already contain large amounts of stable F-actin that arrests the cells.

3.3.2 Role of AC proteins in phagocytosis and antigen presentation

Macrophages lacking AC molecules showed no impaired phagocytosis, in fact BMM lacking cofilin showed a slightly increased phagocytotic activity. A similar observation was made by Adachi et al, who showed that cofilin depletion using antisense oligonucleotides enhances the phagocytic activity of J774.1 cells (Adachi et al., 2002).

In general, phagocytosis is thought to involve the spatial and temporal reorganization of the actin cytoskeleton at the sites of particle engulfment. The current model of internalisation requires four steps (May and Machesky, 2001): First the particle tethers via receptors to the macrophage membrane. This triggers an actin independent membrane protrusion around the particle. In the third step an actin dependent stabilization of the phagocytic cup occurs and the actin network pushes the plasma membrane around the particle (May et al., 2000). Last, the plasma membrane fuses around the particle.

I also found that the first two steps of particle engulfment are actin independent and thus unaffected in macrophages lacking AC molecules. Instead, formation of the phagocytic cup requires F-actin assembly and the final internalization requires actin re-modelling. Lacking cofilin doea not seem to interfere with phagocytic cup formation. In fact, kinetics are faster in macrophages that already contain high levels of F-actin. However, microscopical analysis suggested that the phagocytic cup was stable in cofilin mutant cells providing

evidence that the cells might have a defect in the very last step of resolving the structure. Moreover, this approach to study phagocytosis only focuses on the up-take of a particle. Yet phagocytosis does not end with the up-take of a particle but requires subsequent steps of vesicle transport and modification until a phagolysosome is established. It is only there, that particles are degraded and eventually further processed for antigen presentation.

When antigen presenting cells engulf a pathogen or a foreign structure, they become activated and process foreign proteins in their proteasomes to short peptides. These are presentated in MHC class II molecules to T lymphocytes in order to evoke a cellular immune response. In this multi-step process, I investigated the ability of AC mutant cells to induce a T cell response. In order to circumvent indirect effects of an affected phagocytic activity I used transgenic T cells which recognize a specific peptide from white egg ovalbumin that was added to the cultures. Free MHC class II molecules on the surface of the dendritic cells can bind this peptide and present it directly to T cells, without the requirement of the DC to engulf and process the Ovalbumin protein. Dendritic cells lacking cofilin were severely impaired in inducing a T cell response; instead depletion of ADF did not have an influence on the efficacy of T cell activation. FACS analysis revealed that ADF and cofilin mutant dendritic cells expressed comparable amounts of MHC class II and co-stimulatory molecules, like CD80 and CD86 on their surface, suggesting that the observed differences resulted from a different physiological property.

Antigen presentation requires the establishment of an immunological synapse, a membrane structure that is highly organized and allows the DC to activate naïve T cells. The T cell recognizes through its T cell receptor the peptide:MHCII complex but also requires a second costimulatory signal through additional molecules in order to become fully activated. These two signals have to be presented in a spatially organized manner. Therefore, the actin cytoskeleton has to serve as a platform that dynamically orientates the surface molecules to the right location. Recent studies showed that a sustained actin cytoskeleton rearrangement is necessary for the establishment of a stable immunological synapse (Faure et al., 2004; Billadeau and Burkhardt, 2006; Muller et al., 2006). Dendritic cells lacking cofilin can neither re-model their cytoskeleton nor can they polarize to support the formation of the immunological synapse, which can explain the impaired capacity to mediate T cell activation. Interestingly, inhibition of cofilin on the T cell side using cofilin peptide homologues showed a similar result (Eibert et al., 2004).

3.3.3 A potential role of ADF/cofilin in cell cycle progression

The actin cytoskeleton is also a key regulator of cell cycle progression in eukaryotic cells. In particular the final step in cell division, called cytokinesis, requires the correct regulation of cytoskeletal molecules to allow an equal distribution of cellular contents to both daughter cells (Glotzer, 2005).
The involvement of ADF/cofilin proteins in cell division has been shown in a number of models. In several tumor types (colorectal cancer, pancreatic adenocarcinoma cells) cofilin has been found to be overexpressed (Sinha et al., 1999; Stierum et al., 2003) and inhibition of tumor growth by the use of chemotherapeutic reagents revealed that cofilin expression is reduced (Cecconi et al., 2003). Furthermore, a novel cofilin phosphatase, called chronophin regulates cofilin activity in a precise cell cycle dependent manner (Gohla et al., 2005). In fission yeast ADF1, the sole actin depolymerizing factor, is essential for the formation of the contractile ring during cytokinesis; depletion as well as overexpression of ADF1 results in a failure of cytokinesis (Nakano and Mabuchi, 2006).

I investigated several aspects of cell cycle progression in ADF and cofilin mutant macrophages. Macrophages lacking cofilin had a severe proliferation defect (see 2.3.7) that is likely to be caused by a cytokinesis defect, resulting in multi-nucleated cells (see 2.3.7.1). In agreement with this, cells seemed to have a block in G2/M phase transition, suggested by the reduced phospho-histone H3 level compared to control cells (see 2.3.7.2). On the other hand, macrophages lacking ADF showed no proliferation defects.

Histone phosphorylation is required for chromosome condensation prior to cell division (Hendzel et al., 1997; Goto et al., 1999; Preuss et al., 2003). One could speculate that this block in G2/M transition is an indirect consequence of the cytokinesis defect and the accumulation of nuclei inside the cells. Already at day 3, cofilin mutant cultures contained significantly more cells with two nuclei compared to control cells (data not shown). However, even at later time points only 5% of multinucleated cells (>2 nuclei) were found in cofilin mutant cultures, indicating that bi-nucleated cells divide less frequent and thus have a block in mitosis.

A last possibility to explain the proliferation defect observed in cofilin mutant macrophages is a yet unknown role of cofilin in the nucleus. As described before, cofilin contains a nuclear localization sequence and was found already in 1987 to be a component of nuclear actin rods (Nishida et al., 1987). More evidence that cofilin might play a yet uncharacterized role in transcriptional regulation derives from the experiments I performed to identify novel AC protein interaction partners and will be discussed in the following chapter.

3.4 ADF/cofilin complexes: novel partners for “old” fellows?

Using a proteomics approach, I detected several novel ADF and cofilin ligands. Actin was found in almost all experiments serving as a positive control for a successful affinity purification.

In addition, I detected CAP1 in the cofilin complexes. CAP1 has been shown to directly cooperate with cofilin in a native high molecular weight complex in yeast (Balcer et al., 2003) and several other studies using mammalian cells confirmed the close relationship of CAP1 and cofilin (Moriyama and Yahara, 2002; Bertling et al., 2004). Interestingly, CAP1 was not detected in ADF complexes, which suggests that this protein might specifically interact with cofilin. At the same time this finding provides evidence that ADF and cofilin can be found in different pathways as suggested by the knockout experiments.

Interestingly, a number of nuclear proteins were found in the AC complexes that have not been described to cooperate with cofilin or ADF yet. The identified proteins mainly belong to the class of heterogeneous nuclear ribonucleoproteins (hnRNP), but also a kinase named PRP4m and a TAR binding protein were purified with the complexes.

PRP4m, found in a ADF complex, is the mammalian homologue of a serine/threonine kinase originally found in yeast (Bjorn et al., 1989). In yeast, PRP4 has been shown to be a component of the small ribonucleoprotein particle U4/U6 and to be involved in pre-mRNA splicing (Rosenberg et al., 1991). The identification of a potential kinase that could inactivate ADF in the nucleus is interesting as also the role of AC proteins in the nucleus remains to be elucidated. However, it seems conceivable that AC proteins need to be regulated by specific kinases/phaosphatases also in the nucleus to guarantee their proper function.

TAR binding protein-43 (TBP-43) has first gained attention as a protein that specifically binds to TAR DNA, a regulatory element in the long terminal repeat of HIV. There it can repress HIV-1 gene expression *in vivo* and *in vitro* (Ou et al., 1995). Just recently, a comparative study between TBP-43 proteins from *C. elegans*, *D. melanogaster* and human revealed that TBP-43 in humans and in fly is capable of exon recognition while the worm protein has no effect on exon regulation. Being involved in RNA processing, TBP-43 can be considered an hnRNP, another group of proteins found in ADF/cofilin complexes.

Heterogeneous nuclear ribonucleoproteins (hnRNP) are involved in various nuclear events (Dreyfuss et al., 2002). They are best characterized by their function in transcriptional regulation (Tomonaga and Levens, 1995), splicing

(Caceres et al., 1994; van der Houven van Oordt et al., 2000) and 3'-end processing (Minvielle-Sebastia et al., 1998), for which they bind in various complexes co-transcriptionally to pre-mRNA and many of them remain bound all the way to the ribosomes. The composition of the hnRNP proteins is largely determined by the RNA sequence. The proteins detected in ADF/cofilin complexes have been associated to specific steps of RNA processing: hnRNP A2/B2, H and M are involved in RNA splicing, hnRNP D acts during recombination events and determines mRNA stability, hnRNP U keeps the RNA inside the nucleus until it is finally processed and hnRNP A3 is involved in the cytoplasmatic transport of mRNA. Moreover hnRNP participate in telomere length maintenance (Ishikawa et al., 1993; Eversole and Maizels, 2000) and immunoglobulin gene recombination (Dempsey et al., 1999). Co-purification of hnRNP depends on the presence of RNAs, as RNase digest results in the dissociation of the proteins. Thus, it is not clear yet whether ADF/cofilin molecules directly interact with these proteins or whether they are part of a larger complex, associated with hnRNP.

Actin might be such a bridge. Pendleton et al. showed that cofilin actively transports actin into the nucleus (Pendleton et al., 2003). A physiological role of actin inside the nucleus has been doubted for a long time, since actin is an abundant cellular protein with a high potential for non-specific interactions. However, recent studies provide evidence that actin participates in several nuclear events (Bettinger et al., 2004). Most interesting, with regard to AC complexes, was the finding that actin interacts with hnRNP at sites of active transcription (Percipalle et al., 2001; Percipalle et al., 2003; Kukalev et al., 2005). Moreover, evidence provided by Wu et al. suggests that actin polymerisation might facilitate transcription (Vieu and Hernandez, 2006; Wu et al., 2006). For a long time, the presence of filamentous actin in the nucleus was ruled out since phalloidin staining of cells did not give any positive signal inside the nucleus. The use of a novel antibody, however, resulted in a dotty pattern inside the nucleus, providing evidence for a nuclear localization of actin and supporting the hypothesis that short unconventionally organized F-actin might play a role in this compartment (Gonsior et al., 1999).

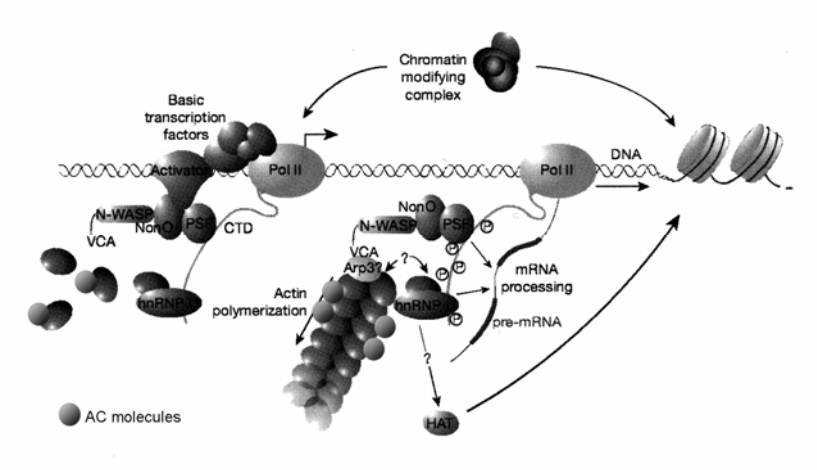

Figure 46: Hypothetical involvement of AC proteins in nuclear actin regulation
AC proteins may regulate actin appearance in the nucleus. Actin is thought to modulate transcription as a component of transcription pre-initition, chromatin remodelling and hnRNP complexes. (modified, taken from Fig. 1 (Vieu and Hernandez, 2006)

It is tempting to speculate that ADF/cofilin serve not only as a carrier for actin into the nucleus, but that they might also be involved in the regulation of the actin structure to modulate some of the newly described functions of actin in the nucleus (see Fig. 46). However, a more detailed analysis will be required to provide evidence and support for this hypothesis. The study of complexes from nuclear extracts could be a way to determine if these interactions really occur in the nucleus. Moreover, immuno-precipitations could offer an appropriate way to prove that endogenous AC proteins are found in complexes regulating transcription.

3.5 Are ADF and cofilin redundant proteins *in vivo*?

In the literature, it is frequently referred to ADF and cofilin as “redundant proteins” and in many experiments little attention was paid to which protein was used. These proteins are highly conserved and antibodies that could discriminate between the two proteins were not at hand. However, the investigation of their biochemical properties showed for example that ADF was able to depolymerize actin filaments faster than cofilin (Arima et al., 1998; Yeoh et al., 2002; Pope et al., 2004). Moreover, the expression patterns of ADF and cofilin have been found to be clearly distinct with ADF being highly expressed in epithelia, whereas cofilin was found to be almost ubiquitously expressed (Gurniak et al., 2005). And finally my analysis of the proteins using a genetic approach resulted in the finding that cofilin is an essential protein during embryogenesis, whereas ADF was dispensable for macrophage function.

In this study, I could show that cofilin, and at lower levels ADF were expressed in bone marrow derived macrophages and that the two proteins localized to regions with a high actin turn-over, like lamellipodia or focal adhesion sites. My analysis of AC complexes led to the conclusion that there exist specific interaction partners for both proteins, besides ligands that can interact with both proteins.

Here I could show for the first time that ADF and cofilin play distinct roles in primary murine macrophages. Macrophages lacking ADF were almost indistinguishable from control cells, whereas cofilin plays a pivotal function in cell polarization and subsequently influences a variety of cellular functions. Since ADF is expressed at lower levels than cofilin, a final answer whether ADF can replace cofilin, under endogenous cofilin expression and regulation, can only be answered after analysis of the transgene mouse that puts ADF under the control of the cofilin promoters upon Cre/loxP induced recombination.

The increasing numbers of publications that prove the importance of the actin cytoskeleton for immune cell function make clear that the underlying regulation of the cytoskeleton plays a yet poorly understood role in immune regulation.

The example of the Wiskott-Aldrich syndrome shows how actin dysregulation caused by a mutation in a single actin-binding protein can result in severe immune deficiencies (Aldrich et al., 1954; Jin et al., 2004). It is tempting to speculate that mutations in AC proteins or their regulation could have a similar impact on the immune system. However, one would expect to find a more severe outcome in the case of a cofilin dysfunction, whereas the strongest effects of an ADF mutation should be expected in epitheliar tissues rather than in immune cells. It will be interesting to see in the future if cofilin can be modified in order to gain control of certain immune cell functions.

4 MATERIALS AND METHODS

4.1 Materials

4.1.1 Glass, plastic and metal wares, laboratory equipment

Description	Source
Analytical balance	*Sartorius AG*, Göttingen
Autoclave	*Schlumbohm Medizintechnik*, Hamburg
Centrifuges	
Megafuge 1.0R, Megafuge 2.0R	*Haraeus-Sepatech,*Hanau
Eppendorf 5415C	*Eppendorf,* Hamburg
Eppendorf 5417R	*Eppendorf,* Hamburg
Avanti J25	*Beckmann*, Munich
Optima TL Ultracentrifuge	*Beckmann*, Munich
CO_2 incubator	*Heraeus Instruments*, Hanau
Confocal microscope „TCS NT“	*Leica*, Wetzlar
Cover slips (∅ 19 mm)	*VWR International*, Darmstadt
Critical Point Drier (CPD7501)	*Polaron/Quorum Technologies,* Sacramento, CA, USA
Cuvette (plastic) for photometer	*Brand*, Wertheim
Cuvette (quarz) for photometer	*Hellma*, Mühlheim
Dissection tools	*Dosch Medizintechnik*, Heidelberg
Douncer	*Kontes Glass Co*, Vineland, NJ, USA
ELISA 96 well pates (microlon)	*Greiner Bio-One GmbH*, Frickenhausen
ELISA reader „Lambda E“	*MWG Biotech*, Ebersberg
FACS Sorter „FACS Calibur“	*Becton Dickinson Immunocytometry Systems*, San Jose, CA, USA
Falcon tubes (15 ml, 50 ml)	*Becton Dickinson*, Heidelberg
Film cassettes	*Siemens*, Munich / *Rego*, Mühlhausen
Fluorescence microscopes	
Axioskop MC-80	*Zeiss*, Oberkochen
Axiovert 100TV	*Zeiss*, Oberkochen
Leica DMR	*Leica*, Wetzlar
Fluoroskan “Ascent FL”	*ThermoLabsystems*, Helsinki, Finland
FPLC “BioLogic Workstation”	*BioRad, Munich*
Footpad measurement device	*Kroeplin GmbH*, Schlüchtern
Gelchambers	
DNA	*EMBL workshop*, Heidelberg
Protein “Mighty small II, SE250/SE260”	*Hoefer/Serva*, Heidelberg
Heatblocks	
“Thermomixer 5436, Thermomixer Compact”	*Eppendorf*, Hamburg
Kodak® BioMax X-Omat AR Film, MR	*Sigma-Aldrich*, Steinheim
Laminar Airflow Cabinet (Lamin Air HB2448)	*Haraeus Instruments*, Hanau
MACS pre-separation filter	*Miltenyi Biotec*, Bergisch Gladbach
MACS separation columns LS	*Miltenyi Biotec*, Bergisch Gladbach
Microscope “Wilovert”	*Hund*, Wetzlar
Microscope slides (SuperFrost Plus)	*Roth*, Karlsruhe
Migration slides (μ-Slide I)	*Ibidi/Integrated BioDiagnostics,* Munich
Needles	*Braun*, Melsungen
Neubauer Chamber	*Brandt*, Melsungen
Nitrocellulose Membrane „GeneScreen Plus“	*Schleicher&Schuell/Whatman,*Kent,UK
PCR machine (PTC-200)	*MJ Research, BioRad*, Munich
Petri dishes	*Sarstedt*, Nürnbrecht
Pipettes	*Gilson,* Bad Camberg
pH meter „MP225“	*Mettler Toledo*, Greifensee, Switzerland
Photometer	*Brandt*, Wertheim
Phosphoimager “BAS 1500 Scanner”	*Fujifilm,* Düsseldorf
Phosphoimagerscreen „BAS cassette 2040“	*Fujifilm,* Düsseldorf

PVDF membrane (Immobilon-P)	*Millipore*, Bedford, MA USA
Raster electron microscope (PSEM 500)	*Philips,* Eindhoven, The Netherlands
Serological Pipets (2, 5, 10, 25, 50 ml)	*Falcon/Becton Dickinson*, Heidelberg
Sonicator "Sonopuls GM200"	*Bandelin*, Berlin
Sterile filters (pore size 0,22 μm and 0,4 μm)	*Millipore*, Bedford, MA USA
Steri-Cups	*Millipore*, Bedford, MA USA
Syringes	*Braun*, Melsungen
Water purification system "Milli-Q"	*Millipore*, Bedford, MA USA
Western Blotting Apparatus (Trans-Blot SD)	*BioRad*, Munich

4.1.2 Chemicals

All chemicals were purchased from the companies *Fluka* (Neu-Ulm), *Merck* (Darmstadt), *Roth* (Karlsruhe) or *Sigma* (Deisenhofen) if not noted otherwise.

4.1.2.1 Reagents for molecular biology

Description	Source
^{32}P-dGTP (3000 Ci/mM)	*Amersham/GE Healthcare*, Munich
Agarose	*Invitrogen*, Karlsruhe
Bacto Agar	*Merck*, Darmstadt
Bacto Tryptone	*Difco*, Detroit, MI, USA
BigDye 3.1 sequencing mix	*Applied Biosystems*, Foster City, CA, USA
BioGel P-6 DG	*BioRad*, Munich
Bovine serum albumin (BSA), Fraction V	*Boehringer Mannheim*, Mannheim
Bromphenol blue	*BioRad*, Munich
Deoxyribonucleoside triphosphates (dNTPs)	*Promega*, Milan, Italy
DNA marker	
λ DNA/ *Eco*91I (*Bst*EII)	*MBI Fermentas*, St. Leon Roth
ΦX174, RF DNA (*Hae*III)	*Invitrogen*, Karlsruhe
1kb Plus DNA Ladder	*Invitrogen*, Karlsruhe
EndoFree plasmid maxi preparation kit	*Qiagen*, Hilden
Gel Extraction Kit (QiaexII)	*Qiagen*, Hilden
Wizard plus plasmid mini preparation kit	*Promega*, Milan, Italy
Yeast extract	*Difco*, Detroit, MI, USA
Xylene Cyanol FF	*BioRad*, Munich
Plasmidvektoren:	
p1.ON$_6$ (#92)	Prepared by C. Gurniak, contains the cofilin probe used in Southern blots.
pTriEx-1 **HTNC**	Prepared and kindly provided by Dr. Edenhofer, *Institute for Genetics, University of Cologne* Contains the HTNC-recombinase that can be expressed in DE3pLacI bacteria.
pFLRT-*Asc*I (#271)	Prepared by J. Sutherland, based on the original pFLRT vector that now contains an *Asc*I restriction site at the position of the former *Asp*718 site.
pΔ6.0 (#88)	Prepared by C. Gurniak, contains a 6 kbp long genomic fragment of cofilin that can be obtained by *Hind*III digest.

ADF subclone(#427)	Prepared by J. Rientjes using ET recombination, genomic sequence of the ADF gene (starts 1. intron, ends after the polyA signal; BAC clone RP2377A2) was introduced into the vector backbone.
cofilin right arm subclone (426)	Prepared by J. Rientjes using ET recombination, genomic sequence downstream of the cofilin gene (BAC clone RP23389K5) was introduced into the vector backbone.
pDRIVE	TA subcloning vector, *Qiagen*, Darmstadt
pGEX2T-cofilin (#101)	Prepared by C Gurniak, contains the cDNA of cofilin n-terminally fused to GST (from pGEX2T).
pGEX2T (#87)	*Clontech Inc.*, USA Bacterial expression vector that generates an N-terminal fusion to GST.
Enzymes:	
Klenow polymerase	*New England Biolabs*, Frankfurt
Alkaline phosphatase, calf intestinal (CIP)	*New England Biolabs*, Frankfurt
Proteinase K	*Merck,* Darmstadt
Restriction endonucleases:	*New England Biolabs*, Frankfurt
*Asc*I (10 U/µl)	5´-GG'CGCGCC-3´
*Bam*HI (20 U/µl)	5´-G'GATCC-3´
*Bst*BI (20 U/µl)	5´-TT'CGAA-3´
*Eco*RI (20 U/µl)	5´-G'AATTC-3´
*Hin*dIII (20 U/µl)	5´-A'AGCTT-3´
*Sal*I (10 U/µl)	5´-G'TCGAC-3´
*Sma*I (20 U/µl)	5´-CCC'GGG-3´
*Xba*I (20 U/µl)	5'-T'CTAGA-3´
*Xho*I (20 U/µl)	5´-C'TCGAG-3´
T4-DNA-Ligase (5 U/µl)	*MBI Fermentas*, St. Leon-Rot
T4-DNA-Ligase buffer	*MBI Fermentas*, St. Leon-Rot
Taq-DNA-Polymerases	
GoTaq Flexi DNA Polymerase	*Promega*, Milan,Italy
Expland Plus	*Roche*, Mannheim
Oligonucleotide primers:	*Metabion*, Martinsried
Primers for cofilin PCR (3XPCR)	
CoIn-Sma5'	5´-CGC TGG ACC AGA GCA CGC GGC ATC-3´
Cof NTS-3'a	5´-CAT GAA GGT TCG CAA GTC CTC AAC-3´
CoIn2-5'a	5´-CTG GAA GGG TTG TTA CAA CCC TGG-3´
Primers for Mx1Cre PCR	
Mx-CreF	5´-CAT GTG TCTTGG TGG GCT GAG-3´
Mx-CreR	5´-CGC ATA ACC AGT GAA ACA GCA T-3´
Primers for ADF PCR	
ADF150'-3'	5´-GAA GAA GGC AAA GAG ATC TT-3´
ADF Int-2-5'	5´-CTA CCT AAA GGG CAT CCT TTC-3´
LacZ-3'	5´-GAT TAA GTT GGG TAA CGC C-3´
dpN_6 (90 O.D. U/µl)	*Pharmacia*, Uppsala, Sweden

The primers used for the cloning of the constructs are listed in chapter 2.2.1.17 and 2.2.1.18.

4.1.2.2 Reagents for biochemical operations

Description	Source
Acrylamide (30%)/Bisacrylamide (0.8%)	*BioRad*, Munich
Ammoniumpersulfate (APS)	*Sigma*, Deisenhofen
Prestained MW-Marker, "SeeBlue Plus 2"	*Invitrogen*, Karlsruhe
Benzonase	*Novagen*, Schwalbach
Bovine serum albumin (BSA), Fraction V	*Boehringer Mannheim,* Mannheim
CNBr activated Sepharose 4B	*Amersham/GE Healthcare*, Uppsala, Sweden
Coomassie Brillant Blue R250	*BioRad*, Munich
ECL	*Amersham/GE Healthcare*, Uppsala, Sweden
Glutathione sepharose 4B	*Amersham/GE Healthcare*, Uppsala, Sweden
Glycine	*Sigma*, Deisenhofen
Imidazole	*Sigma*, Deisenhofen
Lysozyme	*Sigma*, Deisenhofen
Macro-Prep high S Support (MacroS)	*BioRad,* Munich
β-Mercaptoethanol	*Sigma*, Deisenhofen
MES	*Merck*,Darmstadt
Milk powder	*Roth*, Karlsruhe
Nickel sepharose	*Qiagen*, Darmstadt
Protein Markers:	
SeeBlue Plus2 Prestained Standard	*Invitrogen*, Karlsruhe
PageRuler Prestained Protein Ladder	*Fermentas*, St. Leon Roth
Proteinase Complete Inhibitor, EDTA-free	*Roche*, Mannheim
Sucrose	*VWR International*, Darmstadt
L-Tartaric acid (disodium salt)	*Sigma*, Deisenhofen
TEMED	*BioRad*, Munich
Tetramethylbenzidin (TMB)	*Roth*, Karlsruhe
TritonX-100	*Boehringer Mannheim*, Mannheim
Tween20	*Sigma*, Deisenhofen
Thrombin	*Serva*, Heidelberg
ELISA-Kits:	
DuoSet IFNγ ELISA kit	*R & D Systems*, Wiesbaden
DuoSet IL-2 ELISA kit	*R & D Systems*, Wiesbaden

4.1.2.3 Cell culture operations

Description	Source
β-Mercaptoethanol	*Sigma*, Deisenhofen
Dimethyl sulfoxide (DMSO)	*Sigma*, Deisenhofen
DMEM cell culture medium	*Gibco/Invitrogen*, Karlsruhe
Fetal calf serum (FCS)	*Gibco/Invitrogen*, Karlsruhe
FITC-Zymosan	Prepared by W.Witke
Gentamycin	*PAA*, Linz, Austria
HBSS	*Gibco/Invitrogen*, Karlsruhe
HEPES	*Gibco/Invitrogen*, Karlsruhe
Human M-CSF	generous gift from *Genetics Institute*, Boston
Immersion Oil	*Leica*, Wetzlar
L-Glutamine	*PAA*, Linz, Österreich
Non-essential amino acids	*Gibco/Invitrogen*, Karlsruhe
OVA Peptide $Ova_{323-339}$, HPLC purified (ISQAVHAAHAENEAGR)	*Sigma*, Deisenhofen
PBS	*Gibco/Invitrogen*, Karlsruhe
Penicillin/Streptamycin	*Gibco/Invitrogen*, Karlsruhe
polyI:C (27-4732)	*Amersham/GE Healthcare,*
RPMI 1640 culture medium w/o L-glutamine	*PAA*, Linz, Austria
Thioglychollate medium	*DIFCO laboratories/BD,* Heidelberg

Triton-X100	*Boehringer Mannheim,* Mannheim
Trypsin	*Gibco/Invitrogen*, Karlsruhe
Kits:	
BrdU Labeling & Detection. kit II	*Roche,* Mannheim
CyQuant Proliferation Assay	*Molecular Probes/Invitrogen*, Karlsruhe
LIVE/DEAD Assay	*Molecular Probes/Invitrogen*, Karlsruhe
PAN T cell kit	*Miltenyi Biotec*, Bergisch Gladbach
DEADEnd Fluorometric TUNEL system	*Promega,* Milan, Italy
Vybrant Phagocytosis Assay	*Molecular Probes/Invitrogen*, Karlsruhe

4.1.3 Cell lines

The following cell lines were used in this work:

Name	Derived from	Description
IB10	Sv129	ES cells used for targeting
EF	C57BL/6	embryonic feeder cells
L929	C3H	subcutaneous areolar and adipose tissue, *Sigma-Aldrich*, Deisenhofen
Ag8653 myeloma	Balb/c	myeloma cells transfected with the gene for murine GM-CSF (generated by Dr. Brigitta Stockinger, National Institute for Medical Research, Mill Hill, London and generously provided by the Ritter group).

4.1.4 Bacteria

Description	Source
E. coli XL-1 blue	*New England Biolabs*, Bad Schwalbach
E. coli Bl21(DE3)	*Invitrogen*, Karlsruhe

4.1.5 Mouse strains

Mice with the following genotypes were used in this work:

Name	Background	Source
C57Bl/6	C57BL/6	*Charles River*, Wilmington, MA, USA
OT-II	C57BL/6	*Charles River*, Wilmington, MA, USA
ADF$^{-/-}$	C57BL/6xSv129	C. Gurniak, *Witke Lab*
cofilin conditional	C57BL/6xSv129	C. Gurniak, *Witke Lab* (Gurniak et al., 2005)
CD11bCre	C57BL/6	G. Kollias, kindly provided by M. Pasparakis
LysMCre	C57BL/6	B. Clausen (Clausen et al., 1999)
Mx1Cre	SJLxC57BL/6	R. Kühn (Kuhn et al., 1995)

4.1.6 Antibodies, dyes and other high affinity molecules

The table shows the various antibodies, dyes and high affinity molecules used in this study and lists their concentration, basic reactivity and clone number as well as the companies they have been purchased from. In some cases stock solution concentrations, clone or lot numbers were not specified (n.s.) by the manufacturer.

Table 3: Antibodies, dyes and high affinity molecules

Antigen (Species)	Dilution Stock	Reactivity	Clone Lot Number	Source
Immunofluorescence				
Actin (mouse)	1:400	Mouse Actin	C-4	*MP Biomedicals*, Aurora, OH, USA
ADF (rabbit)	1:300 0.8 mg/ml	Human destrin cross-reacts with mouse destrin	GV-13 D8815	*Sigma*, Deisenhofen
cofilin (rabbit)	1:500 n.s.	Recognizes both forms of cofilin (1/2)	KG40	*Witke Lab*
Tubulin (mouse)	1:500	Microtubules	DM1A	*Sigma*, Deisenhofen
anti-mouse IgG Alexa488/594 (goat)	1:200 2 mg/ml	Mouse IgG (H+L)s	A11001/ A11005	*Molecular Probes/ Invitrogen*, Karlsruhe
anti-rabbit IgG Alexa488/594 (goat)	1:200 2 mg/ml	Rabbit IgG (H+L)	A11008/ A11012	*Molecular Probes/ Invitrogen*, Karlsruhe
FACS analysis				
B220-FITC	1:100 1 mg/ml	Mouse extracellular domain of CD45	RA3-6B2	*BD Biosciences*, Heidelberg
CD11b-FITC	1:100 1 mg/ml	Mouse Integrin αM, Mac-1	M1/70	*BD Biosciences*, Heidelberg
CD14-PE	1:100 1 mg/ml	Mouse LPS co-receptor CD14	rmC5-3	*BD Biosciences*, Heidelberg
CD34-APC	1:100 1 mg/ml	Mouse CD34	RAM34	*BD Biosciences*, Heidelberg
Gr1-APC	1:100 1 mg/ml	Mouse Ly-6G/C, Gr-1	RB6-8C5	*BD Biosciences*, Heidelberg
IgM-PE	1:100 1 mg/ml	Mouse μ heavy chain of the haplotype Igh-C^b	AF6-78	*BD Biosciences*, Heidelberg
Western blotting				
Actin (mouse)	1:2000	Mouse Actin	C-4	*MP Biomedicals*, Aurora, OH, USA
Actin (mouse)	1:5 n.s.	Mouse G-actin	hybridoma SN 224-236	*Jan Faix,* Hannover
ADF (rabbit)	1:1000 0.8 mg/ml	Human destrin, cross-reacts with mouse destrin	GV-13 D8815	*Sigma*, Deisenhofen
CapG (rabbit)	1:1000	Mouse CapG	WW12	*Witke Lab*
cofilin (rabbit)	1:500 n.s.	Mouse n-cofilin	KG60	*Witke Lab*
Gelsolin (rabbit)	1:2000 n.s.	Mouse gelsolin		*Witke Lab*
Phospho-Histone	1:1000	Phosphorylated form	06-570	*Upstate*, Lake

H3 (Ser10)(rabbit)	1mg/ml	of murine histone H3 (p-Ser10)		Placid, NZ, USA
Tubulin (mouse)	1:5000	Microtubules	DM1A	*Sigma*, Deisenhofen
anti-mouse IgG HRP (goat)	1:2000 0.8 mg/ml	Mouse IgG (H+L)	31430 98052825	*Pierce*, Rockford, IL, USA
anti-rabbit IgG HRP (goat)	1:2000 0.8 mg/ml	Rabbit IgG (H+L)	31460 98061831	*Pierce*, Rockford, IL, USA
anti-rat IgG HRP (goat)	1:2000 0.8 mg/ml	Rat IgG (H+L)	31470 98063031	*Pierce*, Rockford, IL, USA
Miscellaneous				
CalceinAM	4 mM	Living cells, calceinAM enters cells, upon cleavage, it fluoresces	L3224	*Molecular Probes/ Invitrogen*, Karlsruhe
Ethidium bromide Homodimer (EthD)	2 mM	DNA of dead cells	L3224	*Molecular Probes/ Invitrogen*, Karlsruhe
Hoechst 33342	10 mg/ml 1:30.000	DNA	H-3570	*Molecular Probes/ Invitrogen*, Karlsruhe
Phalloidin Alexa488	1:200 300 U	Filamentous actin	A12379	*Molecular Probes/ Invitrogen*, Karlsruhe
Phalloidin Alexa594	1:200 300 u	Filamentous actin	A12381	*Molecular Probes/ Invitrogen*, Karlsruhe
Streptavidin HRP	1:200 n.s.	Biotin	AEM 374111	*R&D Systems*, Abington, UK

4.1.7 Culture media, buffer and stock solutions

4.1.7.1 Molecular biology

Description	Composition
Ampicillin stock solution (1000×)	50 mg/ml
DNA loading buffer (6×)	0.25% Bromphenol blue 0.25% Xylencyanol FF 15% Ficoll
DNA lysis buffer (low salt)	50 mM Tris, pH 7.5 100 mM NaCl 5 mM EDTA 1% SDS 0.5 mg/ml proteinase K
dNTP-Mix for PCR	2.5 mM dATP 2.5 mM dCTP 2.5 mM dGTP 2.5 mM dTTP
Ethidium bromide stock solution	10 mg/ml Ethidium bromide in H_2O

LAIRD tissue lysis buffer	100 mM Tris-HCl, pH 8.5 5 mM EDTA 0.2% SDS 200 mM NaCl add 100 μg/ml proteinase K before use
OLB	mix A:B:C, 200:500:300 O: 1.5 M Tris-HCl, pH 8.0 0.15 M $MgCl_2$ A: 0.832 ml solution O 18 μl β-Mercaptoethanol 50 μl dATP (10 mM) 50 μl dCTP (10 mM) 50 μl dTTP (10 mM) B: 2 M HEPES-NaOH, pH 6.6 C: dpN_6, 90 O.D. U/ml
Sodium acetate solution for DNA precipitation	3 M Sodium acetate pH 4.6
Southern hybridization buffer	1% BSA 1 mM EDTA 0.5 M Sodium phosphate, pH 7.2 7% SDS
Southern wash buffer	1 mM EDTA 40 mM Sodium phosphate, pH 7.2 1% SDS
TAE buffer (50×)	2.0 M Tris-Base pH 8.3 0.6 M Sodium acetate 0.1 M EDTA
TE buffer	10 mM Tris-HCl 0.1 mM EDTA adjust pH to 8.0, autoclave

Culture medium:

Luria Bertani (LB) medium	10 g Bactotryptone 5 g Yeast extract 10 g NaCl ad 1 l H_2O

For selection purposes the appropriate antibiotic (here: Ampicillin) can be added to the LB broth.

LB agar	15 g agar ad 1 l LB medium, autoclave
SOC medium	0.5% Yeast extract 2.0% Bactotryptone 10mM NaCl 2.5mM KCl 10mM $MgCl_2$ 20mM $MgSO_4$ 20mM glucose

4.1.7.2 Biochemistry

Description	Composition
Ammoniumpersulfat (APS) stock solution	10% APS in H_2O
Coomassie rapid destain	30% isopropanol 6% acetic acid
Comassie destain	10% ethanol 6% acetic acid
Coomassie staining solution	40% Coomassie Brilliant Blue R-250 50% methanol 10% acetic acid
ELISA blocking buffer	1% BSA in PBS
ELISA coating buffer	solution 1: 10 mM Na_2CO_3 solution 2: 20 mM $NaHCO_3$ mix solutions to reach pH 9.6
ELISA substrate buffer	100 mM $NaH_2PO_4 \times H_2O$, pH5.5
ELISA substrate solution	200 µl ELISA TMB solution 12 ml ELISA substrate buffer 1.2 µl 30% H_2O_2
ELISA TMB solution	60 mg Tetramethylbenzidin (TMB) 10 ml DMSO
ELISA stop solution	2 M H_2SO_4
ELISA washing buffer	1×PBS 0.05%(v/v) Tween 20
GST lysis and binding buffer	1xPBS 0.1 mM EDTA 0.1% TX-100
GST elution buffer	15 mM Glutathione in TRIS, pH 8.0
HEPES lysis buffer (HLB)	20 mM HEPES, pH 7.2 50 mM NaCl 5 mM $MgCl_2$ 0.05% Tween-20 freshly add EDTA-free protease inhibitors
HTNC G-dialysis buffer	20 mM HEPES, pH 7.4 600 mM NaCl 50% glycerol
HTNC lysis buffer	1x PTB 1 mg/ml lysozyme 0.2% Tween20
HTNC 10x PTB	500 mM Na_2HPO_4 50 mM Tris adjust pH to 7.8

HTNC Ni-elution buffer	1x PTB 500 mM NaCl 250 mM imidazole
HTNC Ni-wash buffer	1x PTB 500 mM NaCl 0.5% TritonX-100 10 mM imidazole
HTNC S-dialysis buffer	20 mM MES, pH 6.3 5% Sucrose 300 mM NaCl 0.5% Triton-X100
HTNC S-elution buffer	20 mM MES, pH 6.5 5% Sucrose 1.2 M KCl
HTNC S-wash buffer	20 mM MES, pH 6.5 5% Sucrose 300 mM KCl
HTNC TSB	1x PTB 2 M L-tartaric acid (disodium salt) 10 mM imidazole adjust pH to 7.8
IPTG stock solution	1 M in H_20
MacroS binding buffer	20 mM MES pH 6.4 1 mM EDTA 0.1 mM DTT
PBS (20×)	32 g $Na_2HPO_4 \times 2H_2O$ 5.3 g $NaH_2PO_4 \times 1H_2O$ 164 g NaCl ad 1 l H_2O
PHEM buffer	60 mM PIPES 20 mM HEPES 10 mM EGTA 2 mM $MgCl_2$ pH 7.0, 1% Triton-X100
SDS sample buffer (5×)	110 mM Tris-HCl pH 6.8 20% Glycerol 3.8% SDS 8% β-Mercaptoethanol Bromphenol blue, ad libidum
SDS-PAGE running buffer (10x)	30.25 g Tris-base 144.2 g glycine 10 g SDS ad 1 l H_20, pH ~ 8.3, do NOT adjust!
Western Blot transfer buffer (towbin)	25 mM Tris-base 190 mM glycine 20% Methanol (v/v)

Western Blot blocking buffer	5% non-fat milk powder in PBS 0.1% Tween20
Western Blot washing buffer	1×PBS mit 0.1% Tween20

4.1.7.3 Cell biology

Description	Composition
FACS buffer	2.5% FCS and 0.1% sodium acide /PBS
FACS cell fixing solution	1% Paraformaldehyd (PFA)/PBS
Fixative	4% PFA/PBS
Fixative for cofilin staining	15% v/v saturated picric acid solution 4% PFA 1x PHEM buffer pH 6.8
Fixative REM	2% Glutaraldehyde in 0.1 M Sodium-Cacodylate-buffer
Gelvatol mounting medium	make 100 ml solution containing: 0.14 M NaCl 0.01M KH_2PO_4/Na_2HPO_4, pH 7.2 To the 100 ml solution, slowly add 25 g polyvinyl alcohol while stirring, stir o.n., adjust pH to 7.2 the next day. add 50 ml Glycerol, stir over night Store airtight, at -20°C
MACS buffer	1× PBS with 0.5% BSA and 2 mM EDTA
PBS (20×)	32 g $Na_2HPO_4 \times 2H_2O$ 5.3 g $NaH_2PO_4 \times 1H_2O$ 164 g NaCl ad 1 l H_2O
polyI:C stock solution	1 mg/ml in 1×PBS
Red blood cell lysis buffer	10% 0.1 M Tris/HCl pH7.5 90% 0.158 M Ammonium chloride solution
Trypan blue solution	2 mg Trypan blue in 100 ml 1×PBS
Cell culture media:	
Complete DMEM medium	500 ml DMEM 50 ml FCS 5 ml Non-essential amino acids 5 ml HEPES 5 ml Sodium pyruvate 5 ml Penicillin/Streptomycin

DC medium	500 ml RPMI 1640 50 ml FCS 1 ml β-Mercaptoethanol 5 ml Penicillin/Streptomycin 5 ml L-glutamine Mix 1:10 with GM-CSF conditioned SN
ES cell medium	DMEM 4.5 g/l Sodium pyruvate 15% FCS 2 mM L-glutamine 0.1 mM Non-essential amino acids 0.1 mM ß-mercaptoethanol 100 U/ml Penicillin/streptomycin mixture 1000 U/ml Leukemia inhibitory factor (LIF)
ES cell freezing medium	50 ml FCS 40 ml culture medium 10 ml DMSO
Macrophage medium (BMM-medium)	75% complete DMEM medium 25% L929 conditioned medium
RPMI/10% FCS	500 ml RPMI 1640 50 ml FCS 10 ml 1 M HEPES 10 ml 200 mM L-glutamine 2.5 ml 10 mg/ml Gentamycin

4.1.8 Software and analysis tools

Description	Source
Image Acquisition and Analysis	
Openlab 4.01	*Leica*, Wetzlar
Metamorph 6.0	*Molecular Devices*, Downingtown, PA, USA
Leica TCS-NT	*Leica*, Wetzlar
Photoshop 7.0/8.0	*Adobe Systems*, San José, CA, USA
Imaris 4.2	*Bitplane*, Zurich, Switzerland
Miscellaneous	
Office 2003	*Micosoft Cooperation*, Redmond, WA, USA
GraphPad Prism 4.0	*GraphPad Software Inc.*, San Diego, CA, USA
CellQuest Pro 4.0.2	*BD Biosciences*, Rockville, MD, USA,
FlowJo 6.2.1	*Tree Star Inc.,* San Carlos, CA, USA
Ascent	*Thermo Scientific*, Milford, MA,USA
Mausoleum	Java based program, by H.E. Stöffler
Radames	Java based program, by H.E. Stöffler

The significance of deviations was calculated by unpaired T tests or ANOVA analysis. Single stars represent a p-value below 0.05, double stars below 0.01 and triple stars below 0.005. In all graphs, the standard error of means (SEM) is shown.

4.2 Methods

4.2.1 Methods in molecular biology

All DNA and RNA manipulations, unless otherwise specified, were carried out according to Sambrook (Sambrook et al., 1989).

4.2.1.1 Determination of the concentration of nucleid acids

The concentration and purity of DNA solutions was determined by OD using a spectral photometer. Pure DNA solutions are characterized by a ratio A_{260}/A_{280} between 1.8 and 1.95.

4.2.1.2 Polymerase Chain Reaction (PCR)

The polymerase chain reaction represents an elegant method to multiply and/or modify a specific DNA fragment (Saiki et al., 1988). Heat stable DNA polymerases use single stranded DNA for the synthesis of a new complementary DNA strand. Thereby the polymerases depend on the presence of a primer with a free 3'OH group that serves as a starting point for the elongation in 5'→ 3' direction.
For every DNA polymerase the reaction mixture was prepared according to the manufacturer's instruction [ExpandPlus (*Roche*), GoTaq Flexi DNA-polymerase (*Promega*)].

Standard Genotyping Protocols:

PCR mixture:

	1	µl	DNA from tail preparation
	2	µl	10x Taq buffer
	1.5	µl	dNTPs (2.5 mmol)
	1.5	µl	primer A (5 pmol)
	1.5	µl	primer B (5 pmol, unless stated otherwise)
	0.2	µl	Taq DNA polymerase (Promega)
ad	20	µl	ddH_20

cofilin
primer: CoIn-Sma5', Cof NTS-3'a, CoIn2-5'a
program: 3XPCR

Cycles:	94°C	2 min	1x	
	94°C	30 sec		} 35x
	54°C	30 sec		
	68°C	40 sec		

expected products: 380 bp (wildtype), 420 bp (floxed), 170 bp (deleted allele)

Mx1Cre
primer: Mx-CreF/Mx-CreR
program: Mx1

Cycles:	94°C	2 min	1x
	94°C	30 sec	} 35x
	54°C	30 sec	
	72°C	1 min.	
	72.0	5 min	1x

expected PCR product: 250 bp (Cre positive)

ADF
primer: ADF150'-3, ADF Int-2-5', LacZ-3'
program: 3XPCR

Cycles:	94°C	2 min	1x
	94°C	30 sec	} 35x
	54°C	30 sec	
	68°C	40 sec	

expected PCR products: 450 bp (wt), 150 bp (deleted allele).

4.2.1.3 Agarose gel electrophoresis

DNA fragments can be separated according to their size in an agarose gel by an electrical field. Depending on the size of the DNA fragments to be separated, the gels contain between 0.5 % agarose (for fragments up to 30 kb) and 2.0 % agarose (for small DNA fragments until 100 bp). All gels were prepared and run with TAE buffer for 30-60 minutes at 100V.
The DNA samples were mixed with 6x loading buffer and loaded onto the gel. To determine the size of the DNA fragments every gel contained a marker lane. To visualize the DNA ethidium bromide was added to the melted agarose at a concentration of 0.2 μg/ml. The dye intercalates with DNA double strands and fluoresces when exposed to UV light.

4.2.1.4 Gel purification of DNA fragments

To extract DNA fragments of interest from agarose gels the QiaexII kit (*Qiagen*) was used. In brief, the piece of agarose gel containing DNA was separated and melted at 50°C in the presence of buffered glass milk. The DNA binds to the beads and can then be washed, dried and eluted in a small volume.

4.2.1.5 Blunting of DNA fragments

The use of Klenow DNA polymerase allows it to fill up the overhanging ends of a restriction digest. This can be necessary for cloning steps that require blunt ends.

The DNA fragment was incubated in the presence of dNTPs in Klenow buffer and Klenow enzyme for 10 min and 37°C. Klenow polymerase adds dNTPs to the shorter strand of overhanging ends using the complementary strands as a template until both strands reach the same length. Afterwards the enzyme was inactivated by incubation at 70°C for 10 min.

4.2.1.6 Dephosphorylation of DNA fragments

In order to reduce the religation of a vector it can be useful to dephosporylate the free 5'-end after a restriction digest. 0.5 μg/10 μl vector DNA was incubated in CIP-Buffer in the presence of 0.5 u/μl alkaline phosphatase, calf intestinal (CIP), for 1 hr at 37°C. Afterwards the DNA was purified by phenol/ chloroform extraction. 100 μl of DNA solution were added to a 1:1 mixture of phenol/chloroform (pH 7.4), vigorously shaken and centrifuged for 5 min at 14.000 rpm in an eppendorf rotor. The aqueous phase went through a second extraction cycle before the DNA was precipitated by adding 1/10 vol. 3 M sodium acetate (pH 4.6) and 2.5 vol. ice-cold 100 % ethanol. After centrifugation (15 min, 14.000 rpm) the DNA was washed, air-dried and resuspended in a small volume of dH_20.

4.2.1.7 Ligation of DNA fragments

The coupling of two DNA fragments via a phosphodiester binding is called ligation. The enzymes capable to promote this reaction under the consumption of ATP are therefore called ligases.
The reaction took place at 16°C o.n. in a total volume of 10 μl containing 3 units of the T4 DNA ligase, 1 μl 10x T4 ligation buffer as well as the DNA. The ratio of vector to insert employed in all ligations was between 1:4 and 1:7.

4.2.1.8 Production of competent bacteria

4.2.1.8.1 Production of chemically competent bacteria

Chemically competent bacteria cells are quickly prepared but do not exhibit the highest transformation capacity (~10^7 transformants/μg DNA). XL1-Blue cells were grown in pure LB medium to an optical density of OD_{600}≈0.5 – 0.6. The pellet was resuspended in 1/10 volume of freshly made TSB and incubated on ice for 10 min. For long-term storage, 200 μl aliquots were kept frozen at -80°C.

4.2.1.8.2 Production of electro competent bacteria

When higher transformation efficiencies were electro competent bacteria were used. XL-1 blue cells were grown in pure LB medium to an optical density of OD_{600}≈0.6 – 0.7. Growth was stopped by incubating the bacteria 15-30 min on ice, prior to several washing steps (use pre-cooled solutions), in which one decreases the volume of sterile water starting with 500 ml to 1-2 ml with in which the cells are washed. The precipitation occurred at 4.000 rpm in a Heraeus megafuge 2.0R. Aliquots of 50 μl of the final bacteria suspension (containing ≈ 3x10^{10} cells/ml) were prepared and shock frozen in liquid nitrogen. The bacteria can be stored at -80°C.

4.2.1.9 Transformation of bacteria

4.2.1.9.1 Transformation of chemically competent bacteria

Bacteria (100 μl) were thawed on ice and combined with 20 μl 5x KCM, 50 – 100 ng DNA, ad 100 μl ddH_2O. The transformation preparation was incubated for 20 min on ice followed by 10 min at room temperature. The bacteria were split and plated on two plates containing the appropriate antibiotic (50 + 150 μl).

4.2.1.9.2 Transformation of electro competent bacteria

An aliquot of electro competent bacteria (50 µl) was thawed on ice and incubated with 0.1 – 1 ng of DNA for 10 min on ice. The transformation occurred by electroporation (1 mm cuvette, 1.8 kV, 25 µF). Immediately after the pulse, the bacteria were suspended in 1 ml of SOC medium and shaken for 1 hr at 37°C. Different amounts of bacteria were plated on LB plates containing the appropriate antibiotic.

4.2.1.10 Plasmid preparation from bacteria

Plasmids can be multiplied in bacteria for later use. Dependent on the desired amount and purity of the plasmid DNA various ways of preparations can be used.
First bacteria were grown in a culture; 5 ml for a Mini prep, 300 ml for a Maxi prep. The preparation of the plasmids followed the distributor's specifications. The Wizard Mini prep kit (*Promega*) was used for small preparations, for big amounts of endogen-free DNA the Endo-free maxi kit (*Qiagen*) was used.

4.2.1.11 Cryo conservation of bacteria

Long term conservation of bacteria can be achieved by preparation of a glycerol stock. For this purpose, 800 µl of a fresh bacteria culture were mixed with 200 µl 96% glycerol. The glycerol stocks were stored at -80°C.

4.2.1.12 DNA sequencing

To obtain the exact sequence of a DNA the Didesoxy-method was applied (Sanger et al., 1977). Its mechanism is based on the random termination of DNA replication by the insertion of fluorescent ddNTP analoga, which are detectable in a reader.
The sequencing reaction included the following reagents:

	10	ng/100 bp	DNA
	3.2	pmol	primer
	4	µl	BigDye 3.1 (*Applied Biosystems*)
	2	µl	5x Dilution buffer (*Applied Biosystems*)
ad	20	µl	H_20

and the PCR followed this program:

Cycles:	95°C	5 sec	1x
	95°C	15 sec	25x
	52°C	15 sec	
	60°C	3 min.	

The DNA was precipitated by addition of 64 µl 100% ethanol and 16 µl H_20 followed by centrifugation (20 min, 14.000 rpm), and washed with 50 µl 70% ethanol. The DNA was dried and re-dissolved in 10 µl H_20. 2 µl of the sequencing reaction was mixed with 8 µl formamide and heat-denatured before it was sequenced in a capillary sequencer (*Applied Biosystems*).

4.2.1.13 Extraction of genomic DNA from tail-tip

For the genotyping of mice, it is necessary to extract genomic DNA from tissues for analysis. A small piece of tail was cut of (0.4 cm) and incubated over night in DNA lysis buffer at 56°C. The next day the tubes were vortexed to destroy last pieces of connected tissue. After addition of 100 µl saturated NaCl the tubes were shaken vigorously for 2 min and then centrifuged for 15 min at 14.000 rpm to precipitate the proteins. The clear supernatant was transferred into a tube containing 750 µl 100% ethanol. The tube was inverted several times and the precipitated DNA was spun down for 1 min at 14.000 rpm. The supernatant was removed and the DNA air-dried before it was resuspended in 200 µl TE buffer.
In general, 1 µl of this DNA solution was used for the genotyping PCR listed in the appendix A or 20 µl were used for Southern blot analysis.

4.2.1.14 Radioactive labeling of DNA after Vogelstein

20 – 50 ng of a linear DNA fragment was heat denatured (5 min, 100°C), briefly chilled on ice and added to the labelling solution:

	10 µl	OLB
	2 µl	BSA (10 mg/ml)
	5 µl	^{32}P-dGTP, 3000 Ci/mM
	1 µl	Klenow enzyme (5 U/µl)
ad	25 µl	H_20

The mixture was incubated o.n. at RT or 2-3 h at 37°C. The reaction was terminated by the addition of 100 µl stop solution (50 mM Tris-HCl pH 8.0, 20 mM EDTA) and purified using a BioGel column. 1 ml BioGel was given into a 1 ml syringe with a bit of glass wool at the bottom to avoid the flow through of the gel. The column was packed by centrifugation for 2 min at 2000 rpm. The labelled probe was given onto the column and purified by an additional centrifugation (2 min, 2000 rpm, Megafuge) during which the probe travels through the columns while unbound nucleotides remain in the bedding. The probe needs to be denatured (5 min, 100°C) before it can be used in a Southern Blot.

4.2.1.15 Southern blot

For a Southern blot 10-15 µg of genomic DNA were digested o.n. with an appropriate restriction enzyme (in the case of cofilin with *Eco*RI) in total volume of 40 µl. The next day the samples were loaded on a 0.7% agarose gel and slowly separated by size (30 V). A picture with a ruler was taken before the DNA was denatured by washing the gel twice for 30 min in 0.5 M NaOH / 1.5 M NaCl. Prior to the alkaline capillary transfer the gel was equilibrated in transfer buffer before it was placed on a saran wrap and cover with a nitrocellulose membrane (GeneScreen Plus) and 3 whatman papers, all soaked in transfer buffer. On top a pile of paper towels, that was replaced every 6 hrs, build up the used capillary forces to pull the DNA out of the gel onto the membrane. After the transfer the membrane was briefly neutralized in 0.5 M Tris/HCl pH7.4, dried and exsiccated for 1 hr at 75°C.

Non specific binding sites were blocked by incubating the blot for 1 hr in hybridization buffer at 65°C, before the labelled probe was given onto the blot in fresh hybridization buffer and incubated o.n. at 65°C. The next day the blot was washed

several times with Southern Wash before a phosphor imager screen or an X-ray film was exposed.

4.2.1.16 Coning strategy: GST-ADF in pGEX2T

The cDNA of murine ADF was PCR amplified from total gut cDNA, generously provided by C. Gurniak. The obtained fragment was cut with *Bam*HI and *Eco*RI and ligated into the equally digested pGEX2T vector.
Primers for PCR amplification of ADF cDNA:

mADF5': 5'-GATC**GGATCC**ATGGCCTCAGGAGTTCAGG-3'

mADF3': 5'-GC**GAATTC**CTACACAGGGGACCCTTCAAA-3'

4.2.1.17 Targeting construct that replaces cofilin by ADF in mice

The pFLRT-*Asc*I plasmid was used as a base for generating the ADF knock-in targeting construct (plasmid #271, Witke archive).

Step 1:
Subcloning of the fragment to insert between the loxP sites was performed by PCR amplification from a vector (pΔ6.0, #88) generated by C. Gurniak, containing a 6.0 kbp genomic DNA fragment of the cofilin gene including exon 2-4. The vector DNA was isolated and the fragment of interest spanning exon 2-4 of the cofilin gene was amplified by Expand Fidelity PCR^{TM} (*Roche*) in the presence of 3 mM $MgCl_2$ with the following conditions:
The following oligonucleotides were used for the subcloning:

CofInt2aSma-5': 5'-GCCGCTAGGGAAAAGCGCGC -3'

CofpA+100_3': 5'-GGAGATGCCGCTTACTAGGG -3'

PCR program:

Step 1) 94°C	2:00	
Step 2) 94°C	0:30	
Step 3) 59°C	0:30	
Step 4) 72°C	3:20	
Step 5) back to step 2)	9x	
Step 6) 94°C	0:30	
Step 7) 59°C	0:30	
Step 8) 72°C	3:20	+10s/cycle
Step 9) back to step 6)	19 x	
Step10) 72°C	7:00	

Expected fragment length: 3.0 kb

Targeting construct step 1

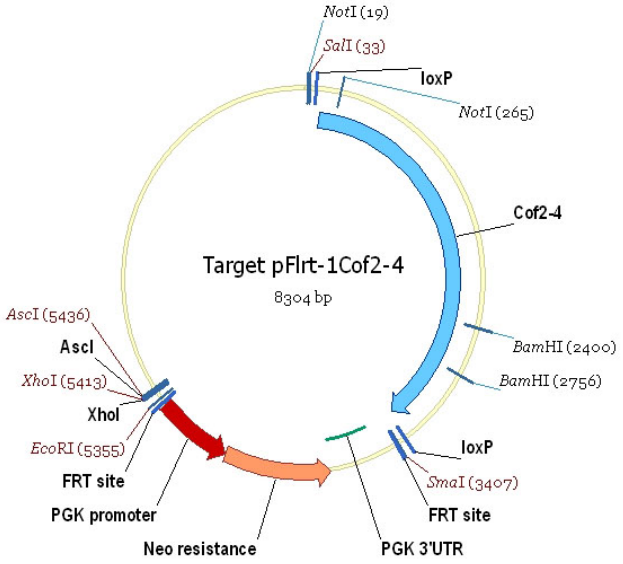

The fragment was subcloned into the pDRIVE vector and sequenced. Clone 8 did not have any mutations in the exons. The vector (#425) was digested with *Eco*RI, the insert was isolated, blunted and transferred into the pFLIRT-*Asc*I vector that was opened between the loxP sites by a digestion with *Bam*HI and was subsequently blunted. Clone 22 was used for the further proceedings.

Step 2

The 5' arm (left arm) for the construct was cut out directly from the pΔ6.0 vector using *Hinc*II/*Sma*I restriction enzymes. The insert (1672 bp) was isolated and ligated into the vector from step 1 (#428). The vector was cut with *Hinc*II and dephosphorylated prior to the ligation. Clone 15 was used for the next cloning steps.

Targeting construct step 2

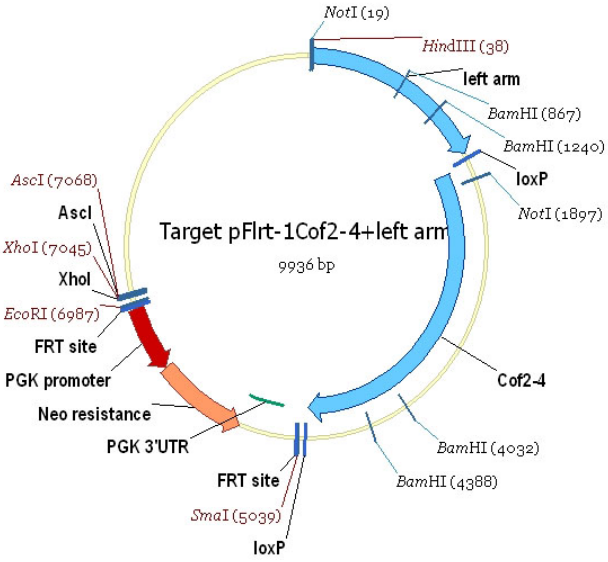

Step 3

Subcloning of the 3' homology arm of the cofilin gene (right arm) was performed by J. Rientjes using ET recombination (BAC clone RP23-389K5). During the subcloning, an *Xho*I restriction site was inserted at the 5' end of the fragment and a *Sal*I/*Asc*I site was inserted at the 3' end respectively. The subclone vector (#426) as well as the targeting vector from step 2 (#429) were amplified and digested with *Xho*I and *Asc*I. The insert was purified and ligated into the dephosphorylated targeting vector. Sequencing confirmed that clone 9 has the correct insertion.

The following oligos were used for the subcloning:

COF down (79 bp): 5'-GCCTTGGAACAGTGCACCCCAACTCAAGAAGGAGATGCCGCTT ACTAGGGCTCGAGAGGTGGCACTTTTCGGGGAAATG-3'

COF up (87 bp): 5'-TCCCTCTCAAGCCCGCCTGGGGATCTTTTCTCCCCTAGCCCCTT CAGAAAGTCGACGGCGCGCCGGGATAACGCAGGAAAGAACATG-3'

Cofilin right arm subclone

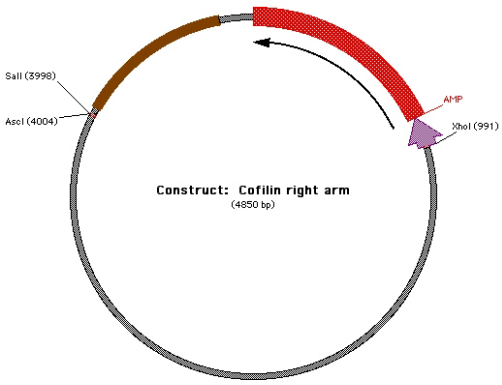

Insert length 3.0 kb

Targeting construct step 3

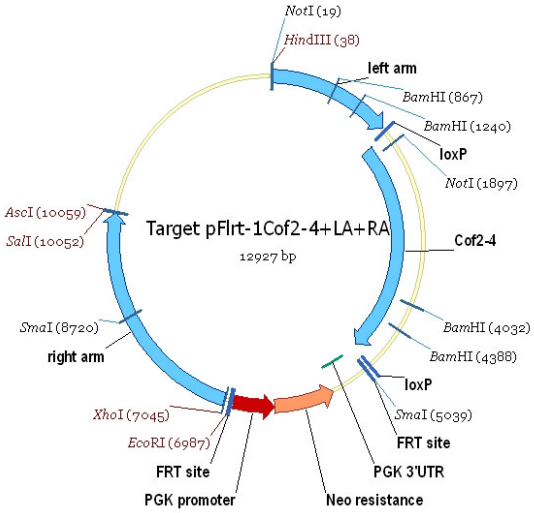

Step 4

Subcloning of the genomic region of the ADF gene encoding exon 2-4 was performed by J. Rientjes using ET recombination (BAC clone RP23-77A2). During the subcloning, a *BstB*I restriction site was inserted at the 5' end of the insert and a *Xho*I site was inserted at the 3' end respectively. Subcloning of the ADF fragment was performed by J. Rientjes using ET recombination from a BAC clone. The subcloned fragment containing the genomic sequence of ADF starting in the first intron, finishing ~ 100 bp downstream of the polyA signal, was flanked by an *Bst*BI side on the 5' end and an *Xho*I side on the 3' end. These restriction sides were used to cut the vector in step 2 as well as the ADF subclone in order to insert the third fragment.

The following oligos were used for the subcloning:

ADF down (79 bp): 5-AATCCATAAACCCTAAGTGAGAGACCTTGTCTCAAAAACAAGAG GGACAGTTCGAAAGGTGGCACTTTTCGGGGAAATG-3'

ADF up (79 bp): 5'-TTACAACTTCCAGAATCCATCACTGAGGGAAGTCAGAACATGA ACTCAAGCTCGAGGGGATAACGCAGGAAAGAACATG-3'

ADF subclone

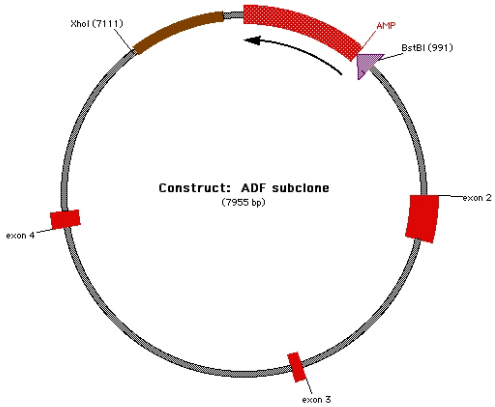

Insert length 6.1 kb

Targeting construct step 4

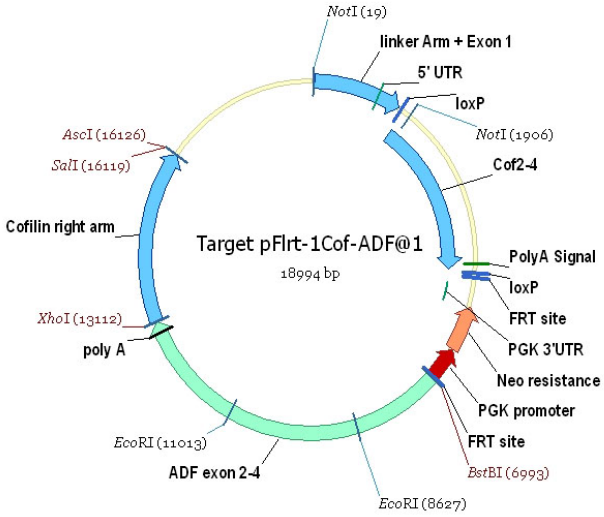

The final targeting vector is 19 kb long (#431) and clone #19 was used to target ES cells.

Correctly targeted ES cell clones were identified by Southern blot using a external 5' probe. The presence of the 5' loxP site was verfied by a PCR spanning the modiefied region in the first cofilin intron.

loxP PCR:
primer:

No. 57 (coinsma-5') : 5' TGC TGT GGA GAC CAA CCT AGC 3'

No. 99 (coinsma-3') : 5' CGC TGG ACC AGA GCA CGC GGC ATC 3'

Cycles:	94°C	2 min	1x
	94°C	30 sec	} 35x
	54°C	30 sec	
	72°C	1 min.	
	72.0	5 min	1x

expected PCR product: 130 bp (loxP present), 100 bp (wild type).

4.2.2 Biochemical methods

4.2.2.1 Sodium dodecylsulfate polyacrylamide gel electrophoresis (SDS-PAGE)

Proteins can be separated according to their size in a SDS-PAGE. The negatively charged SDS molecule binds on average every 2.8 amino acids to protein and abolishes by this mechanism the 3D structure of protein. Thus, the proteins travel in an electrical field according to their size and independent of their structure and charge.
SDS gels were prepared and run with a discontinuous buffer system (Laemmli, 1970):

	15 %	10 %	stack
30 % Acrylamide (ml)	35	23.3	4.8
2 M Tris-HCl, pH 8.8 (ml)	13.2	13.2	…
10% SDS (ml)	0.7	0.7	0.3
H_20 (ml)	21.1	32.8	17.4
0.5 M Tris-HCl, pH 6.8 (ml)	…	…	7.5
10 % APS (ml)	0.44	0.44	0.1
TEMED (ml)	0.08	0.08	0.02
	70	70	30

Protein samples were compounded with 5x loading buffer, heat denatured (5 min, 95°C) and spun down. On every gel, 6 µl marker (prestained for Western Blots) was loaded to determine the size of the proteins. The SDS-PAGE was run for approximately one hour with an electrical current of 125 V.

4.2.2.2 Coomassie staining

The Coomassie Blue staining is a quick but not so sensible method to stain proteins in a SDS-PAGE. The gel is placed in Coomassie staining solution and gently shaken for 30 min until it is completely blue coloured. Then the gel is briefly rinsed in water and destained until the background becomes transparent and distinct bands can be seen.

4.2.2.3 Western blot

Western blotting is a commonly used method to detect proteins in a lysate or culture supernatant by the means of specific antibody.

For Western blots, proteins were electrophoretically transferred onto a polyvinylidone difluoride (PVDF) membrane, using a semi-dry blotting apparatus, by applying 20 V for 1 hr. Prior to the transfer, the PVDF membrane was made hydrophilic by a brief incubation in methanol and gel and membrane were equilibrated in transfer buffer.

After the transfer, the membrane was incubated in blocking solution (4 % non-fat milk powder dissolved in PBS/0.05% Tween20) for 1 hr at RT or o.n. at 4 °C. Primary and secondary antibodies were diluted in blocking solution to the appropriate concentrations. The enhanced chemiluminescence system was used, followed by exposure to x-ray film. Between the antibody incubations, the membrane was washed five times in PBS/0.05% Tween20. For detection, horseradish peroxidase (HRP) conjugated secondary antibodies were used.

4.2.2.4 Expression and purification of recombinant proteins

4.2.2.4.1 Purification of Cre-recombinase expressed in *E. coli*

From a fresh o.n. culture of Bl21(DE3) HTNC-Cre transfected 4 l of prewarmed LB medium were inoculated and grown at 30°C for 3 hrs. To induce HTNC expression 0.5 M IPTG were added and the cells were grown for another 5 hrs at 30°C. Bacteria were collected by centrifugation and the pellet was frozen at –20°C. The frozen pellet was resuspended in 40 ml lysis-buffer and benzonase (*Novagen*) was added (1:1000). 40 ml of TSB buffer was added to the mixture and after a 5 min incubation period the lysate was centrifuged in a TFT45 rotor for 2-3h at 4°C at 30k. The clear supernatant was collected and loaded onto a Nickel-column via a 90ml Dynaloop. The column was extensively washed and the elution took place at a flow rate of 0.5 ml/min over 60 min.

The eluted fractions were checked by coomassie gel and the interesting fractions were pooled and dialysed against 'S-dialysis-buffer'. The precipitate was spun down and the supernatant was loaded onto a Macro-S column. After the washing step the clean HTNC was eluted by a gradient from 0%-100% 0.5 ml/min.

The fractions containing protein were again analyzed on a coomassie gel and the interesting fractions were pooled again and dialyzed against 'G-dialysis buffer'.

4.2.2.4.2 Purification of GST-fused proteins

37°C LB medium containing 50 μg/ml ampicillin was inoculated 1:20 with fresh o.n cultures of respective bacteria harbouring the gene of interest in a pGEX2T vector (Clontech Inc., USA). Cells were grown to an OD600 of 0.8. At this point, protein expression was induced by adding 1 mM IPTG and growing the bacteria further at 37°C for 4-6 hours. Bacteria were then harvested by centrifugation in at 4000 rpm in a JLA 10.500-rotor (Beckmann) for 10 min at 4°C. The pellet was resuspended in GST lysis buffer and subjected to 2 rounds of sonification (2x30s, MS73 probe) and homogenization in a Dounce-homogenizer. After clearing the lysates by a 30 min. spin at 40.000 rpm in a TLA 45 rotor (Beckmann), the supernatant was passed over an appropriate amount of glutathione 4B sepharose, which had been washed and equilibrated with lysis buffer. After extensive washing with cold lysis buffer and briefly with PBS, proteins were eluted in 1 ml fractions with GST elution buffer.

4.2.2.4.3 Purification of recombinant ADF and cofilin

Recombinant GST fusion molecules were incubated o.n. at 18°C with thrombin (1:25). Cleavage was checked by SDS gel electrophoresis and the protein solutions were twice dialyzed against 1 l of MacroS binding buffer. Subsequently AC proteins were separated from GST cation exchange chromatography. One can separate the AC proteins from the GST due to their different isoelectric point (pI). At pH 6.4, GST is positively charged (pI ~ 4.9) and binds to the column while ADF (pI 8.1) and cofilin (pI 7.9) pass through without binding. The fractions containing ADF or cofilin were pooled and dialyzed against PBS.

4.2.2.5 Lysis of tissues and cells

For further processing of lysates, e.g. affinity-chromatography (see below), fresh tissues were shock frozen and routinely lysed in ice-cold HEPES-lysis buffer (HLB). Decomposition was achieved by 30 strokes at 800 rpm in a teflon-pestle Dounce-homogenizer in the cold. After centrifugation at 60.000 rpm at 4°C in a TLA 120.2 rotor (Beckman), the clear supernatant was used for further experiments.

Tissue culture cells were generally lysed in 1xSDS sample buffer in the culture dish after several washes with PBS.

4.2.2.6 Affinity purification of complexes

For GST-complexes, the fusion molecules were incubated o.n. on a wheel at a concentration of 2 mg protein/ml glutathione-sepharose 4B, which was previously washed with PBS several times.

Instead, CNBr activated sepharose had to swell before proteins can bind to it. 1g of sepharose was carefully washed with 500 ml of 1 mM HCl using a glass frit. After a brief wash in PBS sepharose was bound to proteins at a ratio of 0.5 ml of sepharose per mg proteins in 50 ml PBS o.n. at 4°C on a wheel. The next day, the sepharose was collected and washed subsequently with 0.1 M Tris pH 8.0/ 100 mM NaCl, then with 0.1 M Tris pH 8.0, before it was equilibrated in HLB.

For complexes, 6-10 tissues from wild type mice were pooled and lysed as described before. The lysates were passed over the previously washed columns three times. After several washes with HLB the complexes were eluted by boiling the entire sepharose in SDS sample buffer.

4.2.2.7 Separation of G- and F-actin

On day 6 BMM from one 35 mm^2 well were washed twice with PBS, collected and lysed in 200 µl of ice-cold PHEM buffer. After an incubation of 15 min on ice, samples were centrifuged for 10 min in an Eppendorf swing-out rotor at 4°C (10.000 rpm). 150 µl of the supernatant, containing G-actin, were transferred into a fresh tube and mixed with 37.5 µl of 5x SDS sample buffer. The pellet, containing the filamentous actin, was washed twice with ice-cold PHEM buffer and finally resuspended in 250 µl 1x SDS sample buffer. The samples were denatured at 95°C for 5 min and the amount of F- and G-Actin was determined by Western blot and subsequent densitometric measurements.

4.2.3 Cell biology methods

4.2.3.1 General conditions of cell culture and sterilisation

The following cell culture methods were accomplished in a sterile environment using a Laminar Flow Hood. Cells were kept in incubators at 37°C in the presence of 5 % CO_2. Solutions and plastic materials were autoclaved for 20 minutes at 135°C and 2.2 bar pressure prior to use. Glass devices were sterilized for 3 hrs at 180°C.

4.2.3.2 Thawing and freezing of eukaryotic cells

Eukaryotic cells can be stored for a long time in liquid nitrogen (-196°C) and after thawing put into culture. To prevent formation of ice crystals inside the cells 10% DMSO was added to the freezing medium. At least $5x10^6$ cells/ml were transferred into cryo tubes and cooled to -80°C, before they were stored in liquid nitrogen.
After thawing cryo-conserved cells, they were washed twice in medium to remove the toxic DMSO and then seeded for culture.

4.2.3.3 Cell counting

The number of living cells in a culture was determined by the trypan blue exclusion test using a Neubauer counting chamber. The dye can enter into dead cells while the intact membrane of a living cell prohibits the entry of the colour.
An aliquot of a cell suspension was mixed 1:2 with trypan blue solution and counted in a Neubauer chamber. The concentration of the cell suspension can be calculated in consideration of the dilution factor.

4.2.3.4 PolyI:C treatment of Mx1Cre mice

To deplete the conditionally modified cofilin gene, Mx1Cre mice were treated with polyI:C 24 hrs prior to bone marrow preparation. 300 µl polyI:C were injected in a concentration of 1 mg/ml into the peritoneum of a Mx1Cre mouse. PolyI:C leads to an endogenous Interferon type I response in the mouse which in turn leads to the induction of the Cre-recombinase under the control of the Mx1 promotor.

4.2.3.5 Generation and purification of different cell types

4.2.3.5.1 Isolation of cells from the bone marrow

Femur and Tibia of a 6-8 week old mouse were dissected and the remaining tissue was removed. The bones were sterilized in 70% Ethanol and washed in sterile PBS before the bone marrow was flushed out with a syringe using 5 ml of PBS. Cell clusters were dispersed and cells were collected by centrifugation (5 min, 1200 rpm, RT) prior to a red blood cell lysis in 5 ml RBC lysis buffer (5 – 10 min, RT). The reaction was stopped by adding 10 ml medium containing FCS. Cells were collected again by centrifugation, resuspended in 10 ml of the appropriate medium and counted.

4.2.3.5.2 Generation of bone marrow derived macrophages (BMM)

$2x10^6$ isolated bone marrow cells were cultivated in 10 ml BMM medium containing 25% macrophage colony stimulating factor (M-CSF) cell culture supernatant in bacterial Petri dishes (∅10 cm) for 5-7 days. The M-CSF containing cell supernatant was derived from cultures of L929 cells, which express M-CSF. In brief, L929 fibroblasts were grown to confluency, complete DMEM medium was replaced and the cells were incubated for another 12 – 14 days. The L929 conditioned supernatant was collected, filtered and kept at -20°C until use.

4.2.3.5.3 Generation of bone marrow derived dendritic cells (bmDC)

Dendritic cells were generated following the method described by Lutz et al. (Lutz et al., 1999). Briefly, $2x10^6$ bone marrow cells were cultivated in 10 ml DC medium containing 1 ml granulocyte macrophage colony stimulating factor (GM-CSF) cell culture supernatant in bacterial Petri dishes (∅10 cm). The cell supernatant was collected from Ag8653 myeloma cells that had been transfected with the gene for murine GM-CSF (kindly provided by Dr. Brigitta Stockinger, National Institute for Medical Research, Mill Hill, London). On day 3, 10 ml of fresh DC medium was added to the cells. On day 6, half the medium was exchanged. The dendritic cells were used for tests on day 7.

4.2.3.5.4 Induction and harvest of peritoneal exsudate cells (PEC)

If not specified otherwise mice received a single injection of 1 ml 2.5% thioglychollate i.p. 5 days prior to PEC harvest. Mice were desiccated and the skin was carefully removed leaving the peritoneum intact. Using a 10 ml syringe and a 25G needle 10 ml PBS was injected into the peritoneum and removed again. This procedure was repeated two more times before the cells were spun down and resuspended in medium and used for assays.

4.2.3.6 HTNC induced gene deletion *in vitro*

Using a recombinant Cre-Recombinase that can enter cells and nuclei, one can delete a gene *in vitro*. In this work, this protocol was used to confirm the findings of the Mx1Cre deletion by a different approach.
On day 4 of culture, wt and conditional BMM were washed and treated for 6 hrs with a 4 μM dilution of HTNC in serum-free medium. Afterwards the cells were washed again and cultured in BMM medium. After 24 hrs, DNA of treated and untreated samples was prepared and the protein lysates and morphological changes were observed over the following days.

4.2.3.7 Cell based *in vitro* assays

4.2.3.7.1 *In vitro* T cell activation assay

To test the ability of antigen presenting cells to induce an antigen specific T cell response, T cells of a T cell receptor (TCR) transgenic mouse (OT-II) were purified from spleen using the PAN T cell kit (*Miltenyi*). In brief, the spleen was dissected and splenocytes were washed in MACS separation buffer, prior to incubation (15 min, 4°C) with a cocktail of biotinylated antibodies that bind to all cells in the spleen except T cells. Splenocytes were washed and incubated with a secondary anti-biotin antibody bound to magnetic beads. The separation of T cells occurs by passing the splenocytes over a MACS separation column placed into a strong magnetic field that traps all the magnetically labelled cells and allows the T cells to pass through the column. After another washing step, purified T cells can be used in the stimulation assay.

The T cells used in this work are derived from OT-II transgenic mice. They carry T cells with just one specific α/β chain combination that exclusively recognize the $Ova_{323-339}$ peptide of Ovalbumin. Making use of this advantage $1x10^5$ purified T cells were incubated together with 300 ng/ml $Ova_{323-339}$ in the presence of titrated mutant or control DCs ($1x10^5$ -$5x10^3$) for 24 or 48 hrs. At the given time points, supernatant was collected and the levels of IL-2 as well as IFN-γ was determined by ELISA.

4.2.3.7.2 LIVE/DEAD assay

In order to determine the amount of dead cells in a culture the LIVE/DEAD assay (*Molecular Probes*) was used according to the manufacturer's instructions. In brief, BMM were harvested on day 6 of culture by trypsinisation and incubated with dilutions of CalceinAM (an ester that is only cleaved and after that fluorescences by living cells) and Ethidium bromide homodimer that only enters dead cells. The evaluation was done using FACS analysis.

4.2.3.7.3 Attachment and proliferation assay

Mice were injected 72 hours and 24 hours prior to bm preparation with 300 μg polyI:C each. Bm cells were prepared and $1x10^5$ cells were plated into one well of a 48-well plate in 0.5 ml BMM medium (all values in quadruplicates). For every time point (0, 4, 8, 12, 24, 48, 72, 96 hrs) a new 48 well plate was prepared and incubated for the appropriate time. The cells in the plate for 0 hrs were spun down, the medium was carefully removed and the cells were stored at -80°C. The remaining plates were washed vigorously at the given time point and stored as well at -80°C.

The analysis followed the instructions of the CyQuant Proliferation Assay (*Molecular Probes*) according the manufacturer's instructions using 200 μl lysis buffer per well. The assay is based on the quantification of DNA in every well; to be able to compare plates amongst each other a DNA titration was added for every plate. Plates were analysed by Fluoroskan measurement at 485/538 nm.

4.2.3.7.4 Uptake of fluorescently labelled zymosan

On day 6 BMM cultured on cover slips were washed twice with PBS. A 1:100 dilution of FITC-labelled yeast particles in prewarmed BMM-medium, was added to the macrophages for 5 or 15 min. After this incubation period, cells were washed and fixed in 4% PFA/PBS and counterstained with Phalloidin-Alexa546. The evaluation was done manually using a fluorescence microscope counting at least 100 cells from three different mice per time point.

4.2.3.7.5 Phagocytosis assay

On day 6 of culture, BMM were harvested by trypsinization, washed, and counted. In a flat-bottom 96 well plate $1x10^5$ cells were plated in 100 µl medium into the wells. All measurements were at least performed in quadruplicates. After an attachment period of 2 hrs, the medium was removed and replaced by 100 µl of FITC-labelled *E. coli* particles (Vybrant Phagocytosis Assay, *Molecular Probes*). Following a phagocytosis period, the solution was removed and un-internalized particles were quenched by adding trypan blue for 2 min and then aspirated. The absorbance of the plates was read using a Fluoroskan with a wavelength of 485/538 nm.

4.2.3.7.6 BrdU incorporation assay

Dividing cells in bm cultures were detected using the 5'-Bromo-2'-deoxy-uridine Labelling and Detection kit II (*Roche*) according to the manufacturer's instruction. In brief, bm cells grown on cover slips were pulsed for 1 hr with medium containing BrdU (1:1000) prior to fixation in 70% ethanol containing 20 µg/ml glycogen. 1st and 2nd antibody were incubated for 1 hr each, before the cells were mounted in gelvatiol. The number of BrdU-positive and –negative cells were counted for at least 200 cells per genotype and time point. The number of dividing cells is expressed as the percentage of BrdU-positive cells per total counted cells.

4.2.3.7.7 TUNEL apoptosis assay

Apoptotic cells were detected using the DeadEnd Fluorometric TUNEL System kit (*Promega*) according to the manufacturer's instruction. Bm cells grown on coverslips were fixed in 4% PFA/PBS on subsequent days of culture. The cells were incubated with TdT enzyme at 37°C for 60 min and the nuclei were counterstained with Hoechst. At least 200 TUNEL-positive and –negative cells were counted per genotype and time point. The number of apoptotic cells is expressed as the percentage of TUNEL-positive cells per total counted cells.

4.2.3.8 Video microscopy

To analyse the behaviour of living cells, videos were taken using an inverted microscope (Axiovert 100, *Zeiss*) with an incubator. For migration analysis, videos were taken at a frame rate of 4 frames/min with a 16x objective in Ibidi slides (*Integrated BioDiagnostics*), if not stated otherwise. The software used to acquire and analyse the stacks was MetaMorph 6.0 (*Molecular Devices*).

4.2.3.9 Sample preparation for scanning electron microscopy

Macrophages were grown on sterile cover slips for 6 days. Cells were washed twice with PBS and fixed in 2% glutharaldehyde in 0.1 M Sodium-Cacodylate buffer for 30 min. Cover slips were rinsed several times in 0.1 M Sodium-Cacodylate buffer to remove aldyhyde traces, before they were dehydrated in ascending dilutions of 70-100% ethanol in 0.9 % NaCl. Before the samples were sputtered with atomic gold, they were dried in a CO_2 based critical point drier (*Polaron*, CPD7501). Images of macrophages were taken at magnifications between 250x and 5000x in a PSEM 500 scanning electron microscope (*Philips*).

4.2.3.10 Immunostaining

Cultured cells were plated on cover slips. The cells generally were fixed in 4% PFA/PBS for 30 min and permeabilized for 10 min in 0.2 % TX-100/PBS. Cells were washed in 50 mM glycine in PBT (PBS/0.05% Tween20), and incubated in blocking buffer for 1 hr. Primary antibodies were diluted in blocking buffer and incubated for 1 hr. After washing in PBT, fluorescence-conjugated secondary antibodies were allowed to bind for 30 min in the dark diluted in blocking buffer. Nuclei were stained by including a dilution of Hoechst 33342 in PBT in one of the final washing steps. After briefly dipping in water the cover slips were mounted on glass slides in gelvatol.
To visualize cofilin, the cells were fixed with 15% picric acid/ 4% PFA for 1 hour in the dark, followed by several stringent extractions steps. First, the cover slips were dipped we were able to detect cofilin with an affinity purified antibody (KG40).

4.2.3.11 Enzyme-linked immunosorbent assay (ELISA)

A microlon 96-well plate was coated with 100 µl of the capture antibody diluted in PBS (see section 2.1.5) at 4°C o.n. After four-fold washing with PBS/0.05% Tween20 the plates were blocked for 2 hrs at room temperature with 200 µl PBS/1% BSA. At this step, plates can be kept frozen at -20°C for storage and later use. Otherwise, the block buffer was removed and replaced by 50 µl samples at least in duplicates. Additionally a standard reference was serially diluted 1:2 in media (usually starting at a concentration of 4 ng/ml). After an o.n. incubation at 4°C the plates were washed three times with PBS/0.05% Tween20 before 50 µl of the biotinylated detection antibody in PBS/0.1% BSA was given into each well. After 1 hr incubation at room temperature the plates were washed three times and 50 µl streptavidine-horseradish peroxidase (HRP) in PBS/0.1% BSA was added into each well for 30 minutes. The washing step was repeated once more before 100 µl substrate were given into each well. The reaction was stopped with 25 µl 2M H_2SO_4 as soon as the blank controls turned a pale blue shade, and the optical density was measured at 450 nm.

The values measured for the standard reference was plotted against the concentration of cytokine in the corresponding dilution. The equation for the linear section of the curve was used to calculate the concentration of the measured cytokine in the samples.

4.2.3.12 Fluorescence activated cell sorting (FACS) analysis

Flow cytometry is a technique of quantitative single cell analysis. Flow cytometry is based on an optical/mechanical system, in which single cells pass a laser beam. Photomultipliers detect the scattering of the laser beam. The forward scatter correlates with the size of the measured cell, whereas the side scatter indicates its granularity. Additionally different cell populations can be discriminated, if typical surface molecules are marked with antibodies coupled to a fluorescent component. Using fluorescence activated cell sorting (FACS) it is even possible to separate different cell populations marked with different combinations of fluorescing antibodies.

Per staining $2x10^5$ cells were transferred into FACS tubes and spun down (5 min, 1200 rpm, Megafuge 1.0R). The pellet was resuspended in 20 µl F_c-blocking solution and incubated for 15 min at 4°C. Subsequently, antibodies recognizing the desired surface antigens directly coupled to a fluorochrome were added and incubated for for 1 hour on ice. Prior to FACS analysis, the cells were washed three times with FACS buffer and resuspended in 200 µl.

4.2.3.13 Embryonic stem (ES) cell work

4.2.3.13.1 ES cell cultures

IB10 embryonic stem cells derived from 129Sv blastocysts were grown on a feeder layer of embryonic, immortalized fibroblasts (EF-feeders) plated on 0.2% gelatine coated dishes in ES cell medium.

4.2.3.13.2 ES cell transfection

Before transfection, cells were washed twice in PBS buffer, harvested by trypsinization and after washing in electroporation buffer (10mM HEPES buffer in DMEM without FCS) were resuspended at $1x10^7$ cells/ml in a final volume 0.7 ml. Cell suspension was electroporated using a BioRad Gene Pulser set at 250 V/cm and 500 μF for one pulse at RT. 10 μg of linearized plasmid DNA was used for each transfection. After pulsing, cell suspension was diluted in 10ml ES cell medium and plated on 10 cm^2 dishes. Neomycin selection started 1 day after transfection with 0.25 mg/ml G418.

4.2.3.13.3 ES cell selection

After approximately 7 days, single ES cell clones were picked and expanded in 96-well plates grown on EF-layer in selection medium. Once a 70-80% confluency was reached, the clones were washed twice with 100 μl PBS and trypsinized for 5 min with 50 μl trypsin at 37°C. 100 μl ES cell medium was added to the trypsinized clones, which were resuspended by pipetting vigorously, and split into 3 96-well plates. 2 of the 96-well plates were previously plated with an EF-layer, and were used to freeze down and store the clones 2 and 3 days after splitting. The third plate was further expanded on 0.2% gelatine coated dishes to obtain genomic DNA.

4.2.3.13.4 Genomic DNA isolation of ES cells and screening

To prepare genomic DNA from ES cells, cells were grown to confluency in 96-well dishes coated with gelatine, washed with 100 μl PBS, and lysed with 50 μl LAIRD lysis buffer with 100 μg/ml of proteinase K o.n. at 56°C in a humidified chamber. The next day the box was cooled for one hour and genomic DNA was precipitated by adding 100 μl ethanol to each well, followed by incubation for 1-2 hours. Once the filamentous DNA could be observed, the plate was inverted gently to remove the ethanol, and the wells washed 3x with 70% ETOH, air-dried for 15 min and resuspended in 100 μl TE buffer.

Screening of the ES cells clones for homology recombination event was performed by Southern blot.

5 BIBLIOGRAPHY

Abe, H., Nagaoka, R. and Obinata, T. (1993) Cytoplasmic localization and nuclear transport of cofilin in cultured myotubes. Exp Cell Res 206, 1-10.

Abe, H., Ohshima, S. and Obinata, T. (1989) A cofilin-like protein is involved in the regulation of actin assembly in developing skeletal muscle. J Biochem (Tokyo) 106, 696-702.

Adachi, R., Matsui, S., Kinoshita, M., Nagaishi, K., Sasaki, H., Kasahara, T. and Suzuki, K. (2000) Nitric oxide induces chemotaxis of neutrophil-like HL-60 cells and translocation of cofilin to plasma membranes. Int J Immunopharmacol 22, 855-64.

Adachi, R., Takeuchi, K. and Suzuki, K. (2002) Antisense oligonucleotide to cofilin enhances respiratory burst and phagocytosis in opsonized zymosan-stimulated mouse macrophage J774.1 cells. J Biol Chem 277, 45566-71.

Aldrich, R.A., Steinberg, A.G. and Campbell, D.C. (1954) Pedigree demonstrating a sex-linked recessive condition characterized by draining ears, eczematoid dermatitis and bloody diarrhea. Pediatrics 13, 133-9.

Ambach, A., Saunus, J., Konstandin, M., Wesselborg, S., Meuer, S.C. and Samstag, Y. (2000) The serine phosphatases PP1 and PP2A associate with and activate the actin-binding protein cofilin in human T lymphocytes. Eur J Immunol 30, 3422-31.

Arber, S., Barbayannis, F.A., Hanser, H., Schneider, C., Stanyon, C.A., Bernard, O. and Caroni, P. (1998) Regulation of actin dynamics through phosphorylation of cofilin by LIM-kinase. Nature 393, 805-9.

Arima, K., Imanaka, M., Okuzono, S., Kazuta, Y. and Kotani, S. (1998) Evidence for structural differences between the two highly homologous actin-regulatory proteins, destrin and cofilin. Biosci Biotechnol Biochem 62, 215-20.

Ayala, Y.M., Pantano, S., D'Ambrogio, A., Buratti, E., Brindisi, A., Marchetti, C., Romano, M. and Baralle, F.E. (2005) Human, Drosophila, and C.elegans TDP43: nucleic acid binding properties and splicing regulatory function. J Mol Biol 348, 575-88.

Ayscough, K.R. (1998) In vivo functions of actin-binding proteins. Curr Opin Cell Biol 10, 102-11.

Badolato, R., Sozzani, S., Malacarne, F., Bresciani, S., Fiorini, M., Borsatti, A., Albertini, A., Mantovani, A., Ugazio, A.G. and Notarangelo, L.D. (1998) Monocytes from Wiskott-Aldrich patients display reduced chemotaxis and lack of cell polarization in response to monocyte chemoattractant protein-1 and formyl-methionyl-leucyl-phenylalanine. J Immunol 161, 1026-33.

Balcer, H.I., Goodman, A.L., Rodal, A.A., Smith, E., Kugler, J., Heuser, J.E. and Goode, B.L. (2003) Coordinated regulation of actin filament turnover by a high-molecular-weight Srv2/CAP complex, cofilin, profilin, and Aip1. Curr Biol 13, 2159-69.

Bamburg, J.R. (1999) Proteins of the ADF/cofilin family: essential regulators of actin dynamics. Annu Rev Cell Dev Biol 15, 185-230.

Bamburg, J.R. and Bray, D. (1987) Distribution and cellular localization of actin depolymerizing factor. J Cell Biol 105, 2817-25.

Bamburg, J.R., McGough, A. and Ono, S. (1999) Putting a new twist on actin: ADF/cofilins modulate actin dynamics. Trends Cell Biol 9, 364-70.

Bamburg, J.R. and Wiggan, O.P. (2002) ADF/cofilin and actin dynamics in disease. Trends Cell Biol 12, 598-605.

Barnden, M.J., Allison, J., Heath, W.R. and Carbone, F.R. (1998) Defective TCR expression in transgenic mice constructed using cDNA-based alpha- and beta-chain genes under the control of heterologous regulatory elements. Immunol Cell Biol 76, 34-40.

Beller, D.I., Springer, T.A. and Schreiber, R.D. (1982) Anti-Mac-1 selectively inhibits the mouse and human type three complement receptor. J Exp Med 156, 1000-9.

Bernstein, B.W. and Bamburg, J.R. (1982) Tropomyosin binding to F-actin protects the F-actin from disassembly by brain actin-depolymerizing factor (ADF). Cell Motil 2, 1-8.

Bernstein, B.W., Painter, W.B., Chen, H., Minamide, L.S., Abe, H. and Bamburg, J.R. (2000) Intracellular pH modulation of ADF/cofilin proteins. Cell Motil Cytoskeleton 47, 319-36.

Bershadsky, A.D., Vaisberg, E.A. and Vasiliev, J.M. (1991) Pseudopodial activity at the active edge of migrating fibroblast is decreased after drug-induced microtubule depolymerization. Cell Motil Cytoskeleton 19, 152-8.

Bertling, E., Hotulainen, P., Mattila, P.K., Matilainen, T., Salminen, M. and Lappalainen, P. (2004) Cyclase-associated protein 1 (CAP1) promotes cofilin-induced actin dynamics in mammalian nonmuscle cells. Mol Biol Cell 15, 2324-34.

Bettinger, B.T., Gilbert, D.M. and Amberg, D.C. (2004) Actin up in the nucleus. Nat Rev Mol Cell Biol 5, 410-5.

Billadeau, D.D. and Burkhardt, J.K. (2006) Regulation of cytoskeletal dynamics at the immune synapse: new stars join the actin troupe. Traffic 7, 1451-60.

Binks, M., Jones, G.E., Brickell, P.M., Kinnon, C., Katz, D.R. and Thrasher, A.J. (1998) Intrinsic dendritic cell abnormalities in Wiskott-Aldrich syndrome. Eur J Immunol 28, 3259-67.

Bjorn, S.P., Soltyk, A., Beggs, J.D. and Friesen, J.D. (1989) PRP4 (RNA4) from Saccharomyces cerevisiae: its gene product is associated with the U4/U6 small nuclear ribonucleoprotein particle. Mol Cell Biol 9, 3698-709.

Bodin, S., Soulet, C., Tronchere, H., Sie, P., Gachet, C., Plantavid, M. and Payrastre, B. (2005) Integrin-dependent interaction of lipid rafts with the actin cytoskeleton in activated human platelets. J Cell Sci 118, 759-69.

Boillee, S., Yamanaka, K., Lobsiger, C.S., Copeland, N.G., Jenkins, N.A., Kassiotis, G., Kollias, G. and Cleveland, D.W. (2006) Onset and progression in inherited ALS determined by motor neurons and microglia. Science 312, 1389-92.

Borisy, G.G. and Svitkina, T.M. (2000) Actin machinery: pushing the envelope. Curr Opin Cell Biol 12, 104-12.

Caceres, J.F., Stamm, S., Helfman, D.M. and Krainer, A.R. (1994) Regulation of alternative splicing in vivo by overexpression of antagonistic splicing factors. Science 265, 1706-9.

Cammarota, G., Scheirle, A., Takacs, B., Doran, D.M., Knorr, R., Bannwarth, W., Guardiola, J. and Sinigaglia, F. (1992) Identification of a CD4 binding site on the beta 2 domain of HLA-DR molecules. Nature 356, 799-801.

Carlier, M.F., Laurent, V., Santolini, J., Melki, R., Didry, D., Xia, G.X., Hong, Y., Chua, N.H. and Pantaloni, D. (1997) Actin depolymerizing factor (ADF/cofilin) enhances the rate of filament turnover: implication in actin-based motility. J Cell Biol 136, 1307-22.

Carreno, B.M. and Collins, M. (2002) The B7 family of ligands and its receptors: new pathways for costimulation and inhibition of immune responses. Annu Rev Immunol 20, 29-53.

Castellano, F., Chavrier, P. and Caron, E. (2001) Actin dynamics during phagocytosis. Semin Immunol 13, 347-55.

Cecconi, D., Astner, H., Donadelli, M., Palmieri, M., Missiaglia, E., Hamdan, M., Scarpa, A. and Righetti, P.G. (2003) Proteomic analysis of pancreatic ductal carcinoma cells treated with 5-aza-2'-deoxycytidine. Electrophoresis 24, 4291-303.

Chellaiah, M., Kizer, N., Silva, M., Alvarez, U., Kwiatkowski, D. and Hruska, K.A. (2000) Gelsolin deficiency blocks podosome assembly and produces increased bone mass and strength. J Cell Biol 148, 665-78.

Clausen, B.E., Burkhardt, C., Reith, W., Renkawitz, R. and Forster, I. (1999) Conditional gene targeting in macrophages and granulocytes using LysMcre mice. Transgenic Res 8, 265-77.

Cooper, J.A. (2002) Actin dynamics: tropomyosin provides stability. Curr Biol 12, R523-5.

Croft, M. and Dubey, C. (1997) Accessory molecule and costimulation requirements for CD4 T cell response. Crit Rev Immunol 17, 89-118.

Cursiefen, C., Ikeda, S., Nishina, P.M., Smith, R.S., Ikeda, A., Jackson, D., Mo, J.S., Chen, L., Dana, M.R., Pytowski, B., Kruse, F.E. and Streilein, J.W. (2005) Spontaneous corneal hem- and lymphangiogenesis in mice with destrin-mutation depend on VEGFR3 signaling. Am J Pathol 166, 1367-77.

Dai, J., Sultan, S., Taylor, S.S. and Higgins, J.M. (2005) The kinase haspin is required for mitotic histone H3 Thr 3 phosphorylation and normal metaphase chromosome alignment. Genes Dev 19, 472-88.

Dawe, H.R., Minamide, L.S., Bamburg, J.R. and Cramer, L.P. (2003) ADF/cofilin controls cell polarity during fibroblast migration. Curr Biol 13, 252-7.

Dax, C.I., Lottspeich, F. and Mullner, S. (1998) In vitro model system for the identification and characterization of proteins involved in inflammatory processes. Electrophoresis 19, 1841-7.

de Clercq, E. (1980) Interferon inducers. Antibiot Chemother 27, 251-87.

de Hostos, E.L., Bradtke, B., Lottspeich, F. and Gerisch, G. (1993) Coactosin, a 17 kDa F-actin binding protein from Dictyostelium discoideum. Cell Motil Cytoskeleton 26, 181-91.

Dempsey, L.A., Sun, H., Hanakahi, L.A. and Maizels, N. (1999) G4 DNA binding by LR1 and its subunits, nucleolin and hnRNP D, A role for G-G pairing in immunoglobulin switch recombination. J Biol Chem 274, 1066-71.

Derry, J.M., Ochs, H.D. and Francke, U. (1994) Isolation of a novel gene mutated in Wiskott-Aldrich syndrome. Cell 79, following 922.

DesMarais, V., Ichetovkin, I., Condeelis, J. and Hitchcock-DeGregori, S.E. (2002) Spatial regulation of actin dynamics: a tropomyosin-free, actin-rich compartment at the leading edge. J Cell Sci 115, 4649-60.

Didry, D., Carlier, M.F. and Pantaloni, D. (1998) Synergy between actin depolymerizing factor/cofilin and profilin in increasing actin filament turnover. J Biol Chem 273, 25602-11.

Djafarzadeh, S. and Niggli, V. (1997) Signaling pathways involved in dephosphorylation and localization of the actin-binding protein cofilin in stimulated human neutrophils. Exp Cell Res 236, 427-35.

Dreyfuss, G., Kim, V.N. and Kataoka, N. (2002) Messenger-RNA-binding proteins and the messages they carry. Nat Rev Mol Cell Biol 3, 195-205.

Eibert, S.M., Lee, K.H., Pipkorn, R., Sester, U., Wabnitz, G.H., Giese, T., Meuer, S.C. and Samstag, Y. (2004) Cofilin peptide homologs interfere with immunological synapse formation and T cell activation. Proc Natl Acad Sci U S A 101, 1957-62.

Etienne-Manneville, S. (2004) Actin and microtubules in cell motility: which one is in control? Traffic 5, 470-7.

Etienne-Manneville, S. and Hall, A. (2001) Integrin-mediated activation of Cdc42 controls cell polarity in migrating astrocytes through PKCzeta. Cell 106, 489-98.

Eversole, A. and Maizels, N. (2000) In vitro properties of the conserved mammalian protein hnRNP D suggest a role in telomere maintenance. Mol Cell Biol 20, 5425-32.

Faure, S., Salazar-Fontana, L.I., Semichon, M., Tybulewicz, V.L., Bismuth, G., Trautmann, A., Germain, R.N. and Delon, J. (2004) ERM proteins regulate cytoskeleton relaxation promoting T cell-APC conjugation. Nat Immunol 5, 272-9.

Faust, N., Varas, F., Kelly, L.M., Heck, S. and Graf, T. (2000) Insertion of enhanced green fluorescent protein into the lysozyme gene creates mice with green fluorescent granulocytes and macrophages. Blood 96, 719-26.

Feng, Y., Liu, Q. and Xue, Q. (2006) Comparative study of rice and Arabidopsis actin-depolymerizing factors gene families. J Plant Physiol 163, 69-79.

Fenteany, G. and Glogauer, M. (2004) Cytoskeletal remodeling in leukocyte function. Curr Opin Hematol 11, 15-24.

Finkelman, F.D., Svetic, A., Gresser, I., Snapper, C., Holmes, J., Trotta, P.P., Katona, I.M. and Gause, W.C. (1991) Regulation by interferon alpha of immunoglobulin isotype selection and lymphokine production in mice. J Exp Med 174, 1179-88.

Freeman, N.L., Chen, Z., Horenstein, J., Weber, A. and Field, J. (1995) An actin monomer binding activity localizes to the carboxyl-terminal half of the Saccharomyces cerevisiae cyclase-associated protein. J Biol Chem 270, 5680-5.

Fujibuchi, T., Abe, Y., Takeuchi, T., Imai, Y., Kamei, Y., Murase, R., Ueda, N., Shigemoto, K., Yamamoto, H. and Kito, K. (2005) AIP1/WDR1 supports mitotic cell rounding. Biochem Biophys Res Commun 327, 268-75.

Gao, G.F., Tormo, J., Gerth, U.C., Wyer, J.R., McMichael, A.J., Stuart, D.I., Bell, J.I., Jones, E.Y. and Jakobsen, B.K. (1997) Crystal structure of the complex between human CD8alpha(alpha) and HLA-A2. Nature 387, 630-4.

Ghosh, M., Song, X., Mouneimne, G., Sidani, M., Lawrence, D.S. and Condeelis, J.S. (2004) Cofilin promotes actin polymerization and defines the direction of cell motility. Science 304, 743-6.

Glotzer, M. (2005) The molecular requirements for cytokinesis. Science 307, 1735-9.

Gohla, A., Birkenfeld, J. and Bokoch, G.M. (2005) Chronophin, a novel HAD-type serine protein phosphatase, regulates cofilin-dependent actin dynamics. Nat Cell Biol 7, 21-9.

Gonsior, S.M., Platz, S., Buchmeier, S., Scheer, U., Jockusch, B.M. and Hinssen, H. (1999) Conformational difference between nuclear and cytoplasmic actin as detected by a monoclonal antibody. J Cell Sci 112 (Pt 6), 797-809.

Goode, B.L., Drubin, D.G. and Lappalainen, P. (1998) Regulation of the cortical actin cytoskeleton in budding yeast by twinfilin, a ubiquitous actin monomer-sequestering protein. J Cell Biol 142, 723-33.

Gordy, C., Mishra, S. and Rodgers, W. (2004) Visualization of antigen presentation by actin-mediated targeting of glycolipid-enriched membrane domains to the immune synapse of B cell APCs. J Immunol 172, 2030-8.

Goto, H., Tomono, Y., Ajiro, K., Kosako, H., Fujita, M., Sakurai, M., Okawa, K., Iwamatsu, A., Okigaki, T., Takahashi, T. and Inagaki, M. (1999) Identification of a novel phosphorylation site on histone H3 coupled with mitotic chromosome condensation. J Biol Chem 274, 25543-9.

Gurniak, C.B., Perlas, E. and Witke, W. (2005) The actin depolymerizing factor n-cofilin is essential for neural tube morphogenesis and neural crest cell migration. Dev Biol 278, 231-41.

Hara-Kaonga, B., Gao, Y.A., Havrda, M., Harrington, A., Bergquist, I. and Liaw, L. (2006) Variable recombination efficiency in responder transgenes activated by cre recombinase in the vasculature. Transgenic Res 15, 101-6.

Hayashi, M., Kim, S.W., Imanaka-Yoshida, K., Yoshida, T., Abel, E.D., Eliceiri, B., Yang, Y., Ulevitch, R.J. and Lee, J.D. (2004) Targeted deletion of BMK1/ERK5 in adult mice perturbs vascular integrity and leads to endothelial failure. J Clin Invest 113, 1138-48.

Hendzel, M.J., Wei, Y., Mancini, M.A., Van Hooser, A., Ranalli, T., Brinkley, B.R., Bazett-Jones, D.P. and Allis, C.D. (1997) Mitosis-specific phosphorylation of histone H3 initiates primarily within pericentromeric heterochromatin during G2 and spreads in an ordered fashion coincident with mitotic chromosome condensation. Chromosoma 106, 348-60.

Hirayama, A., Adachi, R., Otani, S., Kasahara, T. and Suzuki, K. (2006) Cofilin plays a critical role in IL-8-dependent chemotaxis of neutrophilic HL-60 cells through changes in phosphorylation. J Leukoc Biol.

Hug, H., Costas, M., Staeheli, P., Aebi, M. and Weissmann, C. (1988) Organization of the murine Mx gene and characterization of its interferon- and virus-inducible promoter. Mol Cell Biol 8, 3065-79.

Ichetovkin, I., Grant, W. and Condeelis, J. (2002) Cofilin produces newly polymerized actin filaments that are preferred for dendritic nucleation by the Arp2/3 complex. Curr Biol 12, 79-84.

Ikeda, S., Cunningham, L.A., Boggess, D., Hawes, N., Hobson, C.D., Sundberg, J.P., Naggert, J.K., Smith, R.S. and Nishina, P.M. (2003) Aberrant actin cytoskeleton leads to accelerated proliferation of corneal epithelial cells in mice deficient for destrin (actin depolymerizing factor). Hum Mol Genet 12, 1029-37.

Ishikawa, F., Matunis, M.J., Dreyfuss, G. and Cech, T.R. (1993) Nuclear proteins that bind the pre-mRNA 3' splice site sequence r(UUAG/G) and the human telomeric DNA sequence d(TTAGGG)n. Mol Cell Biol 13, 4301-10.

Janeway, C. (2004) Immunobiology: the immune system in health and disease. Garland Science; Churchill Livingstone, New York, Edinburgh.

Jin, H.K., Yamashita, T., Ochiai, K., Haller, O. and Watanabe, T. (1998) Characterization and expression of the Mx1 gene in wild mouse species. Biochem Genet 36, 311-22.

Jin, Y., Mazza, C., Christie, J.R., Giliani, S., Fiorini, M., Mella, P., Gandellini, F., Stewart, D.M., Zhu, Q., Nelson, D.L., Notarangelo, L.D. and Ochs, H.D. (2004) Mutations of the Wiskott-Aldrich Syndrome Protein (WASP): hotspots, effect on transcription, and translation and phenotype/genotype correlation. Blood 104, 4010-9.

Kabsch, W., Mannherz, H.G., Suck, D., Pai, E.F. and Holmes, K.C. (1990) Atomic structure of the actin:DNase I complex. Nature 347, 37-44.

Kaji, N., Ohashi, K., Shuin, M., Niwa, R., Uemura, T. and Mizuno, K. (2003) Cell cycle-associated changes in Slingshot phosphatase activity and roles in cytokinesis in animal cells. J Biol Chem 278, 33450-5.

Kaplan, G. (1977) Differences in the mode of phagocytosis with Fc and C3 receptors in macrophages. Scand J Immunol 6, 797-807.

Kirchhausen, T. (1998) Wiskott-Aldrich syndrome: a gene, a multifunctional protein and the beginnings of an explanation. Mol Med Today 4, 300-4.

Kohl, J. (2006) The role of complement in danger sensing and transmission. Immunol Res 34, 157-76.

Konakahara, S., Ohashi, K., Mizuno, K., Itoh, K. and Tsuji, T. (2004) CD29 integrin- and LIMK1/cofilin-mediated actin reorganization regulates the migration of haematopoietic progenitor cells underneath bone marrow stromal cells. Genes Cells 9, 345-58.

Kuhn, R., Schwenk, F., Aguet, M. and Rajewsky, K. (1995) Inducible gene targeting in mice. Science 269, 1427-9.

Kuhn, T.B., Meberg, P.J., Brown, M.D., Bernstein, B.W., Minamide, L.S., Jensen, J.R., Okada, K., Soda, E.A. and Bamburg, J.R. (2000) Regulating actin dynamics in neuronal growth cones by ADF/cofilin and rho family GTPases. J Neurobiol 44, 126-44.

Kukalev, A., Nord, Y., Palmberg, C., Bergman, T. and Percipalle, P. (2005) Actin and hnRNP U cooperate for productive transcription by RNA polymerase II. Nat Struct Mol Biol 12, 238-44.

Lamaze, C., Fujimoto, L.M., Yin, H.L. and Schmid, S.L. (1997) The actin cytoskeleton is required for receptor-mediated endocytosis in mammalian cells. J Biol Chem 272, 20332-5.

Lambrechts, A., Van Troys, M. and Ampe, C. (2004) The actin cytoskeleton in normal and pathological cell motility. Int J Biochem Cell Biol 36, 1890-909.

Lee, K.H., Meuer, S.C. and Samstag, Y. (2000) Cofilin: a missing link between T cell co-stimulation and rearrangement of the actin cytoskeleton. Eur J Immunol 30, 892-9.

Linder, S., Higgs, H., Hufner, K., Schwarz, K., Pannicke, U. and Aepfelbacher, M. (2000) The polarization defect of Wiskott-Aldrich syndrome macrophages is linked to dislocalization of the Arp2/3 complex. J Immunol 165, 221-5.

Lutz, M.B., Kukutsch, N., Ogilvie, A.L., Rossner, S., Koch, F., Romani, N. and Schuler, G. (1999) An advanced culture method for generating large quantities of highly pure dendritic cells from mouse bone marrow. J Immunol Methods 223, 77-92.

Maciver, S.K. and Hussey, P.J. (2002) The ADF/cofilin family: actin-remodeling proteins. Genome Biol 3, reviews3007.

Magdalena, J., Millard, T.H. and Machesky, L.M. (2003) Microtubule involvement in NIH 3T3 Golgi and MTOC polarity establishment. J Cell Sci 116, 743-56.

Matsui, S., Matsumoto, S., Adachi, R., Kusui, K., Hirayama, A., Watanabe, H., Ohashi, K., Mizuno, K., Yamaguchi, T., Kasahara, T. and Suzuki, K. (2002) LIM kinase 1 modulates opsonized zymosan-triggered activation of macrophage-like U937 cells. Possible involvement of phosphorylation of cofilin and reorganization of actin cytoskeleton. J Biol Chem 277, 544-9.

May, R.C., Caron, E., Hall, A. and Machesky, L.M. (2000) Involvement of the Arp2/3 complex in phagocytosis mediated by FcgammaR or CR3. Nat Cell Biol 2, 246-8.

May, R.C. and Machesky, L.M. (2001) Phagocytosis and the actin cytoskeleton. J Cell Sci 114, 1061-77.

McGough, A., Pope, B., Chiu, W. and Weeds, A. (1997) Cofilin changes the twist of F-actin: implications for actin filament dynamics and cellular function. J Cell Biol 138, 771-81.

Meberg, P.J., Ono, S., Minamide, L.S., Takahashi, M. and Bamburg, J.R. (1998) Actin depolymerizing factor and cofilin phosphorylation dynamics: response to signals that regulate neurite extension. Cell Motil Cytoskeleton 39, 172-90.

Metchnikoff, E. (1891) Lectures on the comparative pathology of inflammation. Lecture VII. Devlivered at the Pasteur Institute. Translated by F. A.Starling and E. H. Starling, New York: Dover (1968)

Minvielle-Sebastia, L., Beyer, K., Krecic, A.M., Hector, R.E., Swanson, M.S. and Keller, W. (1998) Control of cleavage site selection during mRNA 3' end formation by a yeast hnRNP. Embo J 17, 7454-68.

Misra, U.K., Sharma, T. and Pizzo, S.V. (2005) Ligation of cell surface-associated glucose-regulated protein 78 by receptor-recognized forms of alpha 2-macroglobulin: activation of p21-activated protein kinase-2-dependent signaling in murine peritoneal macrophages. J Immunol 175, 2525-33.

Moon, A.L., Janmey, P.A., Louie, K.A. and Drubin, D.G. (1993) Cofilin is an essential component of the yeast cortical cytoskeleton. J Cell Biol 120, 421-35.

Morgan, T.E., Lockerbie, R.O., Minamide, L.S., Browning, M.D. and Bamburg, J.R. (1993) Isolation and characterization of a regulated form of actin depolymerizing factor. J Cell Biol 122, 623-33.

Moriyama, K., Iida, K. and Yahara, I. (1996) Phosphorylation of Ser-3 of cofilin regulates its essential function on actin. Genes Cells 1, 73-86.

Moriyama, K., Nishida, E., Yonezawa, N., Sakai, H., Matsumoto, S., Iida, K. and Yahara, I. (1990) Destrin, a mammalian actin-depolymerizing protein, is closely related to cofilin. Cloning and expression of porcine brain destrin cDNA. J Biol Chem 265, 5768-73.

Moriyama, K. and Yahara, I. (2002) Human CAP1 is a key factor in the recycling of cofilin and actin for rapid actin turnover. J Cell Sci 115, 1591-601.

Muller, N., Avota, E., Schneider-Schaulies, J., Harms, H., Krohne, G. and Schneider-Schaulies, S. (2006) Measles virus contact with T cells impedes cytoskeletal remodeling associated with spreading, polarization, and CD3 clustering. Traffic 7, 849-58.

Nagaishi, K., Adachi, R., Kawanishi, T., Yamaguchi, T., Kasahara, T., Hayakawa, T. and Suzuki, K. (1999a) Participation of cofilin in opsonized zymosan-triggered activation of neutrophil-like HL-60 cells through rapid dephosphorylation and translocation to plasma membranes. J Biochem (Tokyo) 125, 891-8.

Nagaishi, K., Adachi, R., Matsui, S., Yamaguchi, T., Kasahara, T. and Suzuki, K. (1999b) Herbimycin A inhibits both dephosphorylation and translocation of cofilin induced by opsonized zymosan in macrophagelike U937 cells. J Cell Physiol 180, 345-54.

Nagaoka, R., Abe, H., Kusano, K. and Obinata, T. (1995) Concentration of cofilin, a small actin-binding protein, at the cleavage furrow during cytokinesis. Cell Motil Cytoskeleton 30, 1-7.

Nagata-Ohashi, K., Ohta, Y., Goto, K., Chiba, S., Mori, R., Nishita, M., Ohashi, K., Kousaka, K., Iwamatsu, A., Niwa, R., Uemura, T. and Mizuno, K. (2004) A pathway of neuregulin-induced activation of cofilin-phosphatase Slingshot and cofilin in lamellipodia. J Cell Biol 165, 465-71.

Nakano, K. and Mabuchi, I. (2006) Actin-depolymerizing protein Adf1 is required for formation and maintenance of the contractile ring during cytokinesis in fission yeast. Mol Biol Cell 17, 1933-45.

Nebl, G., Meuer, S.C. and Samstag, Y. (1996) Dephosphorylation of serine 3 regulates nuclear translocation of cofilin. J Biol Chem 271, 26276-80.

Nishida, E., Iida, K., Yonezawa, N., Koyasu, S., Yahara, I. and Sakai, H. (1987) Cofilin is a component of intranuclear and cytoplasmic actin rods induced in cultured cells. Proc Natl Acad Sci U S A 84, 5262-6.

Nishida, E., Maekawa, S. and Sakai, H. (1984) Cofilin, a protein in porcine brain that binds to actin filaments and inhibits their interactions with myosin and tropomyosin. Biochemistry 23, 5307-13.

Nishita, M., Aizawa, H. and Mizuno, K. (2002) Stromal cell-derived factor 1alpha activates LIM kinase 1 and induces cofilin phosphorylation for T-cell chemotaxis. Mol Cell Biol 22, 774-83.

Nishita, M., Tomizawa, C., Yamamoto, M., Horita, Y., Ohashi, K. and Mizuno, K. (2005) Spatial and temporal regulation of cofilin activity by LIM kinase and Slingshot is critical for directional cell migration. J Cell Biol 171, 349-59.

Nishita, M., Wang, Y., Tomizawa, C., Suzuki, A., Niwa, R., Uemura, T. and Mizuno, K. (2004) Phosphoinositide 3-kinase-mediated activation of cofilin phosphatase Slingshot and its role for insulin-induced membrane protrusion. J Biol Chem 279, 7193-8.

Niwa, R., Nagata-Ohashi, K., Takeichi, M., Mizuno, K. and Uemura, T. (2002) Control of actin reorganization by Slingshot, a family of phosphatases that dephosphorylate ADF/cofilin. Cell 108, 233-46.

Ochs, H.D., Slichter, S.J., Harker, L.A., Von Behrens, W.E., Clark, R.A. and Wedgwood, R.J. (1980) The Wiskott-Aldrich syndrome: studies of lymphocytes, granulocytes, and platelets. Blood 55, 243-52.

Okada, K., Obinata, T. and Abe, H. (1999) XAIP1: a Xenopus homologue of yeast actin interacting protein 1 (AIP1), which induces disassembly of actin filaments cooperatively with ADF/cofilin family proteins. J Cell Sci 112 (Pt 10), 1553-65.

Omelchenko, T., Vasiliev, J.M., Gelfand, I.M., Feder, H.H. and Bonder, E.M. (2002) Mechanisms of polarization of the shape of fibroblasts and epitheliocytes: Separation of the roles of microtubules and Rho-dependent actin-myosin contractility. Proc Natl Acad Sci U S A 99, 10452-7.

Ono, S., Baillie, D.L. and Benian, G.M. (1999) UNC-60B, an ADF/cofilin family protein, is required for proper assembly of actin into myofibrils in Caenorhabditis elegans body wall muscle. J Cell Biol 145, 491-502.

Ono, S. and Ono, K. (2002) Tropomyosin inhibits ADF/cofilin-dependent actin filament dynamics. J Cell Biol 156, 1065-76.

Ou, S.H., Wu, F., Harrich, D., Garcia-Martinez, L.F. and Gaynor, R.B. (1995) Cloning and characterization of a novel cellular protein, TDP-43, that binds to human immunodeficiency virus type 1 TAR DNA sequence motifs. J Virol 69, 3584-96.

Palazzo, A.F. and Gundersen, G.G. (2002) Microtubule-actin cross-talk at focal adhesions. Sci STKE 2002, PE31.

Palazzo, A.F., Joseph, H.L., Chen, Y.J., Dujardin, D.L., Alberts, A.S., Pfister, K.K., Vallee, R.B. and Gundersen, G.G. (2001) Cdc42, dynein, and dynactin regulate MTOC reorientation independent of Rho-regulated microtubule stabilization. Curr Biol 11, 1536-41.

Peitz, M., Pfannkuche, K., Rajewsky, K. and Edenhofer, F. (2002) Ability of the hydrophobic FGF and basic TAT peptides to promote cellular uptake of recombinant Cre recombinase: a tool for efficient genetic engineering of mammalian genomes. Proc Natl Acad Sci U S A 99, 4489-94.

Pendleton, A., Pope, B., Weeds, A. and Koffer, A. (2003) Latrunculin B or ATP depletion induces cofilin-dependent translocation of actin into nuclei of mast cells. J Biol Chem 278, 14394-400.

Percipalle, P., Fomproix, N., Kylberg, K., Miralles, F., Bjorkroth, B., Daneholt, B. and Visa, N. (2003) An actin-ribonucleoprotein interaction is involved in transcription by RNA polymerase II. Proc Natl Acad Sci U S A 100, 6475-80.

Percipalle, P., Zhao, J., Pope, B., Weeds, A., Lindberg, U. and Daneholt, B. (2001) Actin bound to the heterogeneous nuclear ribonucleoprotein hrp36 is associated with Balbiani ring mRNA from the gene to polysomes. J Cell Biol 153, 229-36.

Perrin, D., Moller, K., Hanke, K. and Soling, H.D. (1992) cAMP and Ca(2+)-mediated secretion in parotid acinar cells is associated with reversible changes in the organization of the cytoskeleton. J Cell Biol 116, 127-34.

Poljak, R.J. (1991) Structure of antibodies and their complexes with antigens. Mol Immunol 28, 1341-5.

Pollard, T.D. (1986) Rate constants for the reactions of ATP- and ADP-actin with the ends of actin filaments. J Cell Biol 103, 2747-54.

Pollard, T.D., Blanchoin, L. and Mullins, R.D. (2000) Molecular mechanisms controlling actin filament dynamics in nonmuscle cells. Annu Rev Biophys Biomol Struct 29, 545-76.

Pope, B.J., Zierler-Gould, K.M., Kuhne, R., Weeds, A.G. and Ball, L.J. (2004) Solution structure of human cofilin: actin binding, pH sensitivity, and relationship to actin-depolymerizing factor. J Biol Chem 279, 4840-8.

Preuss, U., Landsberg, G. and Scheidtmann, K.H. (2003) Novel mitosis-specific phosphorylation of histone H3 at Thr11 mediated by Dlk/ZIP kinase. Nucleic Acids Res 31, 878-85.

Renoult, C., Ternent, D., Maciver, S.K., Fattoum, A., Astier, C., Benyamin, Y. and Roustan, C. (1999) The identification of a second cofilin binding site on actin suggests a novel, intercalated arrangement of F-actin binding. J Biol Chem 274, 28893-9.

Ressad, F., Didry, D., Xia, G.X., Hong, Y., Chua, N.H., Pantaloni, D. and Carlier, M.F. (1998) Kinetic analysis of the interaction of actin-depolymerizing factor (ADF)/cofilin with G- and F-actins. Comparison of plant and human ADFs and effect of phosphorylation. J Biol Chem 273, 20894-902.

Riol-Blanco, L., Sanchez-Sanchez, N., Torres, A., Tejedor, A., Narumiya, S., Corbi, A.L., Sanchez-Mateos, P. and Rodriguez-Fernandez, J.L. (2005) The chemokine receptor CCR7 activates in dendritic cells two signaling modules that independently regulate chemotaxis and migratory speed. J Immunol 174, 4070-80.

Rodal, A.A., Tetreault, J.W., Lappalainen, P., Drubin, D.G. and Amberg, D.C. (1999) Aip1p interacts with cofilin to disassemble actin filaments. J Cell Biol 145, 1251-64.

Rogers, E.M., Hsiung, F., Rodrigues, A.B. and Moses, K. (2005) Slingshot cofilin phosphatase localization is regulated by Receptor Tyrosine Kinases and regulates cytoskeletal structure in the developing Drosophila eye. Mech Dev 122, 1194-205.

Rosenberg, G.H., Alahari, S.K. and Kaufer, N.F. (1991) prp4 from Schizosaccharomyces pombe, a mutant deficient in pre-mRNA splicing isolated using genes containing artificial introns. Mol Gen Genet 226, 305-9.

Rosmarin, A.G., Weil, S.C., Rosner, G.L., Griffin, J.D., Arnaout, M.A. and Tenen, D.G. (1989) Differential expression of CD11b/CD18 (Mo1) and myeloperoxidase genes during myeloid differentiation. Blood 73, 131-6.

Saiki, R.K., Gelfand, D.H., Stoffel, S., Scharf, S.J., Higuchi, R., Horn, G.T., Mullis, K.B. and Erlich, H.A. (1988) Primer-directed enzymatic amplification of DNA with a thermostable DNA polymerase. Science 239, 487-91.

Sambrook, J., Maniatis, T. and Fritsch, E.F. (1989) Molecular cloning: a laboratory manual. Cold Spring Harbor Laboratory Press, Cold Spring Harbor, N.Y.

Samstag, Y., Eckerskorn, C., Wesselborg, S., Henning, S., Wallich, R. and Meuer, S.C. (1994) Costimulatory signals for human T-cell activation induce nuclear translocation of pp19/cofilin. Proc Natl Acad Sci U S A 91, 4494-8.

Sanger, F., Nicklen, S. and Coulson, A.R. (1977) DNA sequencing with chain-terminating inhibitors. Proc Natl Acad Sci U S A 74, 5463-7.

Sauer, B. and Henderson, N. (1988) Site-specific DNA recombination in mammalian cells by the Cre recombinase of bacteriophage P1. Proc Natl Acad Sci U S A 85, 5166-70.

Schneider, A., Zhang, Y., Guan, Y., Davis, L.S. and Breyer, M.D. (2003) Differential, inducible gene targeting in renal epithelia, vascular endothelium, and viscera of Mx1Cre mice. Am J Physiol Renal Physiol 284, F411-7.

Sen, G.C. and Ransohoff, R.M. (1993) Interferon-induced antiviral actions and their regulation. Adv Virus Res 42, 57-102.

Sinha, P., Hutter, G., Kottgen, E., Dietel, M., Schadendorf, D. and Lage, H. (1999) Increased expression of epidermal fatty acid binding protein, cofilin, and 14-3-3-sigma (stratifin) detected by two-dimensional gel electrophoresis, mass spectrometry and microsequencing of drug-resistant human adenocarcinoma of the pancreas. Electrophoresis 20, 2952-60.

Smith, R.S., Hawes, N.L., Kuhlmann, S.D., Heckenlively, J.R., Chang, B., Roderick, T.H. and Sundberg, J.P. (1996) Corn1: a mouse model for corneal surface disease and neovascularization. Invest Ophthalmol Vis Sci 37, 397-404.

Staeheli, P., Danielson, P., Haller, O. and Sutcliffe, J.G. (1986) Transcriptional activation of the mouse Mx gene by type I interferon. Mol Cell Biol 6, 4770-4.

Stierum, R., Gaspari, M., Dommels, Y., Ouatas, T., Pluk, H., Jespersen, S., Vogels, J., Verhoeckx, K., Groten, J. and van Ommen, B. (2003) Proteome analysis reveals novel proteins associated with proliferation and differentiation of the colorectal cancer cell line Caco-2. Biochim Biophys Acta 1650, 73-91.

Stossel, T.P. (1993) On the crawling of animal cells. Science 260, 1086-94.

Stradal, T.E., Pusch, R. and Kliche, S. (2006) Molecular regulation of cytoskeletal rearrangements during T cell signalling. Results Probl Cell Differ 43, 219-44.

Su, Y., Kondrikov, D. and Block, E.R. (2005) Cytoskeletal regulation of nitric oxide synthase. Cell Biochem Biophys 43, 439-49.

Sumi, T., Matsumoto, K., Takai, Y. and Nakamura, T. (1999) Cofilin phosphorylation and actin cytoskeletal dynamics regulated by rho- and Cdc42-activated LIM-kinase 2. J Cell Biol 147, 1519-32.

Suzuki, K., Yamaguchi, T., Tanaka, T., Kawanishi, T., Nishimaki-Mogami, T., Yamamoto, K., Tsuji, T., Irimura, T., Hayakawa, T. and Takahashi, A. (1995) Activation induces dephosphorylation of cofilin and its translocation to plasma membranes in neutrophil-like differentiated HL-60 cells. J Biol Chem 270, 19551-6.

Takuma, T., Ichida, T., Yokoyama, N., Tamura, S. and Obinata, T. (1996) Dephosphorylation of cofilin in parotid acinar cells. J Biochem (Tokyo) 120, 35-41.

Theriot, J.A. and Mitchison, T.J. (1991) Actin microfilament dynamics in locomoting cells. Nature 352, 126-31.

Tomonaga, T. and Levens, D. (1995) Heterogeneous nuclear ribonucleoprotein K is a DNA-binding transactivator. J Biol Chem 270, 4875-81.

Toshima, J., Toshima, J.Y., Amano, T., Yang, N., Narumiya, S. and Mizuno, K. (2001a) Cofilin phosphorylation by protein kinase testicular protein kinase 1 and its role in integrin-mediated actin reorganization and focal adhesion formation. Mol Biol Cell 12, 1131-45.

Toshima, J., Toshima, J.Y., Suzuki, M., Noda, T. and Mizuno, K. (2001b) Cell-type-specific expression of a TESK1 promoter-linked lacZ gene in transgenic mice. Biochem Biophys Res Commun 286, 566-73.

Toshima, J., Toshima, J.Y., Takeuchi, K., Mori, R. and Mizuno, K. (2001c) Cofilin phosphorylation and actin reorganization activities of testicular protein kinase 2 and its predominant expression in testicular Sertoli cells. J Biol Chem 276, 31449-58.

Valensin, S., Paccani, S.R., Ulivieri, C., Mercati, D., Pacini, S., Patrussi, L., Hirst, T., Lupetti, P. and Baldari, C.T. (2002) F-actin dynamics control segregation of the TCR signaling cascade to clustered lipid rafts. Eur J Immunol 32, 435-46.

van der Houven van Oordt, W., Diaz-Meco, M.T., Lozano, J., Krainer, A.R., Moscat, J. and Caceres, J.F. (2000) The MKK(3/6)-p38-signaling cascade alters the subcellular distribution of hnRNP A1 and modulates alternative splicing regulation. J Cell Biol 149, 307-16.

Van Haastert, P.J. and Devreotes, P.N. (2004) Chemotaxis: signalling the way forward. Nat Rev Mol Cell Biol 5, 626-34.

Vartiainen, M.K., Mustonen, T., Mattila, P.K., Ojala, P.J., Thesleff, I., Partanen, J. and Lappalainen, P. (2002) The three mouse actin-depolymerizing factor/cofilins evolved to fulfill cell-type-specific requirements for actin dynamics. Mol Biol Cell 13, 183-94.

Vasiliev, J.M. (1991) Polarization of pseudopodial activities: cytoskeletal mechanisms. J Cell Sci 98 (Pt 1), 1-4.

Vieu, E. and Hernandez, N. (2006) Actin's latest act: polymerizing to facilitate transcription? Nat Cell Biol 8, 650-1.

Wabnitz, G.H., Nebl, G., Klemke, M., Schroder, A.J. and Samstag, Y. (2006) Phosphatidylinositol 3-kinase functions as a ras effector in the signaling cascade that regulates dephosphorylation of the actin-remodeling protein cofilin after costimulation of untransformed human T lymphocytes. J Immunol 176, 1668-74.

Wang, I., Kao, C.W., Liu, C., Saika, S., Nishina, P.M., Sundberg, J.P., Smith, R.S. and Kao, W.W. (2001) Characterization of Corn1 mice: Alteration of epithelial and stromal cell gene expression. Mol Vis 7, 20-6.

Webb, J.L., Harvey, M.W., Holden, D.W. and Evans, T.J. (2001) Macrophage nitric oxide synthase associates with cortical actin but is not recruited to phagosomes. Infect Immun 69, 6391-400.

Wedlich-Soldner, R. and Li, R. (2004) Closing the loops: new insights into the role and regulation of actin during cell polarization. Exp Cell Res 301, 8-15.

Wells, C.M., Walmsley, M., Ooi, S., Tybulewicz, V. and Ridley, A.J. (2004) Rac1-deficient macrophages exhibit defects in cell spreading and membrane ruffling but not migration. J Cell Sci 117, 1259-68.

Wheeler, A.P., Wells, C.M., Smith, S.D., Vega, F.M., Henderson, R.B., Tybulewicz, V.L. and Ridley, A.J. (2006) Rac1 and Rac2 regulate macrophage morphology but are not essential for migration. J Cell Sci 119, 2749-57.

Witke, W. (2004) The role of profilin complexes in cell motility and other cellular processes. Trends Cell Biol 14, 461-9.

Witke, W., Li, W., Kwiatkowski, D.J. and Southwick, F.S. (2001) Comparisons of CapG and gelsolin-null macrophages: demonstration of a unique role for CapG in receptor-mediated ruffling, phagocytosis, and vesicle rocketing. J Cell Biol 154, 775-84.

Witke, W., Podtelejnikov, A.V., Di Nardo, A., Sutherland, J.D., Gurniak, C.B., Dotti, C. and Mann, M. (1998) In mouse brain profilin I and profilin II associate with regulators of the endocytic pathway and actin assembly. Embo J 17, 967-76.

Wu, X., Yoo, Y., Okuhama, N.N., Tucker, P.W., Liu, G. and Guan, J.L. (2006) Regulation of RNA-polymerase-II-dependent transcription by N-WASP and its nuclear-binding partners. Nat Cell Biol 8, 756-63.

Yang, N., Higuchi, O., Ohashi, K., Nagata, K., Wada, A., Kangawa, K., Nishida, E. and Mizuno, K. (1998) Cofilin phosphorylation by LIM-kinase 1 and its role in Rac-mediated actin reorganization. Nature 393, 809-12.

Ye, M., Iwasaki, H., Laiosa, C.V., Stadtfeld, M., Xie, H., Heck, S., Clausen, B., Akashi, K. and Graf, T. (2003) Hematopoietic stem cells expressing the myeloid lysozyme gene retain long-term, multilineage repopulation potential. Immunity 19, 689-99.

Yeoh, S., Pope, B., Mannherz, H.G. and Weeds, A. (2002) Determining the differences in actin binding by human ADF and cofilin. J Mol Biol 315, 911-25.

Yin, H.L. and Janmey, P.A. (2003) Phosphoinositide regulation of the actin cytoskeleton. Annu Rev Physiol 65, 761-89.

Yonezawa, N., Homma, Y., Yahara, I., Sakai, H. and Nishida, E. (1991) A short sequence responsible for both phosphoinositide binding and actin binding activities of cofilin. J Biol Chem 266, 17218-21.

Yonezawa, N., Nishida, E. and Sakai, H. (1985) pH control of actin polymerization by cofilin. J Biol Chem 260, 14410-2.

Zicha, D., Allen, W.E., Brickell, P.M., Kinnon, C., Dunn, G.A., Jones, G.E. and Thrasher, A.J. (1998) Chemotaxis of macrophages is abolished in the Wiskott-Aldrich syndrome. Br J Haematol 101, 659-65.

Zinkernagel, R.M. and Doherty, P.C. (1997) The discovery of MHC restriction. Immunol Today 18, 14-7.

Appendix A:

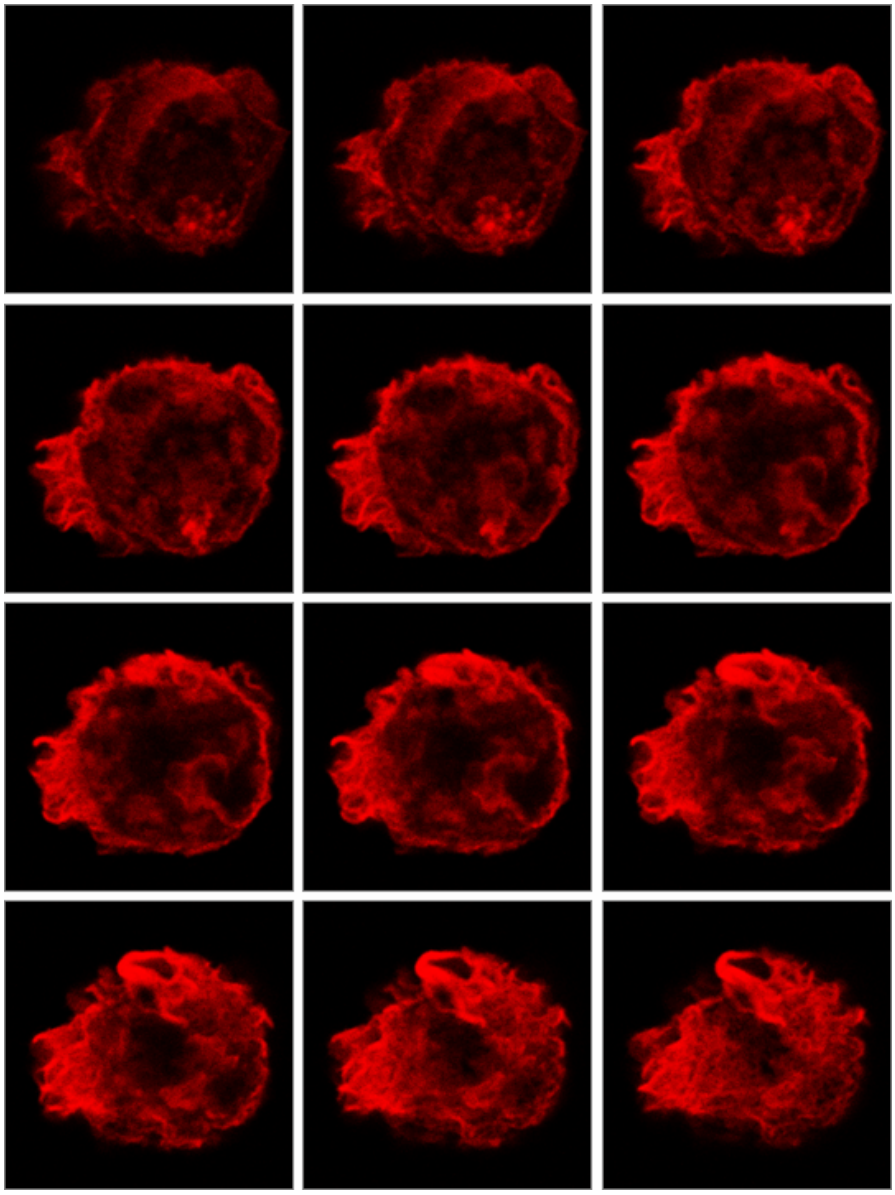

Figure 47: F-actin distribution in a cofilin mutant macrophage
BMM were fixed on day 6 and stained with phalloidin. The images show seqential slides obtained by confocal microscopy. The first image was taken at the contact zone, where the macrophage attaches to the cover slip. The last picture shows the apical surface.